博 士 論 文
(Doctoral Thesis)

Biotechnological application of bacteriophages for controlling citrus canker and citrus bacterial spot

（カンキツかいよう病バイオコントロールへのファージの有効利用）

Abdelmonim Ali Ahmad Ebrahim

広島大学大学院先端物質科学研究科
分子生命科学専攻
Department of Molecular Biotechnology, Graduate School of Advanced Sciences of Matter
Hiroshima University

2015 年 3 月
(March 2015)

目次

(Table of Contents)

主論文
(Main thesis)

CONTENTS

LIST OF FIGURES

LIST OF TABLES

Chapter 1

General Introduction

1.1.The citrus

Citrus, known also as agrumes (sour fruits) by the Romance loanword was originated in Southeast Asia. Today citrus is one of the most important fruit crops with global availability and popularity contributing to human diets. Citrus fruits are high in Vitamin C and contain other important nutrients including folate and potassium, and in fresh form, are good sources of dietary fiber (YuQiu Liu et al., 2012). There are many studies and debates about the origin of citrus with a history full of controversy and interesting legends. Many studies demonstrate that citrus is native to the subtropical and tropical areas of Asia, originating in certain parts of Southeast Asia including China, India, and the Malay Archipelago (Bartholomew and Sinclair, 1952; Sinclair, 1961; Scora, 1975; Ramana et al., 1981; Gmitter and Hu, 1990). It was reported in an old manuscript found among ancient Chinese documents that the earliest reference to citrus was documented during the reign of Ta Yu (around 2205 to 2197 BC) when citrus fruits, particularly mandarins and pummelos, were considered highly prized tributes and were only available for the imperial court (Webber, 1967; Nagy and Attaway, 1980). Lemon was originally grown in India while sweet oranges and mandarins are in China. Recent study suggests that, whereas some commercial species such as oranges, mandarins, and lemons originally came from Southeast Asia, the true origins of citrus fruit are Australia, New Caledonia (off eastern Australia), and New Guinea (Anitei, 2007). Regarding the commercial production of citrus as mentioned above, citrus becomes very important in the agriculture income and citrus industry has a big impact on the economy. The commercial production processing and global trade of citrus has significantly increased since then, placing citrus as the most important fruit in the world (UNCTAD, 2004; Ramana, et al., 1981). The citrus production takes place throughout the tropical and sub-tropical countries of the world.

The main groups of citrus production can be divided into four primary sections: sweet oranges, mandarins (also known as tangerines), grapefruit, and lemons and limes. Orange (*Citrus sinensis*) accounts for almost two thirds of the total citrus production (65%), then tangerine (*C. reticulata*) (21%), lemon (*C. limon*) (6%) and grapefruit (*C. paradisi*) (5.5%). Lime (*C. aurantifolia*), pummelo (*C. grandis*) and citron (*C. medica*) are considering as other significant commercially grown citrus species. Now citrus are grown all over the world in more than 140 countries, but most of the crop grows on either side of a belt around the equator covering tropical and subtropical areas of the world 35°N and 35°S latitudes with cultivation and production concentrated in major regions in the Northern Hemisphere (Ramana et al., 1981; UNCTAD 2004). Annual global production of citrus fruit has witnessed strong and rapid growth in the last several decades, from approximately 30 million metric tons in the late 1960s (FAO, 1967) to a total estimate of over 105 million metric tons between 2000 and 2004, then around 131 million tons on 2012 (FAO, 2012). Brazil is the largest citrus producing country and is the dominant producer of sweet oranges. China and the United States follow where China being the largest producer of mandarins, while the United States leads in grapefruit production. The European Union is also a major producer of sweet oranges, lemons, and mandarins. Mexico is the fifth largest orange producing country.

1.2. Citrus canker disease

Citrus canker disease is one of the most economically damaging diseases affecting citrus worldwide, and is subject to strictly enforced quarantine and eradication laws in many countries worldwide (Gottwald, 2002). Citrus canker is caused by a bacterium that belongs to the *Xanthomonas* genus. *Xanthomona*s (from the Greek *xanthos*,

meaning ‘yellow’, and *monas*, meaning ‘entity’) is a large genus of Gram negative, yellow-pigmented bacteria that are associated with plants. This genus resides at the base of the Gammaproteobacteria (Jun smiss et al., 2010), including 27 species (Figure 1.1) (Ryan et al., 2011). Xanthomonas species can cause serious diseases in ~400 plant hosts, including a wide variety of economically important crops, such as citrus, rice, tomato, cabbage, bean and pepper (Ryan et al., 2011). Individual species can comprise multiple pathovars. Pathogenic species and pathovars of the *Xanthomonas* genus exhibit a high degree of host specificity and many also have tissue specificity, invading either the xylem elements of the vascular system or the intercellular spaces of the mesophyll parenchyma tissue of the host.

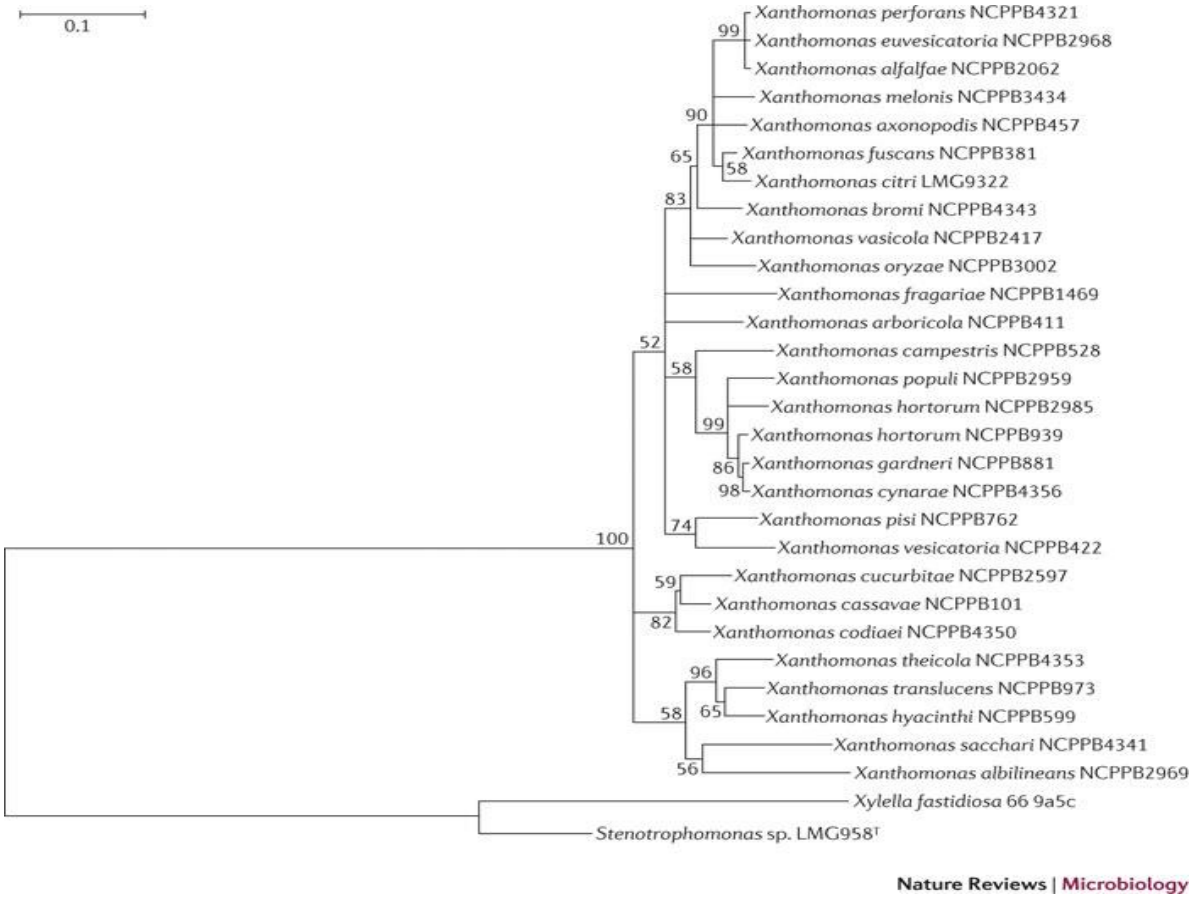

Figure 1.1. (Ryan et al., 2011) Phylogenetic analysis of bacteria within the genus *Xanthomonas* and the related genera *Xylella*, and *Stenotrophomonas*. This neighbour-joining tree is based on the DNA gyrase subunit B (*gyrB*) gene sequence of *Xanthomonas* spp., *Xylella fastidiosa* and a *Stenotrophomonas* sp. Bootstrap values (for 1,000 replicates) are given at the nodes, and branches with <50% bootstrap support were collapsed to better reveal the phylogenetic structure. The scale bar represents 0.1 changes per nucleotide position. In addition to *gyrB*, analysis of 16S–23S ribosomal RNA intergenic spacer sequences and a combination of molecular markers, such as repetitive element sequence-based PCR (rep-PCR), amplified fragment length polymorphism (AFLP) and other fingerprints, have been used to establish the taxonomic status of the genus. A species can contain pathovars, which are pathogenic variants that infect diverse plant hosts and/or exhibit different patterns of plant colonization. Up to 80 pathovars have been recognized so far (Ryan et al., 2011)

1.2.1. Diseases symptoms

All aboveground citrus tissues are susceptible to *X*. *axanopodis* pv. *citri* (*Xac*) infection under field conditions. Typical symptoms of citrus canker including the formation of circular, water soaked lesions become visible about 7 to 10 days after infection, and while they are initially circular in shape, they may become irregularly shaped later on. As the lesions age, they become tan or brown with water-soaked margins usually surrounded by a chlorotic or yellow halo, and they may be visible on the upper surface of the leaf. Eventually, the lesions become corky or spongy and the centers may become crater-like. In case of heavy infection occurs, citrus canker causes defoliation and premature fruit drop; an essential diagnostic symptom is citrus tissue hyperplasia. The most critical period for fruit rind infection is during the first 90 days after petal fall (Graham et al., 1992; Gabriel, 2001). The pathogen can infect almost all citrus varieties. In general, grapefruit, Mexican lime, and trifoliate orange are highly susceptible to all pathotypes of Citrus Canker (CC). Early oranges are moderately to highly susceptible; sour orange, lemons, and sweet orange are moderately susceptible; and mandarins are moderately resistant (Schubert et al., 2001).

1.2.2.The causal agent

Citrus canker disease is caused by two phylogenetically distinct groups of Xanthomonads (Gabriel, 2001). Each group contains subgroups that are differentiated primarily on the basis of host range (Table 1.1) (Ashma et al., 2003). The first phylogenetically distinct group is the Asiatic group, named *Xanthomonas citri* ex Hasse (Gabriel et al., 1989; synonyms: *X*. *campestris* pv. *citri* Dye pathotype A and *X*. *axonopodis* pv. *citri* Vauterin). The second phylogenetically distinct group is the

South American group, named *X*. *campestris* pv. *aurantifolii* Gabriel (Gabriel et al., 1989; syn = *X*. *campestris* pv. *citri* Dye and *X*. *axonopodis* pv. *aurantifolii* Vauterin). The Asiatic type of citrus canker (pathotype A), caused by the *X*. *axonopodis* pv. *citri* (*Xac*) strains that originated from Asia, is by far the most widespread and severe form of the disease with a host range on all citrus varieties. *Xac* is the bacterium that causes the disease most often referred to as 'citrus canker' (Stall and Civerolo, 1991). Cancrosis B or false canker (pathotype B) caused by the *X*. *axonopodis* pv. *aurantifolii* is a minor canker disease found on lemons in Argentina, Paraguay, and Uruguay. This pathotype has a limited host range on lemon, Mexican lime, sour orange and pummelo (Civerolo 1984). Cancrosis C (pathotype C) also caused by the *X*. *axonopodis* pv. *aurantifolii* has been found in Brazil and its host range is limited to Mexican lime (Schubert et al., 2001). Reason for this host range limitation of type B and C is unknown (Ashma et al., 2003). Another group of strains (A* pathotype) was isolated in southwest Asia in the 1990s. These strains constitute a subgroup of the A pathotype, *X*. *axonopodis* pv. *citri*, but their host range is limited to Key lime (Vernierie et al., 1998). An A^W Pathotype strain was also found in Florida with a host range limited to Mexican lime (Sun et al., 2000).

To identify and differentiate the pathotypes of *Xac* bacteria belonging to various pathotypes, a variety of methods can be used including physiological and biochemical assays (Verniere et al., 1991; Verniere et al., 1993), serological approaches (Civerolo and Fan, 1982; Alvarez et al., 1991), phage typing (Verniere et al., 1998), protein profiles (Vauterin et al., 1991), fatty acid analysis (Graham *et al*. 1990; Vauterin *et al*. 1991), DNA-DNA hybridization (Vauterin et al., 1991), restriction-fragment length polymorphism (Hartung and Civerolo, 1989; Graham et al., 1990), plasmid DNA fingerprints (Pruvost et al., 1992), and specific primer pairs (Hartung et al., 1993;

Cubero and Graham, 2002; Sun et al., 2004). Moreover, Southern hybridization with a *pth*A probe reveals distinct profiles among strains in pathotype A, pathotype B, pathotype C, and pathotype E (Swarup et al., 1992). And rep-PCR with BOX and ERIC primer pairs has been used to separate pathotypes of *Xac* or to differentiate strains in the same pathotype. The rep-PCR technique also allows evaluating the diversity of *Xac* in certain geographic areas of the world (Cubero and Graham, 2002).

Table 1.1. Relative pathogenicity of all known *X. citri* strain groups on four Citrus species (Brunings and Gabriel, 2003)

Canker Group	*C. sinensis* *(Sweet orange)*	*C. paradisi* (Grapefruit)	*C. limon* (Lemon)	*C. aurantifolii* (Mexican lime)
X. citri pv. *citri* A	+++	++++	+++	++++
X. citri pv. *citri* A*	−	−	−	++++
X. citri pv. *citri* A^W	−	HR	−	++++
X. citri pv. *aurantifolii* B	+	+	+++	++++
X. citri pv. *aurantifolii* C	HR	HR	HR	++++

+ Weak canker; ++++ strong canker; − no symptoms; HR, hypersensitive response.

1.2.3. Epidemiology and disease life cycle

A comprehensive report on the epidemiology of citrus canker disease can be referred to Gottwald et al. (2002). The pathogen is spread by rain splash and rains spread the diseases over short distances. The bacterium enters its hosts naturally by rain splash directly through natural opening, stomata and wounds; there is no evident epiphytic growth stage. Disease initiation by T3S requires tight attachment to host mesophyll cells, either by way of *hrp* pili (He, 1998) or by way of type IV pili. Tropical storms, hurricanes, and tornadoes can spread the bacteria for several miles. Windbreaks surrounding citrus plantings, especially when facing the prevailing wind direction, can limit the spread of citrus canker by wind (Gottwald et al., 2002a). The diseases

significantly increase in its incidence and severity in case of the presence of citrus leafminer, *Phyllocnistis citrella* Stainton (*Lepidoptera*: *Gracillariidae*), (Gottwald et al., 2002b). Although citrus leafminer does not vector of the pathogen, its feeding activity provides entry points for the bacterium (Belasque et al., 2005). The larvae mine the lower surface of newly emerging leaves or flush growth (Heppner, 1993). These leaves become the most susceptible to infection by canker. In addition, the environment inside the leaves that infected by leafminer is highly favorable for the development of the canker bacterium because the serpentine mines under the leaf cuticle caused by the larvae of the leafminer, provide ample wounding on new growth to greatly amplify citrus canker infection (Sohi and Sandhu, 1968 Sinha et al., 1972; Cook, 1988; Rodrigues, 1998).

Disease life cycle and the infection proces of the pathogen is illustrated in Figure 1.2. The bacterium multiplies in lesions in the infected area (leaves, stem and fruits). When there is free moisture on the lesions, the bacteria propagate at a high level and ooze out and can be dispersed to new growth and other plants. Rainwater collected from foliage with lesions contains bacterial cells between 10^5 to 10^8 cfu/ml (Goto, 1992; Stall, 1980). Multiplication of bacteria occurs mostly while the lesions are still expanding, and numbers of bacteria produced per lesion are also related to general host susceptibility. Wounds made by thorns, insects such as the Asian leaf miner, blowing sand, and pruning are also factors that can increase the spread of the pathogen (Timmer, 2000). Moreover, Studies of inoculum associated with water congestion after rain storm have demonstrated how as few as 1 to 2 bacterial cells forced through stomatal openings can lead to infection and lesion formation (Gottwald and Graham, 1992; Graham et al., 1992). The bacterium remains alive in the margins of the lesions in leaves and fruit until they fall and begin to decompose.

Bacteria also survive in lesions on woody branches up to a few years of age. Bacteria that ooze onto plant surfaces die upon exposure to drying. Death of bacteria is accelerated by exposure to direct sunlight. Exposed bacteria survive only a few days in soil and a few months in plant refuse that is incorporated into soil, but in case of infected tissues the bacteria can survive inside such tissues for years (Goto, 1992).

The *pthA* gene which is a member of *avrBs3*/*pthA* gene family is essential for *Xac* A to cause canker disease. It has been reported that *pthA* is required for the formation of canker on citrus. When *pthA* inserted into other Xanthomonads confers an ability to induce canker on citrus (Swarup et al., 1991). Moreover it was demonstrated that *pthA* is not only necessary for citrus canker disease but also it was sufficient to developed the diagnostic symptoms of citrus canker when it was expressed by itself inside host (citrus) cells (Duan et al., 1999). Furthermore, rapture of citrus epidermal and canker developing when *pthA* was delivered to the host by *Agrobacterium tumefaciens* and *E. coli*, respectively, but the symptoms were much reduced compare to *X.citri* control (Duan et a*l*., 1999; Kanamori and Tsuyumu, 1998). This function of *pthA* was limited to the citrus host. In transient expression assays of *pthA* in tobacco, bean, cotton and poplar, no canker symptom was observed, instead a rapid plant defence reaction known as hypersensitive response (HR) was observed (Duan et al., 1999). It is worth mentioning here that *pthA* is the first member of *avrBs3*/*pthA* gene family to be recognized as being necessary for pathogenicity on a host (Swarup et al., 1991). This is interesting because the function of pthA as an avirulent factor by trigger of HR when it was expressed in host plants other than citrus, indicating that R genes from those plants may provide useful transgenic resistance in citrus (Swarup et al., 1992)

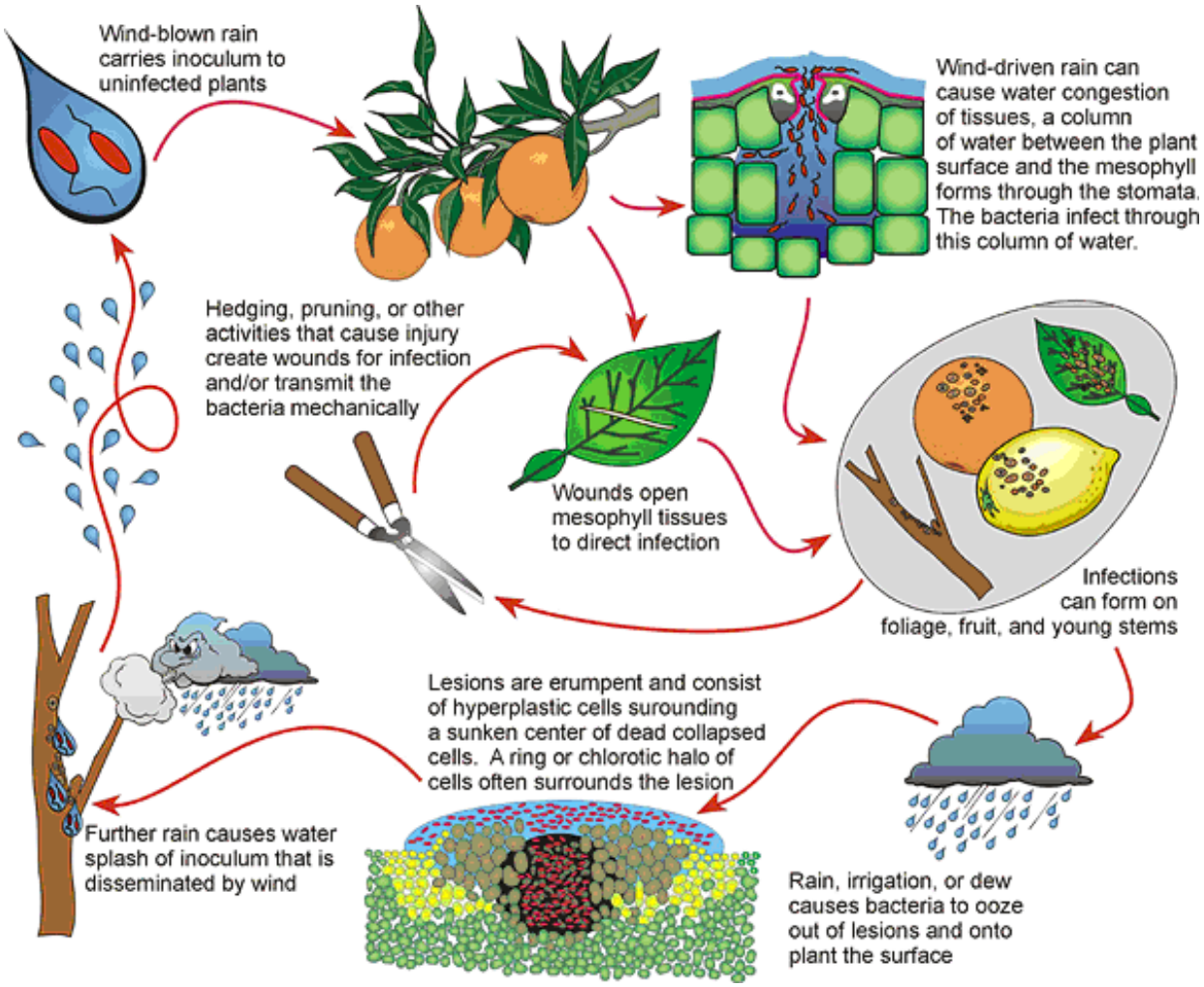

Figure 1.2. Citrus canker disease cycle (Gottwald, 2002)

1.2.4. Disease management

Quarantine measures to stop the introduction or establishment of the pathogen are applied in the countries, which are free of the diseases or where the disease has been eradicated. As a disease exclusion measure, they prohibit importation of plant materials from areas infected with canker (Gottwald et al., 2001). This is because historically, outbreaks of citrus canker in many countries occurred by introduction of the disease from other infected area. For example it was reported that the disease outbreaks in U.S., New Zealand, Australia and South Africa were originated in Asian countries. Once the disease was detected in any continuities, this is always met by carrying an eradication programs in which all infected and exposed citrus is destroyed (Gottwald et al., 2001). In case of newly-established outbreaks, eradication programs that started immediately were successful in eradication of citrus canker in some area including Mozambique, New Zealand, Australia, South Africa, the Fiji Islands and twice from the US, while failed in many other areas such as Argentina, Uruguay, Paraguay, and more recently in Florida (Rybak, 2005; Schubert, 2001; Stall and Civerolo, 1991).

Unfortunately, quarantine and eradication measurements have filled to provide complete control of citrus canker and although many citrus-producing countries appling strictly the quarantine programs by prohibit the importation of plant material from citrus canker-endemic areas, outbreaks continuously occur in new areas of these countries. Also as mentioned above in many cases, eradication efforts failed and have met with limited success in controlling the spread of the disease (Hogg, 1985; Koizumi, 1985; Schubert et al., 2001; Stall, 1987). Thus, new strategies are recently followed in regions where canker disease is endemic. This is by implementing integrated management programs which rely most heavily on the planting of resistant

varieties of citrus (Leite, and Mohan, 1990), production of disease-free nursery stock by locating nurseries outside of citrus canker areas and/or indoors (Leite and Mohan, 1990), restricting disease spread by establishing windbreaks and fences around groves, using preventative copper bactericides (Leite, and Mohan, 1990; Stein et al., 2005), and by controlling Asian leafminer. Cultural practices include windbreaks, and pruning or defoliation of diseased summer and autumn shoots, considering as important measures for the disease managment (Kuhara, 1978; Leite and Mohan, 1990; Stall and Seymour, 1983). Windbreaks alone or in combination with copper sprays may reduce disease incidence on leaves and fruits to non-detectable levels on field resistant cultivars (Kuhara, 1978). Pruning and defoliation of diseased shoots in combination with copper sprays as a complete control has also been effective for controlling canker. Pruning of the citrus trees is performed during the dry season, when the environmental conditions are less favorable for spread of the bacterium from pruned to adjacent non-infected trees. Moreover, fresh fruit for internal and export markets is subject to inspection protocols for freedom of citrus canker symptoms on fruit in orchards and sanitation treatments in the packinghouse (Leite, 2005).

Chemical Control. Copper based bactericides spray is a common method for controlling citric canker worldwide. These sprayers are used to protect the fruits from the infection and to reduce the inoculum on the new flushes. Environmental conditions, cultivars susceptibility and the implementation of other control methods are important factors that can affect positively or negatively the suppression of the disease by copper spray. Control of citrus canker with copper sprays may be achieved in the case of resistant or moderately resistant cultivars, whereas in the case of susceptible cultivars using copper spray alone for controlling the canker is not

effective (Koizumi, 1977; Kuhara, 1978; Leite, 1990, Leite et al., 1987; Stall, 1983). The timing and number of times of copper sprays for effective control is different from case to case. It depends on many factors including susceptibility of the citrus cultivar, the age of the citrus trees, environmental conditions, and the adoption of other control measures. In general, 3 to 5 times copper sprays are required for effective control of citrus canker on citrus cultivars with intermediate levels of resistance (Leite, 1990), whereas, in years with weather that is highly favorable for the pathogen and for epidemic development of citrus canker, up to 6 times sprays may be recommended (Leite, et al 1987). However, using copper compounds associates with many problems. The extended use of copper sprays in agriculture led to soil contamination, the emergence of copper tolerant phytobacterial strains ((Marco, and Stall , 1983)), which reduced the efficacy of copper bactericides. This is why we are in need of alternative control methods. These alternative methods may include the systemic acquired resistance (SAR) inducers, which have been used effectively against many of bacterial plant diseases (Ji, et al., 2004; Louws et al., 2001; Maxson-Stein et al., 2002), but have not been effective in controlling Asiatic Citrus Canker (ACC) (Graham and Leite, 2004). Another method is the developing a strategy of biological control agents, including antagonistic foliar bacteria, plant growth promoting bacteria, and bacteriophages. Bacteriophages have been successfully used for controlling many bacterial plant pathogens (Balogh, et al., 2003; Byrne, et al., 2005; Ji, 2006) and are also promising candidates for control of ACC (Balogh et al., 2008).

1.3. Bacteriophages

1.3.1. Brief history

Bacteriophages or phages are bacterial viruses that invade bacterial cell. The real discovery of bacteriophages was by Twort in 1915 and by d'Herelle in 1917, when independently they reported on filterable and transmissible agents of bacterial lysis (Summers, 2005). Although the early results of using bacteriophages as a control agent for bacterial pathogens were very promising, the discovery of broad-spectrum activity of antibiotics in the 1940s led to the decline of research controlling bacterial diseases with bacteriophages (Summer, 2001). However, during this period, phage therapy had been practiced mainly in human healthcare in some European countries (Slopek et al., 1987; Kutter et al., 2009)

Regarding agriculture field, phages were first found to be associated with plant pathogenic bacteria in 1924 when Mallmann and Hemstreet (1924) reported that the filtrate of decomposed cabbage inhibited the growth of *Xanthomonas campestris* pv. *campestris*. In 1926, Moore proposed that phages could be used as agents against bacterial pathogens. At the same time, Kotila and Coons, (1925) succeed to use bacteriophage to control the black leg disease of potato caused by *Erwina atroseptica*. Then, Tomas, (1935) could reduce the Stwart's wilt of corn caused by *Pantoea stewartii* by treat the seeds with phages. By 2005, the first phage-containing pesticide (AgriPhageTM) was registered with the U.S. Environmental Protection Agency (http://www.omnilytics.com/products/agriphage) (Balogh, 2010). Actually, there are many factors that reattract again the attention of the researches and reincrease the interest in bacteriophage therapy in biomedical and agriculture fields. These factors include, the appearance of multi resistant bacterial strains, as well as the lack of

discovering new and effective antibiotics fields (Slopek et al., 1987; Kutter et al., 2009; Jones et al., 2007). The emergence of such antibiotics resistance strains results in loss of control in many crop diseases, including bacterial spot of tomato and pepper and fire blight of apple and pear (Cooksy, 1990; Thayer and stall, 1961; Louws, 2001).

Other factors have contributed to a renew of interest in developing bacteriophage-based disease control methods in modern agriculture, such as the expanding knowledge based on successful phage applications in medicine (Kutter et al., 2009; Kutateladze et al., 2010; Sulakvelidze et al., 2001), the raise and widespread of copper resistant bacterial strains in the field (Marco and Stall, 1983), and increase of toxic levels in the environment due to the continual use of copper spray.

Therefore, it becomes favorable and urgent to replace chemical methods with more effective and environment friendly alternatives. Thus, the search for eco-friendly alternatives results in re-evaluation of phage therapy (Balogh et al., 2010).

Bacteriophages have been successfully used for controlling many plant bacterial pathogens including *Xanthomonas* spp. (bacterial spot of tomato, peach, geranium and citrus, onion-blight, walnut blight, and citrus canker) (Balogh, et al., 2008; civerolo, and Kiel, 1969; Sccardi, et al., 1993; Flaherty, 2000; McNeil et al., 2001; Flaherty, 2001), *Erwinia* spp. (fire blight, bacterial soft rot) (Svircev et al., 2005), *Streptomyces* (potato scab) (McKenna et al., 2001), *Pseudomonas* spp. (bacterial blotch of mushroom) (Munsch et al., 1995), and *Ralstonia* (bacterial wilt of tobacco) (Tanaka et al., 1990). And then, the first bacteriophage product was registered with U.S. Environmental Protection Agency in 2005 by OmniLytics Inc., Salt Lake City, UT (EPA Registration # 67986-1) and recently the bacteriophages are commercially

available in the United States for treatment of bacterial spot and bacterial speck of tomato and pepper (*Xanthomonas campestris* pv. *vesicatoroia* and *Pseudomonas syringae* pv. *tomato*) (Balogh et al., 2010).

As biological control agents targeting phytopathogens, phages have many advantages. First, phages are viruses that specifically infect bacteria. They have no direct negative effects on animals or plants. Second, infection of a bacterium by a virulent phage typically results in rapid viral replication, followed by the lysis of the bacterium and the release of numerous progeny phages, which can proceed to infect new bacterial cells. Therefore, the numbers of phage will expand when target pathogens are encountered and the therapy effects will essentially be amplified in response to the bacterial infection. Phages are natural entity and they have the potential to infect antibiotic or heavy metal resistant bacteria. Moreover, phages preparation, storage and application are easy and inexpensive compared with chemical methods (Greer, 2005). Furthermore, there is also interest in the use of phage in the detection of phytopathogens (Frampton et al., 2012).

1.3.2. Citrus canker and bacteriophages

There are several reports on bacteriophages found in association with citrus canker. In Japan, Wakimoto's phages Cp1 and Cp2 have been well known as two representative virulent phages, which specifically attack citrus canker bacteria. Of a total of 1256 isolates collected in wide range survey, only 17 (1.4 percent) were resistance to both Cp1 and Cp2 (Takushi, 1974). Goto found that both Cp1 and Cp2 had wide host ranges and more than 97% of Xac strains present in Japan were sensitive to one of these two phages (Goto, 1992). In Japan Wide range surveys for distribution patterns of *X*. *citri* strains, results obtained from the year 1968 through 1971 showed, a very

contrasting pattern in the distribution of *X*. *citri* strains. This can be noted in that a great majority of the isolates from Satsuma orange sources were Cp2-sensitive whereas from other varieties, both Cp1-sensitive and Cp2-sensitive strains appear in varying proportions depending upon the difference in localities or orchards (Takushi, 1974). In general, the Japanese *Xac* strains comprised two groups: the strains of the first one originated mostly from Unshu orange (*Citrus unshu*) and were sensitive to Cp2 only, whereas the members of the second group had a variety of hosts and were sensitive only to Cp1 (Balogh, 2006). These phages have been used for detection of the pathogen (Goto and Morita, 1971). Another *Xac* phage (Cp3), which was also isolated in Japan, had a tadpole shape with a spherical head and long tail (Goto et al., 1980.). Goto et al. (1980) found that strains of the B pathotype (*X*. *axonopodis* pv. *aurantifolii*) could be distinguished from type A strains (*Xac*) based on sensitivity to phage Cp3, with all B strains being sensitive to Cp3 and all A strains resistant to Cp1 and Cp2. Canker C strains were differentiated from canker A strains by their resistance to both Cp1 and Cp2 (Stall, and Civerolo, 1991).

Balogh et al. (2006) were able to isolate many *Xac* phages and evaluated their usability as a cocktail mixture for controlling citrus canker in greenhouse trials in Florida and in nursery trials in Argentina, where they found that bacteriophages reduced citrus canker disease severity both in greenhouse and field trials.

Phages CPl15 and CP122, which were isolated from canker lesions on grapefruit and Liucheng sweet orange, respectively, were found to be very specific with respect to lysis of test bacterial strains. When used jointly, they lysed 135 (97-8%) out of 138 *Xanthomonas eampestris* pv. *citri* Taiwanese *strains* isolated from the canker lesions on leaves, twigs, and fruits of various citrus species, cultivars, and hybrids. These

phages, however, did not lyse *Xanthomonas* strains that did not cause citrus canker, or any other bacteria tested isolated from soil, clinical or environmental samples. Thus, the authors concluded that CPl 15 and CP122 phages could be used also for specific detection of *Xac* in Taiwan (Wu et al., 1993).

There are also many filamentous phages were isolated for *Xac*. Dai te al, 1980 were able to isolate the first filamentous phage from *X*. *campestris* pv. *citri*. This phage was designated Cf. It showed a narrow host range forms and an unusually clear but tiny plaque of the host within 12 hours post infection. The infection with Cf neither killed nor drastically prevented host cells from propagation. But the rate of the host cell division was severely related. Another two phages XCf1 and XCf2 were isolated from a Japanese *X*. *campestris* pv *citri* isolates. These two phages were similar in particle of length (800-1100 nm). Both phages were heat resistant and they can tolerate temperature of 80^{o}C for 10 min, but they were sensitive to chloroform treatment. Serological inactivation tests indicate that both phages are closely related (Hiroshi et al., 1980).

Cf1t is another filamentous phage isolated from *Xac*. This phage also formed turbid plaques and its DNA was found to integrate into the host chromosome (Fann and Kuo, 1988; Kuo et al., 1987; Kuo, et al., 1991; Sheh et al., 1991). Moreover, a virulent form spontaneously arisen from a temperate phage Cf1t was designated Cf1tv (Kuoo et al., 1994).

Temperate phage PXC7 that was isolated from Japanese *Xac* strain XCJ18 produces small turbid plaques with irregular borders and is sensitive to chloroform (Wu, 1972). When *Xac* strain XCJ19 was lysogenized with PXC7, its colony morphology changed from smooth to dwarf and became resistant to phage Cp2 (Wu, 1972). Bacteriophages

were also found in citrus canker lesions in Argentina in 1979 (Balogh, 2006).

1.3.3. Considerations for using bacteriophages for plant disease control

In spite of the successful cases and the promising of using bacteriophages as biocontrol agents against many plant bacterial diseases, phage therapy is still associated with many problems, disadvantages and challenges that have been raised (Jones et al., 2013). These include the narrow host range and high specificity (Greer, 2005), which put phages at a disadvantage against other anti bacterial material such as antibiotics. Also the requirement of certain number of the pathogen (10^4-10^6 cfu/ml) may limit the phage activity. Furthermore the emergency of resistance mutant is a practical problem, which significantly limits the use of bacteriophages as abiocotrol agent (Okabe and Goto, 1963). Other major affecting factors maybe the environmental effects such as temperature, pH, physiology of bacterium and the inactivation by UV light (Jones, 2013). These environmental factors have great negative impact on the ability of phage to infect the target pathogen as well as on the persistence of phages in the phyllosphere and rizosphere. Moreover one concern maybe phage mediated transducing undesirable characteristics into host cells, such as virulence factors (Vidaver, 1976). In addition, the consumer perception of adding phages to the food products could be also a reason of limiting the utilization of phage as a biocontrol agent. Lastly, it has been reported that in some cases the phages have negative side effects in agriculture due to inhibition of beneficial bacteria such as the reduction in symbiotic nitrogen fixing bacterial growth and nitrogen content of cowpea (Ahamd and Morgan, 1994)

For all above reasons and many others, the use of bacteriophages as an effective biocontrol strategy that can replace the using of antibiotics and chemical methods still faces significant challenges. So a number of factors should be taken into our

consideration regarding the use of phages as abiocontrol agent in agriculture (Jones, 2012). Thus, there are many strategies that developed to maximize the effectiveness of phages and to come over the above mentioned factors, including the application strategy, the proper assay for phage selection, and the using of phages as a part of integrated management strategy.

Application strategy is an important factor that may decrease or increase the phage affectivity. For foliar pathogen, the phyllosphere is always associated with a harsh condition including the high UV and visible light irradiation and desiccation. These limit the phage survival and cause a rapid degradation for phages when applied to aerial parts (Gill and Abdon, 2003; Iriarte et al, 2007; Balogh et al, 2002; Balogh et al, 2003; Civerolo and Keil, 1969; McNeil et al, 2001). It was also noted that the isolation of phages from aerial plant tissue was pretty hard (Flaherty, 2001; Gill, 2003; Okabe et al, 1963). Gill and Abedon (2003) suggested that phage can live longer and easily isolated from soil than from leaves and this is why phage therapy might be meet with a greater success in rhizosphere. The low level of moisture on the phyllosphere condition can be another important factor that may cause negative impact on phages activity (Johnson, 1994). Therefore, many researches showed that the timing of phage application is an essential factor to extend the persistence of phages on aerial condition and subsequently to encourage the biocontrol. Significant reduction of peach bacterial spot with phage treatment was achieved only when the treatments was applied one hour or one day before inoculation with the pathogen. There was no significant reduction in the pathogen population when the phages were applied one hour or one day after inoculation (Civerolo and Keil, 1969). In the case of *Erwinia amyloovara*, the phage treatment was successful to reduce the fire blight on apple blossoms when the phage mixture was applied at the same time as the

pathogen. On other hand, there was no significant affect when the phages applied one day before the inoculation (Schnabel et al., 1999). On cabbage the most effective treatment with phages bringing a significant reduction of black rot of cabbage disease caused by *Xanthomonas campestris* pv *campestris* and bacterial spot of paper, caused by *X*. *campestreis* pv *vesicatoria* was occurred when phages were applied at the day of inoculation (Bargamin, 1981).

Furthermore the time of the day when phages are applied is also of great importance, that may affect positively or negatively the activity of the phages. This is because the sunlight irradiation is the most detrimental factor that causes reduction of the phage persistence on the canopy. Therefore phages should be applied to avoid exposeing to direct sunlight in order to inccrease their lifetime and activity. This was demonstrated by Balogh et al. (2003) when they achieved more significant reduction of the tomato bacterial spot by applying the phage treatments in the early evening compared with the morning application. Also it is highly recommended to apply the phages when enough moisture is available on the leaves, because the phages can only interact with the host in the presence of free moisture on the leaf (Jones, 2012).

Another strategy to increase the phage persistence is to use formulated phages. In order to reduce the dramatic inactivation of phages on leaf surfaces after application, some formulations (protectors) have been developed. It was reported that when skim milk was added to phage suspension, the phage persistence on the leaf surface was improved (Balogh et al, 2003; Iriarte et al., 2007). Although, the treatment of phage with skim milk resulted in the improvement of phage activity, causing more reduction in the diseases and increases in the yield (Obradovic et al., 2004; Obradovic et al., 2005), Balogh et al. (2008) found that there was no reduction in the citrus canker

disease severity in case of applying phages in combination with skim milk. Thus it is obvious that more effective formulations are required to improve the phage therapy.

Another approach that can be used for improving the persistence of the phages is by applying the phage where phage-sensitive bacterial host is present. This will give the phage an advantage to multiply and persist at higher levels than on surface without host (Balogh, 2006). Tanaka et al. (1990) demonstrated this to reduce the tobacco wilt disease, when they used an avirulant strain of *Ralstonia solanacearum* as a host for phage that can infect both the virulent and avirulent strains. This combination of the phage and the avirulent strain significantly improved disease control over using the avirulant strain alone. Similar strategy was reported by Svirecv et al. (2005) for controlling fire blight of pear, by selecting phages based on the ability to lyse both the traget pathogen *Erwinia amylovora* and an antagonistic phyllosphere bacterium, *Pantoea agglomerans*. Even *P. agglomerans* itself is a biological control agent for *E. amylovora*, the result showed that when it served as a phage carrier and also as a propagator of phage on the inoculation sites, the control of the disease was significantly improved. Another strategy that can be use to improve the phage persistence is to develop an attenuated strain of bacterial pathogen that can also serve as phage propagator on the canopy. This method resulted in increasing the period of phage persistence in greenhouse studies. This was demonstrated by Iriarte et al. (2012) when they succeeded to significantly improve the phage persistence on tomato leaves by adding an attenuated strain of *X. perforans* with a disrupted *OpgH* gene.

1.3.4. Phage classification

Phages are classified on the basis of their nucleic acid type and on morphology. Based on the nucleic acid type, phages include viruses with double stranded DNA (dsDNA;

the vast majority), single-stranded DNA (ssDNA), double-stranded RNA (dsRNA; very rare), and single stranded RNA (ssRNA).

Based on morphology, there are tailed phages, which exhibited approximately 96 % of phages and CFP (cubic, filamentous or pleomorphic), which represent approximately 4% of examined phages (Ackermann, 2007). The tailed phages are varied in size and structure. Tails are helical and generally provided with fixation structures (baseplates, spikes, and fibers). There is no envelope and particles adsorb to their hosts and infect them from the outside. These phages contain linear, double stranded DNA and have icosahedral or elongated heads. The progeny phages are assembled via complex pathways; with phage DNA entering preformed capsids. Tailed phages are belonging to the order *Caudovirales*. This order has three families, the *Myoviridae* with a neck, a contractile tail, and a central tube. This family includes phages that tend to be larger than phages of other groups. The second family is the *Siphoviridae*. Phages belong to this family are characterized by their long non-contractile tails, flexible or rigid tubes. Siphoviruses are the most numerous of tailed phages. The third family is the *Podoviridae* in which the phages have non-contractile short tails.

The second type of phages based on the morphology is the cubic phages. “Cubic” denotes cubic symmetry and icosahedral shape. Phages within this group are belong to many families including *Micorviridae* where the virions contain ssDNA as the genome and with no envelope, very small and provided with 12 knob like capsomers, *Corticoviridae* with dsDNA genome, the virons have a multilayered, lipid-containing capsid and circular DNA, *Teciviridae* with dsDNA genome, *Leviviridae* with ssRNA, and *Cystoviridae* in which the phages are dsRNA.

The third groups are the filamentous phages. This group includes the phages, which are belonging to the *Inoviridae*, *Lipothrixviridae*, and *Rudivirdae* families. Genomes of inoviridae are ssDNA. Particles are excreted from infected cells without killing the host. In many cases, the DNA of these phages can be integrated into the host genome. Those phages were found infecting *Pseudomonas*, *Vibrio*, *Xanthomonas*, and other genera. In the case of *Lipothrixviridae*, the particles are long rods with lipoprotein envelope. *Rudivirade* including filamentous phages that have straight rods shape without envelopes.

The last morphology group is the pleomorphic phages, which include phages belonging to *Plasmaviridae*, *Fuselloviridae*, *Salteprovirus*, *Guttaviridae*, *Ampullaviridae*, *Bicaudaviridae* and *Globuloviridae* families. All are with dsDNA.

Table 1.2. Overview of bacteriophage families (Akermann, 2007)

Shape	Order or family	Nucleic acid, particulars, size	Member	Number
	Caudovirales	dsDNA (L), no envelope		
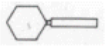	*Myoviridae*	Tail contractile	T4	1312
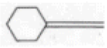	*Siphoviridae*	Tail long, noncontractile	λ	3262
	*Podoviridae*	Tail short	T7	771
	*Microviridae*	ssDNA (C), 27 nm, 12 knoblike capsomers	ϕX174	38
	*Corticoviridae*	dsDNA (C), complex capsid, lipids, 63 nm	PM2	3?
	*Tectiviridae*	dsDNA (L), inner lipid vesicle, pseudo-tail, 60 nm	PRD1	19
	*Leviviridae*	ssRNA (L), 23 nm, like poliovirus	MS2	38
	*Cystoviridae*	dsRNA (L), segmented, lipidic envelope, 70–80 nm	ϕ6	3
	*Inoviridae*	ssDNA (C), filaments or rods, 85–1950 x 7 nm	fd	66
	*Plasmaviridae*	dsDNA (C), lipidic envelope, no capsid, 80 nm	MVL2	5

From: Ackermann, 2007. C, circular. L, linear

1.4. The scope of this study

Asiatic citrus canker (ACC), which is caused by the phytopathogenic bacterium *Xanthomonas axonopodis* pv. *citri*, is one of the biggest problems in citrus production worldwide. Given the difficulties in controlling this disease using conventional methods, considerable efforts have been made to find alternative strategies. Recently, biological controlling agents, especially bacteriophages, have been successfully used in several plant diseases (Yamada, 2009) and are also promising candidates for control of ACC. However there are many challenges that are limiting the success of bacteriophages as biological control agent. Thus, there have been many efforts to solve these problems and find the best condition that can maximize the benefit from phages for controlling bacterial diseases.

Molecular characterizations and studies of the biology and ecology of phages are very important aspects to understand the phage-host interaction and to figure out the most important characteristics of bacteriophages to be used as biological control agents. The first subject of this study was to make a full characterization of the historical *Xanthomonas* Cp1 and Cp2 phages. These molecular studies would help in providing an explanation for the molecular mechanism of host selection by these phages. Such molecular studies will be very useful for understanding the nature of these phages and their interaction with the host cell, which may improve their usage as biocontrol agents against citrus canker disease as well as a detection and classification tools for the bacterial strains.

My second goal was to find a better solution that may contribute to solving the major challenge associated with the use of phages, mainly instability of phages during treatment of field crop plants. In many reports, this was managed by getting detailed information about the phage nature and by using different application and conditions.

In this study, I could isolate and characterize a novel filamentous phage designated XacF1 which can infect *X*. *axonopodis* pv. *citri* (*Xac*). This phage was shown to have a great impact on the virulence reduction in the infected cells. The infection by XacF1 caused loss of virulence in *X*. *axonopodis* pv. *citri*. This would be a promising method of phage therapy to solve the problem of phage instability because in contrast to lytic phages, filamentous phages do not kill the host cell but establish a persistent association between the host and phage.

Chapter 2

Characterization of bacteriophages Cp1 and Cp2, the strain-typing agents for *Xanthomonas axonopodis* pv. *citri*

2.1. Abstarct

The strains of *Xanthomonas axonopodis* pv. *citri*, the causative agent of citrus canker, are historically classified based on bacteriophage (phage) sensitivity. Nearly all *X. axonopodis* pv. *citri* strains isolated from different regions in Japan are lysed by either of phage Cp1 or Cp2; Cp1-sensitive ($Cp1^S$) strains have been observed to be resistant to Cp2 ($Cp2^R$) and *vice versa*. In this study, genomic and molecular characterization was performed for the typing agents Cp1 and Cp2. Morphologically, Cp1 belongs to the *Siphoviridae*. Genomic analysis revealed that its genome comprises 43,870-bp dsDNA, with 10-bp 3'-extruding cohesive ends, and contains 48 open reading frames. The genomic organization was similar to that of *Xanthomonas* phage phiL7, but it lacked a group-I intron in the DNA polymerase gene. Cp2 resembles morphologically *Escherichia coli* T7-like phages of *Podoviridae*. The 42,963-bp linear dsDNA genome of Cp2 contained terminal repeats. The Cp2 genomic sequence has 40 open reading frames, many of which did not show detectable homologs in the current databases. By proteomic analysis, a gene cluster encoding structural proteins corresponding to the Class III module of T7-like phages was identified on the Cp2 genome. Therefore, Cp1 and Cp2 were found to belong to completely different virus groups. In addition, we found that Cp1 and Cp2 use different molecules on the host cell surface as phage receptors and that host-selection of *X. axonopodis* pv. *citri* strains by Cp1 and Cp2 is not determined at the initial stage by binding to receptors.

2.2. Introduction

Citrus canker, caused by *Xanthomonas axonopodis* pv. *citri* (syn, *Xanthomonas campestris* pv. *citri* or *Xanthomonas citri*), is a widespread disease in citrus-producing areas of the tropical and subtropical world (Civerelo, 1984; Gottwald et al., 2002). Different types of citrus canker, corresponding to different pathotypes of *X. axonopodis* pv. *citri*, have been reported (Stall and Civerolo, 1991). The Asiatic type, caused by *X. axonopodis* pv. *citri* pathotype A, is the most widespread and the most economically important citrus canker. The host range of pathotype A strains is wider than that of the other pathotypes, including most citrus varieties (Stall and Civerolo, 1991). *X. axonopodis* pv. *citri* pathotype A strains are separated into two groups based on their sensitivity to phages Cp1 and Cp2 (Wakimoto, 1967; Obata, 1974). Phage typing with Cp1 and Cp2 was first demonstrated by Wakimoto, 1967. Wakimoto found that nearly all strains isolated from different regions in Japan were lysed by either Cp1 or Cp2, and that Cp1-sensitive ($Cp1^S$) strains were resistant to Cp2 ($Cp2^R$) and *vice versa*. Cp1 and Cp2 phages were morphologically different: Cp1 showed a head-tail structure, whereas Cp2 consisted of a polyhedral head without tail (Wakimoto, 1967). In a larger survey, Obata found that $Cp1^R/Cp2^S$ strains predominated in major citrus-producing regions in Japan, with the exception of Hiroshima Prefecture where $Cp1^S/Cp2^R$ strains predominated (Obata, 1974). Two different strain types can occur in a mixture on the same single leaf of a tree, but one single lesion usually consists of a single strain.

Notably, the sensitivity of *X. axonopodis* pv. *citri* strains to Cp1 and Cp2 is associated with differences in their physiological features and canker aggressiveness. *X. axonopodis* pv. *citri* strains of $Cp1^S/Cp2^R$ can assimilate mannitol, while $Cp1^R/Cp2^S$ strains cannot (Goto et al., 1980). All strains of $Cp1^R/Cp2^S$ are canker

aggressive to citrus variety "Otachibana", whereas all the strains of $Cp1^S/Cp2^R$ are weakly aggressive (Shiotani et al., 2000). The $Cp1^R/Cp2^S$ strains generate a 1.8 kbp specific fragment by rep-PCR (Louws et al., 1994) using Enterobacterial repetitive intergenic consensus (ERIC) primers. The 1.8 kbp band corresponds to a region encompassing XAC1661 (Isxac3 transposase) and XAC1662 (*repA*) within an insertion element in the genomic sequence of *X*. *axonopodis* pv. *citri* strain 306 (Shiotani, 2007). Most strains of $Cp1^S/Cp2^R$ contain *hssB3.0*, a member of the *avrBs3*/*pthA* (avirulence and pathogenicity) gene family (Swarup et al., 1992; Szurek et al., 2002), which is responsible for the suppression of virulence on a *Citrus grandis* cultivar; however, $Cp1^R/Cp2^S$ strains lack this gene (Shiotani et al., 2007). These results suggest some relatedness between Cp1/Cp2 sensitivity and the virulence and pathogenic features of *X*. *axonopodis* pv. *citri* strains.

In contrast to the large contribution toward characterization of host strains, very little information is available about the nature or identity of phages Cp1 and Cp2. Concerning Cp1 and Cp2, the following issues are of particular interest: (i) the virological identification and phylogenetic relationships of these phages, (ii) the origin of the above-mentioned 1.8 kbp sequence on the host genome and its possible association with a phage sequence, (iii) *hssB3.0* and its possible association with a phage sequence, and (iv) the molecular mechanism of host selection by these phages. As a first step toward exploring these issues, the present study performed genomic and molecular characterization of Cp1 and Cp2.

2.3. Materials and methods

2.3.1. Bacterial strains and phages.

MAFF (Ministry of Agriculture, Forestry and Fisheries) strains of *X*. *axonopodis* pv. *citri* were obtained from the National Institute of Agrobiological Sciences, Japan.

Strain KC33 (Shiotani et al., 2000) was obtained from National Institute of Fruit Tree Science, National Agriculture and Food Research Organization, Japan. Their origins and sensitivity to Cp1 and Cp2 are listed in Table 1. Bacteriophages Cp1 and Cp2 (Wakimoto, 1967; Obata, 1974) were obtained from the Yokohama Plant Protection Station, Japan. Strains MAFF 301080 and MAFF 673010 were used as hosts for routine propagation of Cp1 and Cp2, respectively. Bacterial cells were cultured in nutrient broth (NB) medium (BBL, Becton Dickinson and Co., Cockeysville, MD, USA) at 28°C with shaking at 200-300 rpm. An overnight culture of bacterial cells grown in NB was diluted 100-fold with 100 ml fresh NB in a 500 ml flask. To collect sufficient phage particles, 1 L of bacterial culture (10 × 100 ml cultures) was grown. When the cultures reached 0.2 units of OD_{600}, the phage was added at a multiplicity of infection (moi) of 0.1. After further growth for 9-18 h, the cells were removed by centrifugation with a R12A2 rotor in a Hitachi himac CR21E centrifuge (Hitachi Koki Co. Ltd., Tokyo, Japan), at 8,000 × g for 15 min at 4°C. The supernatant was passed through a 0.45 μm membrane filter and phage particles were precipitated by centrifugation with a P28S rotor in a Hitachi XII100□ centrifuge at 40,000 × g for 1 h at 4°C and dissolved in SM buffer (50 mM Tris-HCl at pH 7.5, 100 mM NaCl, 10 mM $MgSO_4$, and 0.01% gelatin). Purified phages were stored at 4°C until use. Bacteriophage particles purified by CsCl-gradient ultracentrifugation (with a P28S rotor in a Hitachi XII100□□ultracentrifuge) (Kawasaki et al., 2009) were stained with Na-phosphotungstate before observation in a Hitachi H600A electron microscope, according to the method of Dykstra, 1994. λ phage particles were used as an internal standard marker for size determination. For host range determination, standard plaque-forming assays (Sambrook and Russell, 2001) or lysis zone formation spot tests (Yamada et al., 2007) were performed.

Table 2.1 Bacterial strains and Bacteriophages used in this study

Strain	Host (citrus)	Phage type [b]	Source
Xanthomonas axonopodis pv. *citri*			
MAFF 301077	*C. limeon*	$Cp1^S/Cp2^R$	NIAS[C]
MAFF 301080	*C. sinensis*	$Cp1^S/Cp2^R$	NIAS
301080 R1		$Cp1^R/Cp2^R$	This study
MAFF 311130	*C. iyo*	$Cp1^R/Cp2^R$	NIAS
MAFF 302102	C. sp	$Cp1^R/Cp2^S$	NIAS
MAFF 673001	*C. atsudaidai*	$Cp1^R/Cp2^S$	NIAS
MAFF 673010	C. sp	$Cp1^R/Cp2^S$	NIAS
673010 R2		$Cp1^R/Cp2^R$	This study
MAFF 673011	*C. limeon*	$Cp1^S/Cp2^R$	NIAS
MAFF 673013	C. sp	CP_1^S/CP_2^R	NIAS
MAFF 673018	C. sp	$Cp1^R/Cp2^S$	NIAS
MAFF 673021	*C. limeon*	$Cp1^R/Cp2^S$	NIAS
KC33	*C. iyo*	$Cp1^S/Cp2^S$	Shiotani et al. (10)
Xanthomonas axonopodis pv. *citri phages*			
Cp1			Wakimoto (5)
Cp2			Wakimoto (5)

[a] All strains originated in Japan.

[b] Sensitivity to phages CP_1 and CP_2 ; S= sensitive, R= resistance.

[c] National Institute of Aerobiological Sciences, Japan.

2.3.2. Single-step growth experiment

Single-step growth experiments were performed as previously described (Hung et al., 2003; Calrson et al., 1994), with some modifications. Strains MAFF 301080 and MAFF 673010 were used as hosts for Cp1 and Cp2, respectively. Cells (0.1 U of OD_{600}) were harvested by centrifugation and resuspended in fresh NB (ca. 1×10^8 CFU/ml) to a final culture volume of 10 ml. Phage was added at an m.o.i of 1.0 and

allowed to adsorb for 10 min at 28°C. After centrifugation and resuspending in the initial volume of NB with decimal dilution to a final volume of 10 ml, the cells were incubated at 28˚C, the cells were incubated at 28°C. Samples were taken at intervals (every 10 min up to 3.5 h for Cp1 and every 30 min up to 5 h for Cp2) and the titers were determined by the double-layered agar plate method.

2.3.3. Phage adsorption test

Phage adsorption was assayed as follows: when fresh bacterial cultures (10 ml) reached 0.1 units of OD_{600}, the phage (10 µl) was added at an m.o.i of 0.1. After incubation for 10 min at 28°C, the cells were removed by centrifugation with a R12A2 rotor in a Hitachi himac CR21E centrifuge at 8,000 × g for 10 min at 4°C. The supernatant was subjected to a plaque assay, where strains MAFF 301080 and MAFF 673010 were used as a host for Cp1 and Cp2, respectively. *Escherichia coli* JM109 was used as a negative control in phage adsorption.

2.3.4. DNA manipulation and sequencing

Standard molecular biological techniques for DNA isolation, digestion with restriction enzymes and other nucleases, and construction of recombinant DNAs were followed, according to Sambrook and Russell, 2001. Phage DNA was isolated from the purified phage particles by phenol extraction. For genome size determination, the purified phage particles were embedded in 0.7% low-melting-point agarose (InCert agarose, FMC Corp, Philadelphia, PA, USA) and after treatment with proteinase K (1 mg/ml, Merck Ltd., Tokyo, Japan) and 1% Sarkosyl, subjected to pulsed-field gel electrophoresis in a CHEF MAPPER electrophoresis apparatus (Bio-Rad Lab., Hercules, CA, USA) according to the method of Higashiyama and Yamada, 1991. Shotgun sequencing was performed at Hokkaido System Science Co., Ltd. (Sapporo, Japan) using a Roche GS Junior Sequence System. The draft assembly of the obtained

sequences was assembled using GS De novo Assembler v2.6. The analyzed sequences corresponded to 94 and 40 times the final genome sizes of Cp1 (43,860 bp) and Cp2 (42,963 bp), respectively. Potential open reading frames (ORFs) larger than 150 bp (50 codons) were identified using Glimmer (Delcher et al., 1999) and GeneMark. Homology searches were performed using BLAST/RPS-BLAST (Altschul et al, 1997) against the UniProt sequence database (Uniprot, 2007) and the NCBI/CDD database (Wheeler et al., 2007), using an E-value lower than e^{-4} as a cutoff for notable similarity. Multiple-sequence alignments were generated using the DNASIS program (version 3.6; Hitachi Software Engineering, Co., Ltd., Tokyo, Japan). For phylogenetic analysis of RNA polymerase (RNAP) proteins, the unrooted dendrogram was constructed with the Treeview tool using the maximum likelihood method based on a complete protein sequence alignment of RNAP proteins from other phages using ClustalX. The Cp1 cohesive ends (*cos*) sequence was determined as follows. A 6.8 kbp *Pst*I fragment of Cp1 DNA was dissociated into two fragments (4.3 and 2.5 kbp) after heating at 70°C for 15 min. The dissociated bands were recovered from the agarose gel and treated with T4 DNA polymerase to form blunt ends. The nucleotide sequence of these bands was determined. By comparing the nucleotide sequences with each other and with the Cp1 genomic sequence, the *cos* sequence was determined according to Fujiwara et al. (2011).

2.3.5. Southern and dot blot hybridization

Genomic DNA from bacterial cells was prepared by a mini-preparation method, according to Ausubel et al. (1995). After digestion with various restriction enzymes (*Eco*RI, *Eco*RV, *Hin*dIII, and *Hin*cII), DNA fragments were separated by agarose gel electrophoresis, blotted onto a nylon membrane (Biodyne, Pall Gelman Laboratory, Closter, NJ, USA), hybridized with probes (the entire Cp1 DNA by combining all the

*Hinc*II fragments and the entire Cp2 DNA with all the *Hinc*II fragments), labeled with fluorescein (Gene Images Random Prime labeling kit; Amersham Biosciences, Uppsala, Sweden) and detected with a Gene Images CDP-Star detection module (Amersham Biosciences). Hybridization was performed in buffer containing 5 × SSC, 0.1% SDS, 5% liquid block and 5% dextran sulfate for 16 h at 65°C. The filter was washed at 60°C in 1 × SSC and 0.1% sodium dodecylsulfate (SDS) for 15 min, and then in 0.5% SSC and 0.1% SDS for 15 min with agitation, according to the manufacturer's protocol. The hybridization signals were detected by exposing the filter onto an X-ray film (RX-U, Fuji Film, Tokyo, Japan).

2.3.6. SDS-polyacrylamide gel electrophoresis (SDS-PAGE) and LC-MS/MS analysis

Purified phage particles were subjected to SDS-PAGE (10-12 % (wt/vol) polyacrylamide) according to Laemmli (1970). Protein bands were visualized by staining the gel with Coomassie brilliant blue, excised from the gel, digested with trypsin and subjected to liquid chromatography-tandem mass spectrometry (LC-MS/MS) (LTQ Orbitrap XL, Thermo Fisher Scientific, Osaka, Japan) analysis at the Natural Science Center for Basic Research and Development, Hiroshima University.

2.3.7. Staining of bacterial cells by SYBR Gold-labeled phages

Phage labeling and observation of phage treated bacterial cells were performed according to Mosier-Boss et al. (2003). To 100 ml of the phage lysate, 10 µl of 10^4 × SYBR Gold (Molecular Probes, Inc., Eugene, OR, USA) in DMSO was added. After 10 min, the labeled phage particles were precipitated by centrifugation with a P28S rotor in a Hitachi XII100□ centrifuge at 40,000 × g for 1 h at 4°C. Three washes using 1 × PBS were done to ensure the removal of excess SYBR Gold. A 1 ml sample of an overnight culture of *X*. *axonopodis* pv. *citri* was mixed with 4 ml NB and

allowed to grow until an OD_{600} of 0.5 was reached. A 10µl sample of the bacterial culture was added with 10 µl SYBR Gold-labeled phage and incubated for 10 to 60 min. As a control, a culture of *E. coli* JM109 was treated in the same way. After fixation with 30 µl 4% paraformaldehyde in PBS, the mixture was added with 5 ml ddH_2O and filtered through a membrane filter (0.2 µm pore size, Steradisc, Krabo, Osaka, Japan). The bacterial cells were observed under a fluorescence microscope system with filter sets (Olympus BH2 fluorescence microscope; Olympus, Tokyo, Japan). Microscopic images were recorded with a CCD camera (Kyence VB-6010; Osaka, Japan).

2.3.8. Nucleotide sequence accession number

The sequence data for the Cp1 and Cp2 genomes have been deposited in the DDBJ database under accession nos. AB720063 and AB720064, respectively.

2.4. Results and discussion

2.4.1. Cp1 and Cp2 belong to different virus families

Morphology indicates that Phages Cp1 and Cp2 belong to different virus families: Cp1 as a member of *Siphoviridae* and Cp2 as a member of *Podoviridae*. The purified particles of Cp1 and Cp2 were negatively stained and examined by transmission electron microscopy. Cp1 particles had an icosahedral capsid of 60 ± 5 nm in diameter with a long noncontractile tail of 135 ± 10 nm long by 12 ± 2 nm wide (Figure 2.1). This morphology was almost the same (though in smaller dimensions) as that reported preliminarily for CP1 particles replicated in strain N6101 as a host (Arai et al., 1974), indicating that, morphologically, Cp1 belongs to the family *Siphoviridae*. By contrast, Cp2 particles showed an icosahedral capsid of 60 ± 5 nm in diameter with a short tail of 15 ± 5 nm long (Figure 2.1), indicating that Cp2 has a

typical structure of the family *Podoviridae*. In a preliminary work, this phage was reported to have larger polyhedral particles without a tail (Arai et al., 1974). These results raised the question of whether Cp1 and Cp2 are related to each other in infection and replication in host strains.

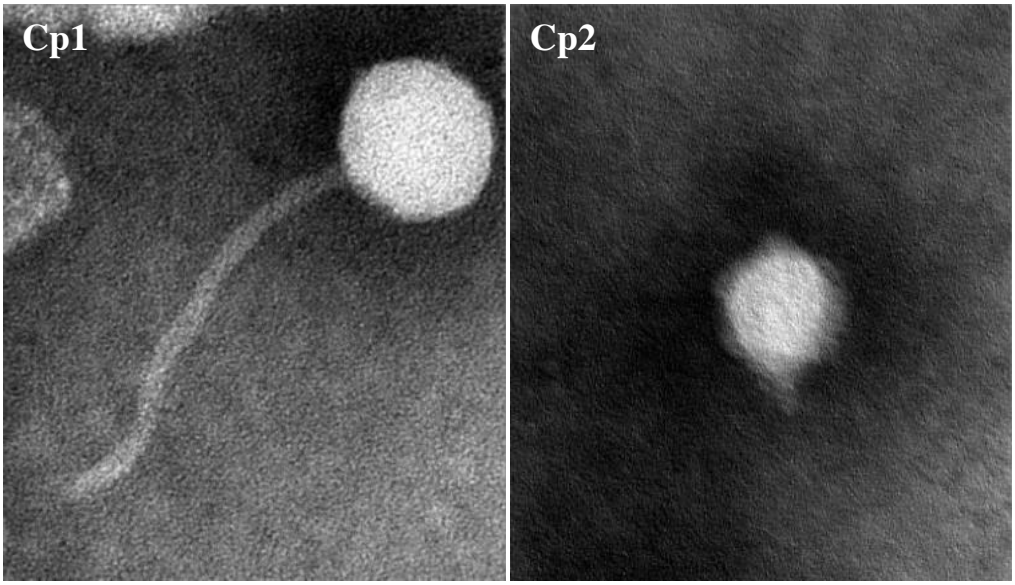

Figure 2.1. Morphology of Cp1 and Cp2 particles. The purified particles of Cp1 and Cp2 were negatively stained and examined by transmission electron microscopy. Cp1 particles had an icosahedral capsid of 60 ± 5 nm in diameter with a long non-contractile tail of 135 ± 10 nm long by 12 ± 2 nm wide (n=20). Cp2 particles showed an icosahedral capsid of 60 ± 5 nm in diameter with a short tail of 15 ± 5 nm long (n = 20).

2.4.2. Comparison of infection cycle of Cp1 and Cp2

Both Cp1 and Cp2 form clear plaques with various *X*. *axonopodis* pv. *citri* strains including those shown in Table 2.1 as hosts (Wakimoto, 1967; Obata, 1974). The infection cycle of each phage was characterized by a single-step growth experiment with appropriate hosts. The growth curves are compared in Figure 2.2 In the case of Cp1 replication, the latent period was ~ 60 min, followed by a rise period of 20-30 min, giving an entire cycle of 80-90 min. The average burst size was 20 plaque-forming unit (PFU) per infected cell. For Cp2 replication, the latent period was ~90 min, with a 60-min raise period, taking 150-180 min for a single growth cycle. The burst size was approximately 100 PFU/cell. These results showed that Cp1 infected and replicated more rapidly than Cp2, but the burst size was much smaller than Cp2. These results contrasted with the observation that more than 600 progeny phages were formed in an infected bacterial cell for both Cp1 and Cp2, as detected by electron microscopy (Arai et al., 1974). The burst size of a phage may depend on the host strain, culture medium, culture conditions, cell age and multiplicity of infection (moi) (Hadas et al., 1997). The net ratio of infective to non-infective phage particles in the progeny population, and frequent re-adsorption of phage particles onto cell debris, may partly explain this discrepancy.

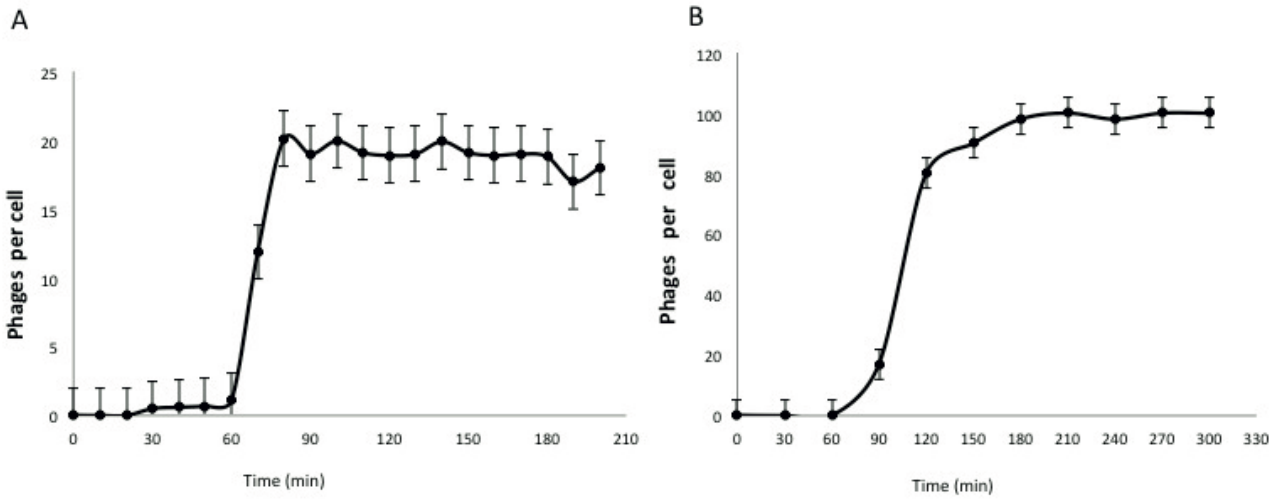

Figure 2. 2. Single-step growth curves for Cp1 (A) and Cp2 (B). The plaque-forming units (PFUs) per infected cell in cultures of MAFF 301080 for Cp1 and MAFF 673010 for Cp2 at different time postinfection are shown. Samples were taken at intervals (every 10 min up to 3.5 h for Cp1 and every 30 min up to 5 h for Cp2). Error bars indicate standard deviation (n = 3).

2.4.3. Genomic analyses of Cp1: gene organization and homology to other phages. The Cp1 genome was a linear double-stranded (ds) DNA of approximately 44 kbp, as determined by pulsed-field gel electrophoresis (PFGE) (data not shown). The nucleotide sequence of the Cp1 genome was determined using shotgun sequencing of DNA purified from phage particles. Sequences were assembled into a circular contig of 43,870 bp, suggesting the presence of terminal repeats. The exact termini of the Cp1 genome were determined to have a 10-nucleotide (nt) 3'-protruding *cos* site (5'-CCAGTTGTCT, corresponding to position 43,861-43,870) at either end. The Cp1 genome had a G + C content of 53.3%; this value was significantly lower than that of the host genome (e.g. 64.7% for strain 306, accession no. NC_003919). When the databases were searched using BLAST and BLASTX programs for sequences homologous to the Cp1 DNA sequence, extensive homologies were detected in the genome sequence of *X*. *campestris* phage phiL7 (accession no. EU717894), *X*. *oryzae* phage OP1 (accession no. AP008979), and *Xanthomonas* phage Xp10 (accession no. AY299121). All these phages are siphoviruses infecting species of *Xanthomonas*, which is consistent with the Cp1 morphological features. An extended collinearity of the nucleotide sequence homology, with several short interspersed divergent islands, was detected throughout almost the entire genomic region between Cp1 and phiL7, which gave the highest similarity score (Figure 2.3).

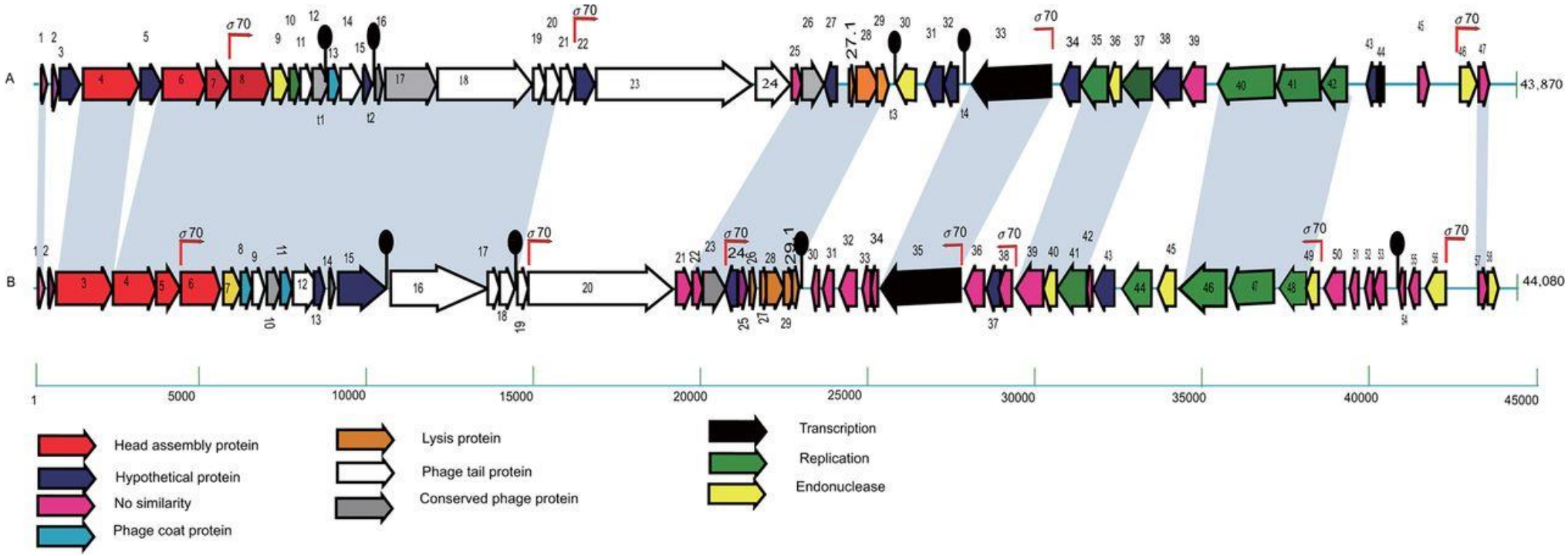

Figure 2.3. Genomic organization of phages Cp1 (A) and phiL7 (B). Colored arrows indicate the directions and categories of the genes. Broken arrows and black knobs indicate the □□□-type promoters and predicted terminators for transcription, respectively. No simirarity: using an E-value lower than e^{-4} as a cutoff for notable similarity.

Forty-eight potential ORFs comprising 50 or more codons, starting with ATG or GTG as the initiation codon, and with a Shine-Dalgarno ribosome-binding sequence preceding the initiation codon, were detected in the Cp1 genome. The genome was divided into left and right arms by the ORF29 and ORF30 intergenic region, with genes on the two arms transcribed convergently (Figure 2.3). The 48 deduced proteins included: (i) 27 that had database homologs of known function, including phage structural proteins, DNA packaging proteins, and proteins involved in DNA replication, transcription and lysis; (ii) 19 hypothetical proteins in the databases, including many phiL7 proteins; and (iii) two proteins with no similarities in the databases (Table 2.2). The gene organization of Cp1 was compared with that of phiL7 in Figure 2.3. Compared with the phiL7 gene organization, *p21*, *p25*, *p26*, *p30-p34*, *p36-p38*, *p42*, *p45*, *p49-p52*, *p55* and *p56* of phiL7, most of which were without similarity in the databases, were missing from Cp1 and instead *orf3*, *orf5*, *orf30-orf32*, *orf34*, o*rf44* and *orf45* were inserted or replaced in the Cp1 genome. Some of these genes, such as *p45*, *p49*, and *p56* of phiL7 and *orf3*, *orf5*, and *orf30* of Cp1 encoded HNH endonuclease, GIY-YIG endonuclease or group-I intron endonuclease, suggesting their involvement in gene rearrangements, especially horizontal gene movements. However, the group-I intron inserted in the DNA polymerase gene (*p44-p46*) in phiL7 (Lee et al., 2009) was missing from the corresponding region of the Cp1 gene (*orf40*).

Interestingly, Cp1 encodes a viral RNA polymerase (RNAP; ORF33) (a single-subunit RNAP similar to the T7-type enzymes). Sequence analysis showed that Cp1 ORF33 was 71.4% identical to phiL7 p35 (ACE75775.1) and 31.5% identical to T7 RNAP (NP_041960) (Figure 2.4A). Cp1 ORF33 also showed 40-50% amino acid sequence identity with RNAPs of other *Xanthomonas* phages, such as Xp10

(AAP58699.1), OP1 (BAE72738.1), and Xop411 (ABK00180.1) (Figure 2.4A). All-important amino acid residues identified in T7 RNAP for structure and function (Cheetham et al., 1999; Osumi et al., 1992) were conserved among these RNAPs. Their phylogenetic relationship is shown in Figure 2.4B. The siphovirus Xp10 was shown to rely on both host and phage RNAPs, and the shift from host to phage RNAP is regulated by phage protein p7 (Semenova et al., 2005). Xp10 p7 (73 aa) is encoded by gene p45L, located after the replication module of the Xp10 genome. A similar regulation may work in Cp1 because ORF44 encoding 66 aa with a sequence similarity to inhibitors of transcriptional initiators and terminators (33% identical to Xp10 p45L; AAP58713.1), was located at the corresponding position on Cp1 DNA (Figure 2.3). Like Xp10, the protein encoded by ORF44 may function to inhibit host RNAP and act as an antiterminator, allowing RNAP to pass through the intrinsic terminator for expression of the late genes (Semenova et al., 2005).

Furthermore, we detected a homolog of the OP1 tail fiber protein (Tfb, OP1-ORF25), which was thought to be involved in host range determination, mediated by variation in the combination of repetitive motifs at the N-terminus (Inoue et al., 2006).

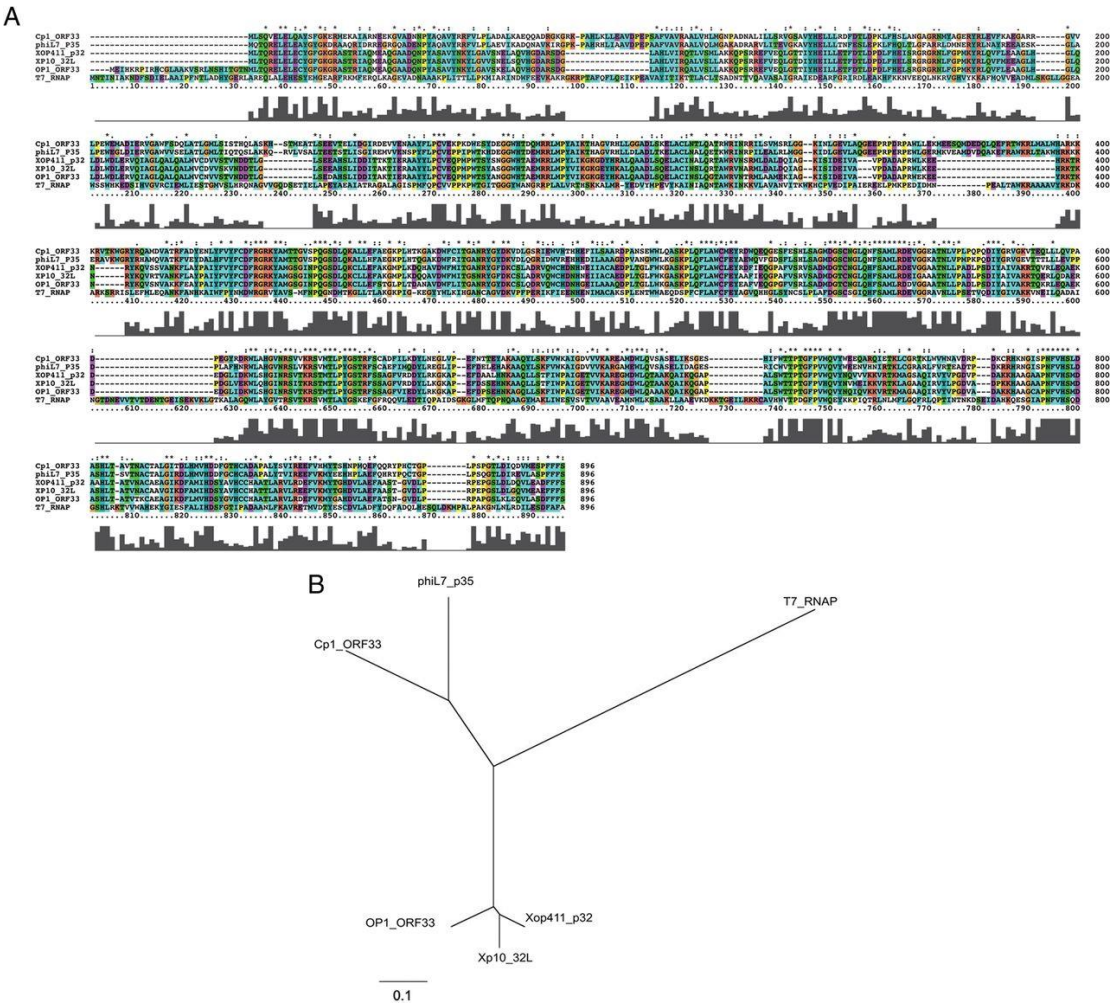

Figure 2.4. Comparison of amino acid sequences of RNA polymerases (RNAP) encoded by *Xanthomonas* phages. (A) The amino acid sequence of Cp1 ORF33 (AB720063) was aligned with those of phiL7 p35 (ACCE75775.1), Xop411 p32 (ABK00180.1), Xp10 32L (AAP58699.1), OP1 ORF33 (BAE72738.1) and coliphage T7 RNAP (NP_041960.1) using ClustalX. The ClustalX coloring scheme depends on both residue type and the pattern of conservation with column (http://www.cgl.ucsf.edu/chimera/docs/ContributedSoftware/multalignviwer/cxcolor.html). Conservative scores are drawn below the alignment. (B) The unrooted dendrogram was constructed with the Treeview tool using the maximum likelihood method based on a complete protein sequence alignment of RNAP proteins from other phages.

Table 2.2. Predicted ORFs found in Cp1 genome

Coding sequence	Strand	Position (5 \to 3\)	G+C (%)	Length (aa)	Mass (kDa)	Amino acid identity/similarity to best homologs	FASTA score (E value)
ORF1	+	106-333	59.3	76	7.94	p01 PHIL7	43 (0.025)
ORF2	+	392-628	52.5	78	8.44	P02 phil7- hypothetical protein	84 (8e-13)
ORF3	+	635-1315	53.9	226	25.06	group 1 intron GIY-YIG endonuclease (*Pseudomonas stutzeri Kos6)*	123 (1e-30)
ORF4	+	1349 -3054	54.6	568	61.58	p03 phiL7-Terminase large sub unit	730 (0.0)
ORF5	+	3079- 3723	50.4	214	23.71	group 1 intron GIY-YIG endonuclease (*Pseudomonas stutzeri Kos6)*	109 (9e-26)
ORF6	+	3734-5029	55.1	431	46.65	p04 phiL7-Putative head portal protein	652 (0.0)
ORF7	+	5026-5745	50.6	239	25.23	p05 phiL7-Protease of the CIPp family	288 (5e-76)
ORF 8	+	5760-6944	59.6	394	41.7	p06 phiL7- Head protein	641 (0.0)
ORF9	+	7029-7526	49.1	165	18.51	p07 phiL7- HNH endonuclease	180 (1e-43)
ORF10	+	7528-7863	53.8	111	12.6	p08 phiL7- Phage coat protein	111 (6e-23)
ORF11	+	7863-8237	52.1	124	13.16	p09 phiL7- Head- tail Joint	187 (8e-46)
ORF12	+	8227-8694	49.1	156	17.17	p10 phiL7-Conserved phage protein I	172 (6e-52)
ORF13	+	8691-9047	50.1	118	13.17	p11 phiL7- Phage coat protein	177 (7e-43)
ORF14	+	9057-9695	55.6	212	22.24	p12 phiL7- Major tail	288 (3e-76)
ORF15	+	9695-9997	55.0	100	10.9	p13 phiL7- Hypothetical protein	170 (8e-41)
ORF16	+	10102-10311	57.2	69	8.05	p14 phiL7-Conserved phage protein II	79.1(7e-25)
ORF17	+	10406-11917	50.8	503	56.34	p15 phiL7- Hypothetical Protein	590(0.0)
ORF18	+	11963-14827	55.4	953	99.34	p16 phiL7-Tail length tape measure protein	992 (0.0)
ORF19	+	14827-15189	48.7	121	13.81	p17 phiL7- Tail protein I	179 (2e-43)
ORF20	+	15189-15647	52.1	152	16.79	p18 phiL7- Tail protein II	225 (3e-57)
ORF21	+	15665-16051	54.2	129	14.62	Xop411 phage, p21, Peptidoglycan hydrolase	174 (7e-42)
ORF22	+	16064-16669	52.0	201	23.05	Bacillus phage G, G3MAX5 (Gp595)	62 (9e-08)
ORF23	+	16710-21431	53.8	1573	167.72	- OP1_ORF21,Putative tail component protein. - p20 phiL7- Tail protein III	2048(0.0) 1496(0.0)
ORF24	+	21478-22554	51.7	358	37.68	OP1_ORF25,Deduced tail fiber protein	77 (6e-12)
ORF25	+	22556-22855	49.3	98	10.48	p22 phiL7- hypothetical protein	125 (2e-27)
ORF26	+	22857-23543	46.8	228	23.91	p23 phiL7- Conserved Phage protein	253 (23-65)
ORF27	-	23540-23908	51.3	122	13.39	p24 phiL7- Hypothetical protein	200 (1e-63)
ORF27.1	+	24387-24587	50.9	66	7.046	P27 phiL7- putative holin	48 (7e-5)
ORF28	+	24591-25130	53.9	179	19.83	p28 phiL7- Phage type lysozyme	265 (2e-69)
ORF29	+	25099-25467	51.0	122	13.5	p29 phiL7- Hypothetical protein	110 (7e-23)
ORF30	-	25676-26327	53.2	200	22.27	group I intron endonuclease (D6TZN2)	71 (1e-10)

Table 2.2. Continued

Coding sequence	Strand	Position (5 \to 3\)	G+C (%)	Length (aa)	Mass (kDa)	Amino acid identity/similarity to best homologs	BLAST score (E value)
ORF31	-	26558-27104	50.8	181	19.39	*Hemophilus parasuis* SH0165 (Interrupted gp229, phage associated)	160 (8e-45)
ORF32	-	27100-27534	53.7	144	14.35	F7T9I5(Putative uncharacterized protein)	69 (3e-10)
ORF33	-	27912-30327	53.6	804	91.43	p35 phiL7- RNA polymerase	1212 (0.0)
ORF34	-	30601-31164	54.3	187	21.14	*Pantoea* phage LIMEzero (F4N9T4), Putative uncharacterized protein	86 (3e-15)
ORF35	-	31175-32026	50.4	283	32.35	p39 phiL7- Putative DNA polymerase III	456 (e-126)
ORF36	-	32013-32408	53.5	131	14.64	p40 phiL7- Endonuclease VII	134 (4e-30)
ORF37	-	32405-33334	56.0	309	34.35	p41 phiL7- Exonuclease	312 (5e-83)
ORF38	-	33334-34215	57.1	293	32.02	ADQ2- *Caulobacter* Cd1 Phage, Putative Un characterized protein	133 (4e-11)
ORF39	-	34229-34936	55.3	235	26.6	Unknown	
ORF40	-	35296-37014	53.2	572	63.96	p46 phiL7- DNA polymerase lacking N-trminal exonuclase	550(e-154)
ORF41	-	37073-38365	55.5	430	48.35	p47 phiL7- Replicative helicase of the DnaB family	408 (e-113)
ORF42	-	38350-39177	52.0	275	30.6	p48 phiL7-DNA primase of the DnaG family	239 (4e-61)
ORF43	-	39758-40066	43.8	102	12.21	Xop411_p 45 Hypothetical protein	74 (1e-11)
ORF44	-	40063-40263	42.1	66	7.46	Xp10_45L, 7K protein; inhibitor of transcription initiation and anti-terminator	35.8(0.13)
ORF45	+	41309-41626	53.2		11.55	Unknown	-----
ORF46	+	42546-43075	46.9	175	20.24	p07 phiL7- HNH endonuclease	166 (4e-50)
ORF47	+	43111-43425	45.6	104	12.38	p57 phiL7	57 (1e-06)

2.4.4.Genomic analyses of Cp2: gene organization and homology to other phages.

The Cp2 genome was also a linear ds DNA of approximately 43.0 kbp, based on PFGE analysis (data not shown). The Cp2 DNA isolated from phage particles was subjected to shotgun sequencing. Sequences were assembled into a circular contig of 42,963 bp, also suggesting the presence of terminal repeats. The precise sequence of the repeat was not determined. The Cp2 genome had a G + C content of 66.7%, comparable with that of the host genome (ca. 64.7%). To find homologous sequences, nucleotide sequences from Cp2 were used to search sequence databases. Short-ranged homologies were found in the sequences of *Azospirillum brasilense* Sp245 plasmid (accession no. HE577328; E-value, 2e-11 (84 bit)) and *Burkholderia pseudomallei* bacteriophage phi1026b (accession no. AY453853; E-value, 5e-09 (76 bit)). Interestingly, a sequence in the genome of *X*. *axonopodis* pv. *citri* strain 306 also showed some homology to the Cp2 genome (accession no. AE008923; E-value, 8e-08 (72 bit)). The homologous sequence corresponded to a single gene (*orf32* of Cp2, encoding a single-strand binding protein). However, the 1.8 kbp region, including XAC1661 (Isxac3 transposase) and XAC1662 (*repA*) of strain 306, which was specifically amplified by rep-PCR for $Cp1^R$/$Cp2^S$ strains (Shiotani, 2007), did not show any sequence homology with the Cp2 genome. Forty potential ORFs were identified in the Cp2 genome. The 40 deduced proteins included: (i) 20 that had database homologs of known functions, including phage structural proteins, DNA processing proteins, and lysis proteins; (ii) 16 hypothetical proteins showing marginal similarities with unknown proteins of various origins; and (iii) four proteins with no similarities in the databases (Table 2.3). The ORF map is shown in Figure 2.5. Morphologically, Cp2 belongs to the family *Podoviridae*. The genome of coliphage T7, the representative of T7-like phages of the *Podoviridae*, generally consists of

three functional gene clusters: one for early functions (class I), one for DNA metabolism (class II), and the other for structural proteins and virion assembly (class III) (Dunn and Studier, 1983). For the Cp2 genome, the assignment of classes I-III was difficult because of the lack of sufficient information about each gene, especially about key genes, such as RNAP, DNA metabolism, and structural proteins. After identifying genes for structural proteins, we tentatively assigned the three functional modules according to the T7 gene arrangement (Figure 2.5). In this Cp2 gene arrangement, the putative class I module contained ORF32 (with similarity to ssDNA-binding proteins), ORF33 (HNH endonuclease), ORF34 (YqaJ-like recombinase), and ORF35 (ERF family protein) (Table 2.3). The Cp2 putative class II region contained ORF39 (with a marginal similarity to DNA polymerase gamma-1 subunit), ORF40 (pyocin-like), ORF3 (Holliday junction resolvase), and ORF5 (lysozyme) (Table 2.3). The details for class III, consisting of ORF13-ORF29, are described below.

We could not find a gene for RNAP in the Cp2 genome. In general, T7-like podoviruses use phage-encoded RNAP for predominant expression of phage genes (Molineux, 1999). T7-RNAP encoded in the class I module (early expressed by host RNAP) specifically recognizes phage promoters of class II and class III genes for the shift of gene expression. However, several podoviruses that have the RNAP gene in the class II module showed a high dependency on the host RNAP for the expression of phage genes (Carlson, 1994; Ceyssens et al., 2006). Marine phages VpV262 and SI01, which share extensive homology with T7, lack a phage RNAP (Hardies et al., 2003), indicating absolute dependency on the host RNAP for the expression of phage genes. Therefore, the lack of an RNAP gene in the Cp2 genome is not surprising. Searching promoter sequences throughout the Cp2 genome using ORFinder only revealed typical □□□□promoters (data not shown). Notably, the *Siphovirus* Cp1

contained an RNAP gene that is phylogenetically related to RNAP genes of T7-like phages. In the genomes of siphoviruses such as *Xanthomonas* phage Xp10, as well as Xop411 and OP1, a cluster of □-like structural genes is connected to other gene clusters arranged in the reverse orientation, such as the T7-like class II and class I genes (Yuzenkova et al., 2003).

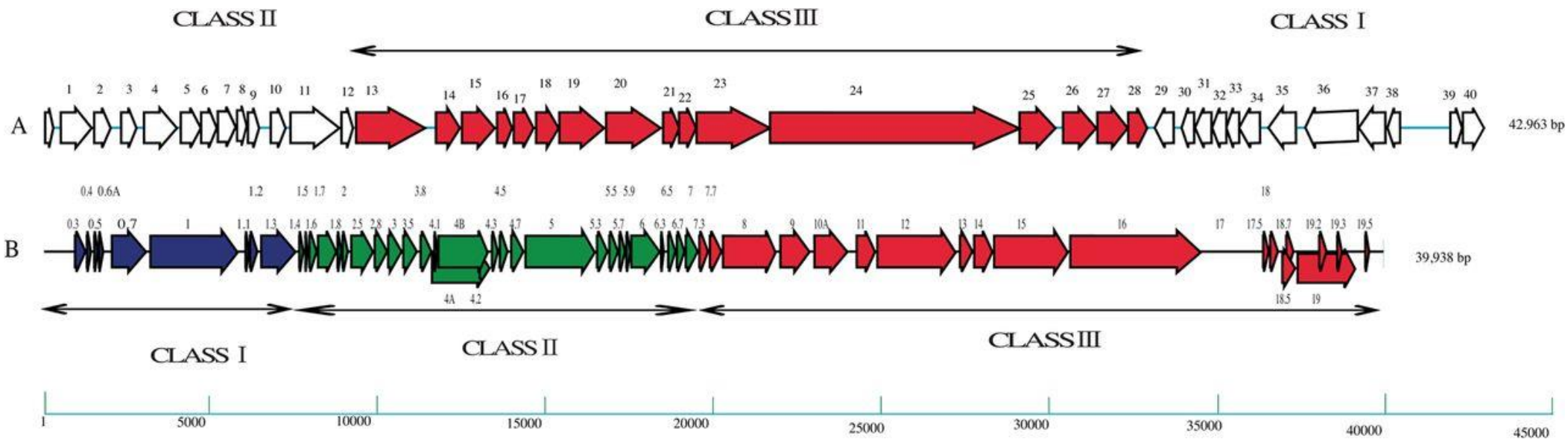

Figure 2.5. Genomic organization of phages of Cp2 (A) and *Escherichia coli* T7 (B). Arrows indicate the sizes and directions of the genes. The typical podovirus genome represented by T7 phage consists of three functional modules: class I, class II, and class III, as shown in (B) (Dunn and Studier, 1983). Putative class I, class II, and class III modules for Cp2 are shown in different colors in (A).

Table 2.3. Predicted ORFs found in Cp2 genome

Coding sequence	Strand	Position (5 \to 3\)	G+C (%)	Length (aa)	Mass (kDa)	Amino acid identity/similarity to best homologs	FASTA score (E value)
ORF1	+	454-1398	66.8	314	34.88	phage protein Gp37/Gp68.	329(3e-108)
ORF2	+	1364-1945	63.2	193	18.1	hypothetical protein F116p34 (*Pseudomonas* phage F116)	106 (6e-26)
ORF3	+	2262-2717	66.8	151	16	holliday junction resolvase , RUSA	112 (2e-28)
ORF4	+	2836-3952	73.9	372	32.71	no similarity	-----
ORF5	+	4030-4632	70.5	200	21.46	phage lysozyme (*Burkholderia multivorans* CF2)	127(1e-32)
ORF6	+	4635-5108	64	157	16.46	hypothetical protein SSKA14_3083 (*Stenotrophomonas* sp. SKA14)	51 (3e-06)
ORF7	+	5105-5662	67.3	185	20.37	hypothetical protein SSKA14_2891 (*Stenotrophomonas* sp. SKA14)	80 (1e-12)
ORF8	+	5665-5979	67.6	104	11.61	hypothetical protein XVE_1166 (*Xanthomonas vesicatoria* ATCC 35937)	59(1e-09)
ORF9	+	6031- 6360	67.3	109	11.45	No similarity	-----
ORF10	+	6712-7149	65.8	145	16.1	hypothetical protein Pden_3755 (*Paracoccus denitrificans* PD1222)	59 (4e-09)
ORF11	+	7289-8815	67	508	56.21	putative phage terminase B protein [*Enterococcus* phage phiEf11]	196 (7e-53)
ORF12	+	8820-9158	65.3	112	11.95	Bbp20 (*Bordetella* phage BPP-1)	58(4e-09)
ORF13	+	9234 -11294	67.6	686	74.87	bacteriophage head to tail connecting protein	300 (2e-89)
ORF14	+	11629-12354	65.8	241	25.11	endoprotease (*Pantoea* sp. aB)	84 (1e-16)
ORF15	+	12398-13411	63.1	337	36.38	putative major capsid protein (*Pseudomonas* phage AF)	257 (8e-80)
ORF16	+	13447-13893	66.6	148	15.35	hypothetical protein AF_009 (*Pseudomonas* phage AF)	73 7e-14)
ORF17	+	13947-14537	59.5	196	19.98	no similarity	---
ORF18	+	14607-15290	67.3	227	24.71	putative tail tubular protein A (*Pseudomonas* phage AF)	89(1e-18)
ORF19	+	15292-16683	65.7	463	49.5	putative phage protein p13 (*Hydrogenophaga* sp. PBC)	155 (9e-38)
ORF20	+	16683-18395	65.1	570	61.81	*Salmonella* phage epsilon15	350(5e-07)
ORF21	+	18392-18868	64.5	158	17.7	hypothetical protein PhiV10p16 (*Escherichia* phage phiV10)	112 (3e-28)
ORF22	+	18868-19371	67.5	167	17.11	hypothetical protein Q5W_4240 (*Hydrogenophaga* sp. PBC)	64 (2e-12)
ORF23	+	19371-21563	68.8	730	79.04	putative structural lysozyme (*Pseudomonas* phage AF)	94(4e-17)
ORF24	+	21566-29002	68.2	2478	267.54	hypothetical protein AF_016 (*Pseudomonas* phage AF)	506(9e-143)
ORF25	+	29002-30111	63.5	369	40.13	endo-N- acetylneuraminidase (Endosialidase) family protein, end_tail_spike	79 (4e-13
ORF26	+	30289-31314	64.2	341	35.78	LysM domain protein (*Xanthomonas citri* pv. *mangiferaeindicae*)	115(1e-24)
ORF27	+	31311-32243	60.9	310	33	putative tail fiber protein (*Pseudomonas* phage PT2)	64(9e- 09)
ORF28	+	32233-32808	61.0	191	21.69	tail fibre protein (*Pseudomonas* phage LUZ19)	74 (2e-13)
ORF29	-	33018-33584	67.6	188	21.26	hypothetical protein YPK_2318 (*Yersinia pseudotuberculosis* YPIII)	70 (6e-12)
ORF30	-	33829-34191	63.8	120	12.84	N4 Gp49/Sf6 protein 66 phage family protein (*Acinetobacter baumannii* OFCO211)	110 (6e-29)
ORF31	-	34225-34710	64.9	161	17.68	Orf76(Pseudomonas phage D3)	73 (2e-13)
ORF32	-	34723-35160	62.7	145	16.35	Single-stranded DNA binding protein (*Xanthomonas translucens* pv. *graminis* ART-Xtg29)	173 (5e-52)
ORF33	-	35157-35534	65.3	125	13.27	- hypothetical protein Bphy_1919 (*Burkholderia phymatum* STM815) - bacteriophage-like protein (*Ralstonia solanacearum* GMI1000]	106 (2e-26) 103(2e-25)

Table 2.3. Continued

Coding sequence	Strand	Position (5 \to 3\)	G+C (%)	Length (aa)	Mass (kDa)	Amino acid identity/similarity to best homologs	BLAST score (E value)
ORF30	-	33829-34191	63.8	120	12.84	N4 Gp49/Sf6 protein 66 phage family protein (*Acinetobacter baumannii* OFCO211)	110 (6e-29)
ORF31	-	34225-34710	64.9	161	17.68	Orf76(Pseudomonas phage D3)	73 (2e-13)
ORF32	-	34723-35160	62.7	145	16.35	Single-stranded DNA binding protein (*Xanthomonas translucens* pv. *graminis* ART-Xtg29)	173 (5e-52)
ORF33	-	35157-35534	65.3	125	13.27	- hypothetical protein Bphy_1919 (*Burkholderia phymatum* STM815) - bacteriophage-like protein (*Ralstonia solanacearum* GMI1000]	106 (2e-26) 103(2e-25)
ORF34	-	35534-36157	65.5	207	23.36	YqaJ-like viral recombinase domain; pfam09588 (*Xanthobacter autotrophicus* Py2)	207(7e-64)
ORF35	-	36385-37227	64.4	280	30.33	ERF family protein (*Burkholderia glumae* BGR1)	179 (7e-51)
ORF36	-	37496-39031	69.3	511	56.94	hypothetical protein F116p18 (*Pseudomonas* phage F116)	73(4e-11)
ORF37	-	39072-39896	65.9	274	29.27	protein of unknown function (DUF2303)(Vibrio phage VvAW1)	190 (2e-55)
ORF38	-	39951-40325	63.4	124	13.04	hypothetical protein VvAW1_00024c (Vibrio phage VvAW1)	76 (3e-15)
ORF39	+	41829-42176	66.7	115	12.48	Predicted: DNA polymerase subunit gamma-1 (*Callithrix jacchus*)	35 (2.2)
ORF40	+	42178-231	62.6	338	36.7	- hypothetical protein (*Escherichia* phage TL-2011b) "PhdYeFM_antitox" - Pyocin large subunit-like protein [Pseudomonas sp. R81]	140(1e-35) 127(3e-31)

2.4.5. Proteomic analyses of Cp1 and Cp2 virions

Using SDS-PAGE in conjunction with LC-MS/MS, we identified virion proteins of Cp1 and Cp2. In the case of Cp1, at least 10 proteins, ranging from 13 kDa and ca. 120 kDa, were separated by SDS-PAGE (Fig. 5A). All these proteins were recovered, in-gel digested and subjected to mass spectrometric analysis. The results are shown on the right side of Figure 2.6A. The identified proteins include p5 (unknown protein), p6 (head portal protein), p8 (head protein), p14 (major tail protein), p18 (tail length tape major protein), p23 (tail fiber protein), p28 (lysozyme), p29 (hypothetical protein) and p31 (unknown protein). We observed oligomerization of two proteins. The major head protein (p8; calculated to be 41.7 kDa) was detected at a position corresponding to ~200 kDa in SDS-PAGE, suggesting oligomers consisting of five subunits. In addition, p5 (unknown protein) has a calculated molecular mass of 23.71 kDa, but was observed at a position corresponding to 60-70 kDa, suggesting this protein exists as a trimer. These subunits may be covalently linked in the phage particles. For other proteins, the observed size was close to the calculated size. In the Cp1 genomic analysis, we detected a homolog of the OP1 tail fiber protein (Tfb, OP1-ORF25), which was thought to be involved in host range determination, mediated by variation in the combination of repetitive motifs at the N-terminus (Swmwnova et al., 2005). However, the corresponding Cp1 ORF (ORF24) was much smaller (358 aa residues) compared with OP1-ORF25 (431 aa residues) and the similarity was limited to 42 aa residues at the N-terminus (67% identity) without any following repetitive motifs. Indeed, this protein was not detected among the Cp1 structural proteins (Figure 2.6A). It is unknown whether this protein is involved in host range determination. Instead, a large protein corresponding to ORF23 (1574 aa residues) was detected (Figure 2.6A), which showed significantly high similarity to tail fiber

proteins of several phages; 22R of Xp10 (accession no. Q7Y5J5), p22 of Xop411 (accession no. A5H1M5) and p20 of phiL7 (accession no. C4ML20). This protein might be involved in determining the host range, as suggested by Lee et al. (2007; 2009).

For Cp2 virions, at least 13 proteins, ranging from 16 kDa and ca. 300 kDa, were separated by SDS-PAGE (Figure 2.6B). All of these proteins were recovered and subjected to mass spectrometric analysis as above. The results are shown on the right side of Fig. 5B. The proteins identified were from the ORFs 13 to 28 cluster on the Cp2 map (Figure 2.5), giving a putative structural module (class III) of T7-like phages. From this cluster, p14 (endoproteinase), p17 (unknown protein), and p21 (hypothetical protein) were not detected. The identified proteins included p13 (head-tail connecting protein), p15 (major capsid protein), p18 (tail tubular protein A), p23 (structural lysozyme), p24 (lysin-like protein), p25 (end-tail-spike protein), P26 (LysM domain protein), p27 (tail fiber protein) and p28 (tail fiber protein). Among these, p23 (structural lysozyme; calculated to be 79 kDa) gave three ladder bands around 80–130 kDa, which suggested processing and oligomerization of this protein

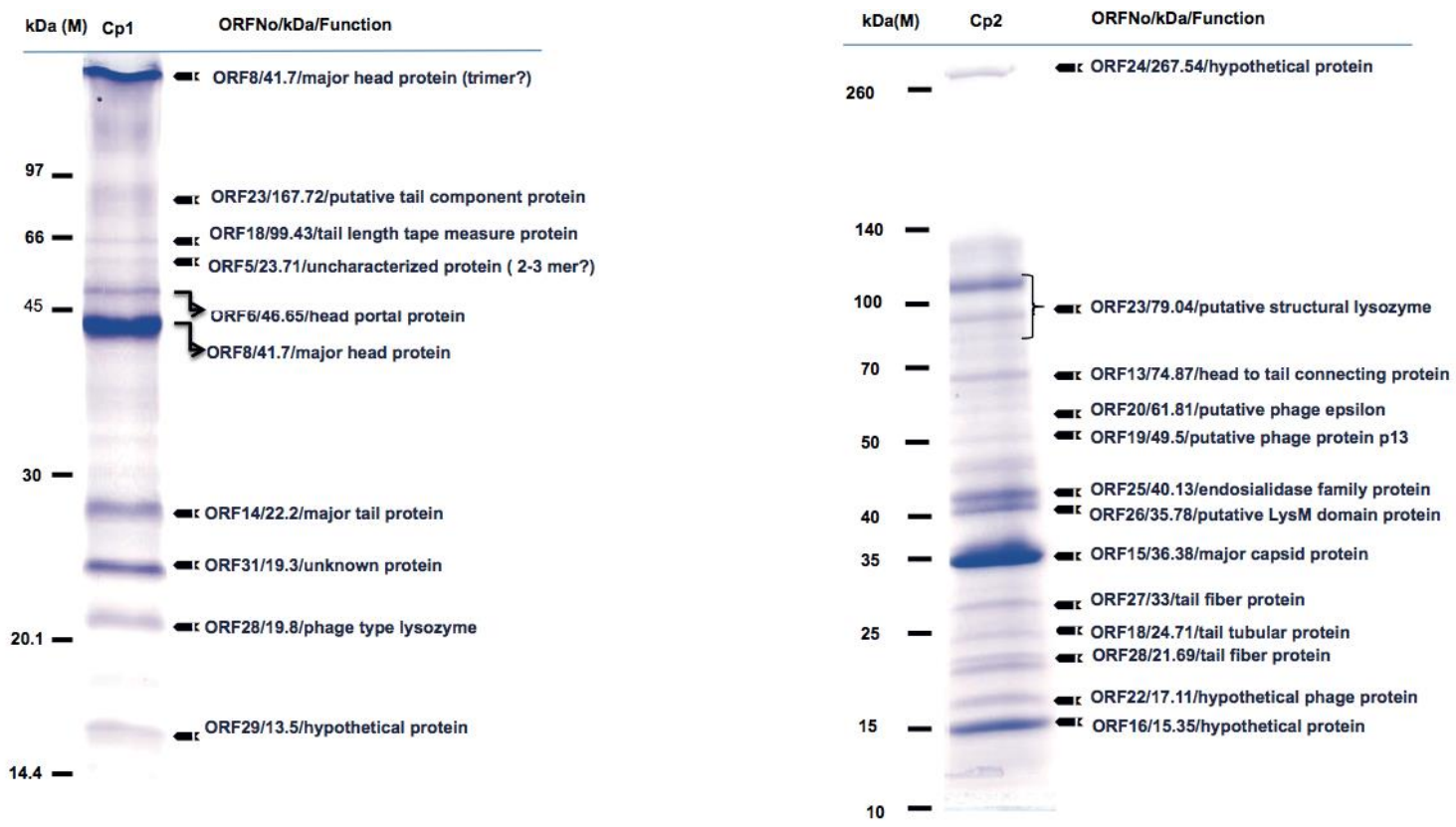

Figure 2.6. Proteomic analysis of Cp1 (A) and Cp2 (B) particles. Proteins of purified phage particles were separated in 10% (wt/vol) polyacrylamide gel by SDS-PAGE and stained with Coomassie brilliant blue. The protein bands were recovered, digested in gel, and subjected to LC-MS/MS analysis. On the right are the descriptions of the genes, their deduced molecular sizes based on the ORF sequences, and their possible functions. Positions of size markers are shown on the left. For some protein bands, possible oligomerization of the phage protein was observed.

2.4.6. Host selection by Cp1 and Cp2

As described above, phages Cp1 and Cp2, practically used for phage-typing of *X. axonopodis* pv. *citri* strains, were found to belong to completely different virus groups. This raises the question of how these phages discriminate host strains. The initial and essential event for a phage to succeed in infection is attachment of the phage particles to the host surface receptors. Therefore, differential adsorption of Cp1 and Cp2 to host cells was examined, according to the method described in Materials and Methods. The results shown in Table 2.4 indicated that both $Cp1^S/Cp2^R$ and $Cp1^R/Cp2^S$ strains (MAFF 301080 and MAFF 673010, respectively) adsorbed Cp1 and Cp2 efficiently. Even a $Cp1^R/Cp2^R$ strain (MAFF 31130) also adsorbed Cp1 and Cp2 almost equally. To further investigate the relationship between Cp1 and Cp2 infection, we isolated resistant mutants from the host strains. When a spontaneous mutant showing $Cp1^R$ from MAFF 301080 was subjected to phage adsorption assay, it did not adsorb Cp1 but did absorb Cp2, as did its wild type (Table 2.4). This mutant also showed $Cp2^R$. In the same way, a spontaneous mutant showing $Cp1^R/Cp2^R$ from MAFF 673010 did not adsorb Cp2, but did absorb Cp1 (Table 2.4). Moreover, when cells of MAFF 301080 ($Cp1^S/Cp2^R$) were first treated with Cp2 particles at an m.o.i of 5 and then subjected to plaque assay with Cp1, the number of plaques that appeared were almost the same as that with untreated cells (data not shown). Similar results were obtained for MAFF 673010 ($Cp1^R/Cp2^S$) cells with pretreated with Cp1 and assayed for Cp2 infection. Taken together, these results indicated that Cp1 and Cp2 use different molecules on the host cell surface as phage receptors and that discrimination of strains by Cp1 and Cp2 is not at the initial stage by binding to receptors, but at some stage(s) afterwards.

Table 2.4. Adsorption of Cp1 and Cp2 to bacterial strains

Strain	Phage type	Phage adsorption	
		Cp1	Cp2
MAFF 301080	$Cp1^S/Cp2^R$	100	>99
301080 R1	$Cp1^R/Cp2^R$	0	>99
MAFF 673010	$Cp1^R/Cp2^S$	>99	100
673010 R2	$Cp1^R/Cp2^R$	>99	0
MAFF 31130	$Cp1^R/Cp2^R$	>99	>99
E. coli JM109		0	0

Another question arose as to what happens to the phage DNA after cell attachment in the case of non-host strains. To answer this question, SYBR Gold-labeled phages were added to cells of *X. axonopodis* pv. *citri* strains and the movement of SYBR Gold-phage DNA was monitored. SYBR Gold-labeled phage attached to host cells (observed after 10-20 min post infection) and bacterial cells were not stained at 10 min post infection (Fig. 6AB, left panels) but some cells became stained at 20 min post infection, possibly by injection of phage DNA (Fig. 6AB, right panels). As shown in Fig. 2.6 C and D, after 30 min post infection, Cp1 DNA seemed to be injected into most cells of MAFF 673010, MAFF 31130 and MAFF 301080. Similarly, Cp2 DNA seemed to be injected into most cells of MAFF 301080, MAFF 31130 and MAFF 673010. With cells of *E. coli* as the control, Cp1 and Cp2 did not attach to the cells and no injection of DNA occurred (data not shown). Once the phage DNA was introduced into cells, it was retained stably for a certain period. In the case of resistant strains, cell growth continued after phage addition. Host restriction/modification systems may contribute to this host selection, but its importance is not clear because Cp1 and Cp2 progenies produced from strain KC33 ($Cp1^s/Cp2^s$) showed exactly the same host range as their original phages (data not

shown). These results suggested that host selection by Cp1 and Cp2 may occur at or after immediate early expression of phage genes.

In the genome of hosts such as strain 306 (accession no. NC_603919), there are no sequence elements that showed significant homology with Cp1 or Cp2 sequences. The 1.8 kbp region containing a transposon that was specifically amplified by rep-PCR from genomic DNA of $Cp1^R/Cp2^S$ strains (Shiotani et al., 2000) and the region containing avrBs3/pthA varying between $Cp1^S/Cp2^R$ and $Cp1^R/Cp2^S$ strains (Shiotani, 2007) did not show any nucleotide sequence homology with the Cp1 and Cp2 genomes. Dot blot and Southern blot hybridization of genomic DNA from 11 strains tested (Table 2.1) showed no significant hybridization signals with Cp1 DNA or Cp2 DNA as a probe (data not shown). Therefore, no direct connection between the host genome and Cp1/Cp2 genomes was detected.

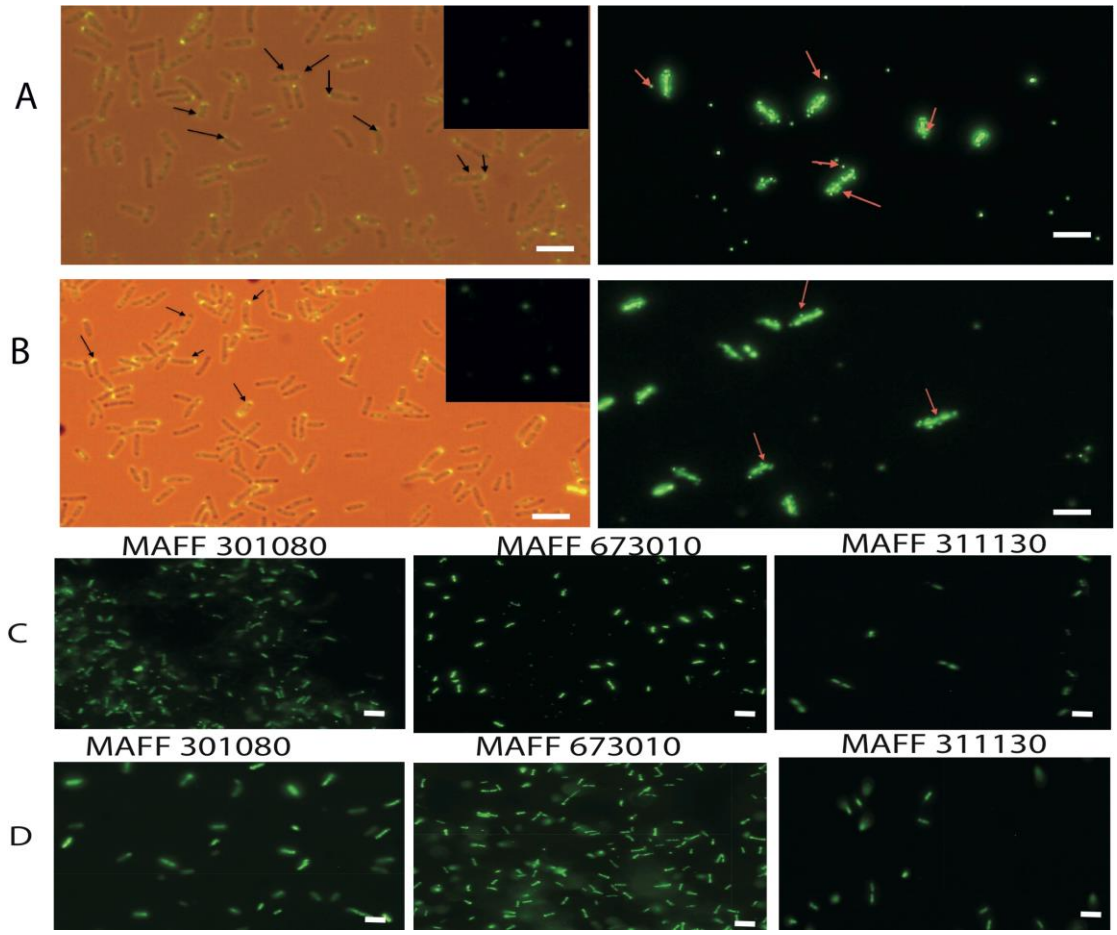

FIG. 2.7. Attachment of SYBR Gold-labeled phage particles to bacterial cells and staining the cells by possible injection of phage DNA. (A) Cp1 particles were added to cells of host strain MAFF 301080 and (B) Cp2 particles were added to cells of host strain MAFF 673010. Cells from A and B were observed under a fluorescence microscope at 10 min (moi = 1, left panel) and 20 min (moi = 10, right panel) post infection. Showing the attachment of the phage particles to the bacterial cell surface. Phage particles appear as tiny spots (arrows). At 10 min post infection, bacteria cell were not stained (bright and dark fields), while cells became stained at 20 min post infection (dark field). Cp1 (C) and Cp2 (D) particles were also added to cells of MAFF 301080 ($Cp1^S/Cp2^R$), MAFF 673010 ($Cp1^R/Cp2^S$), and MAFF 311130 ($Cp1^R/Cp2^R$). Cells were observed under a fluorescence microscope at 30 min post

infection. Bacterial Cells were stained by SYBR Gold, indicating injection of phage DNA into the $Cp1^S/Cp2^R$ or $Cp1^R/ Cp2^S$ as well as $Cp1^R/Cp2^R$ cells. Bar = 10 μm.

2.5. Conclusion

Bacteriophages Cp1 and Cp2, traditionally used as phage-typing agents for *X. axonopodis* pv. *citri* strains, were found to belong to completely different virus groups. Cp1 was characterized as a phiL7-like siphovirus, but without a group-I intron in the genome, and Cp2 was classified as a new podovirus with genes lacking detectable homologs in the current databases. The host *hssB3.0* and XAC1661-XAC1662 sequences were not related to either Cp1 or Cp2 sequences. Both Cp1 and Cp2 efficiently attached to host cells, even if those are resistant strains.

Chapter 3

The filamentous phage XacF1 causes loss of virulence in *Xanthomonas axonopodis* pv. *citri*, the causative agent of citrus canker disease

3.1. Abstract

In this study, filamentous phage XacF1, which can infect *Xanthomonas axonopodis* pv. *citri* (*Xac*) strains, was isolated and characterized. Electron microscopy showed that XacF1 is a member of the family *Inoviridae* and is about 600 nm long. The genome of XacF1 is 7325 nucleotides in size, containing 13 predicted open reading frames (ORFs), some of which showed significant homology to Ff-like phage proteins such as ORF1 (pII), ORF2 (pV), ORF6 (pIII), and ORF8 (pVI). XacF1 showed a relatively wide host range, infecting seven out of 11 strains tested in this study. Frequently, XacF1 was found to be integrated into the genome of *Xac* strains. This integration occurred at the host *dif* site (*att*B) and was mediated by the host XerC/D recombination system. The *att*P sequence was identical to that of *Xanthomonas* phage Cf1c. Interestingly, infection by XacF1 phage caused several physiological changes to the bacterial host cells, including lower levels of extracellular polysaccharide production, reduced motility, slower growth rate, and a dramatic reduction in virulence. In particular, the reduction in virulence suggested possible utilization of XacF1 as a biological control agent against citrus canker disease.

3.2. Introduction

Xanthomonas axonopodis pv. *citri*, *Xac* (syn. *Xanthomonas campestris* pv. *citri*), is the causative agent of Asiatic citrus canker disease (ACC), one of the most serious citrus plant diseases in the world (Civerolo, 1984; Graham et al., 2004). Under natural conditions, the bacterium can invade all aboveground parts of plants, entering through natural openings and wounds (Brunings and Gebriel, 2003; Vojnov et al., 2010). A characteristic symptoms include raised corky lesions surrounded by a water or oil-soaked margin on leaves, stems, and fruits, including defoliation, twigs dieback, general tree decline, blemished fruit, and premature fruit drop in severely infected trees (Graham et al., 2004). Management of ACC relies on an integrated approach that includes: (i) replacement of susceptible citrus species with resistant ones; (ii) production of disease-free nursery stock; (iii) reduction of pathogen spread by establishing windbreaks and fences around groves; (iv) preventative copper sprays; and (v) application of insecticide to control Asian leafminer. Because of the limited effectiveness of the current integrated management strategies, citrus canker disease continues to be an economically serious problem for field-grown crops worldwide (Balogh et al., 2010). Hence, alternative control methods are necessary.

Bacteriophages have recently been evaluated for controlling a number of phytobacteria and are now commercially available for some diseases (Balogh et al., 2010). The use of phages for disease control is a fast expanding area of plant protection, with great potential to replace existing chemical control measures. Bacteriophages have been used effectively for controlling several diseases caused by *Xanthomonas* species, including, peach bacterial spot, caused by *X*. *campestris* pv. *pruni*, geranium bacterial blight, caused by *X*. *campestris* pv. *pelargonii*, tomato bacterial spot caused by *Xanthomonas euvesicatoria* and *Xanthomonas perforans*, and

onion leaf blight caused by *X*. *axonopodis* pv. *allii* (Flaherty et al. 2000; Flaherty et al. 2001; Balogh et al., 2003; Lang et al., 2007; Obradovic et al., 2004; Obradovic et al., 2005). Major challenges of agricultural use of phages arise from the inherent diversity of target bacteria, high probability of resistance development, and weak phage persistence in the plant environment (Balogh et al., 2008; Balogh et al., 2010). Very recently, utilization of filamentous phages as a disease management strategy has been investigated, and application will likely increase in the future (Askora et al., 2009; Addy et al., 2012). The filamentous ϕRSM phages have dramatic effects on the virulence of *Ralstonia solanacearum*. Infection of *R*. *solanacearum* cells with ϕRSM3 decreased their growth rate, twitching motility, movement in tomato plant stems, extracellular polysaccharide (EPS) production, and *phcA* expression, resulting in loss of virulence (Addy et al., 2012). This strategy using filamentous phage might be expanded to control various diseases, including citrus canker disease. In contrast to lytic phages, filamentous phages do not kill the host cells but establish a persistent association between the host and the phage (Askora et al., 2009; Addy et al., 2012). This is an advantage of filamentous phages to solve the problem of bacteriophages easily inactivated by sunlight UV irradiation (Balogh, et al., 2010).

In the current study, we isolated and characterized a novel filamentous phage and showed that changes occurred at a cellular level in *X*. *axonopodis* pv. *citri* strains following infection. This filamentous phage might be a unique biological agent for use against bacterial citrus canker disease.

3.3. Material and methods

3.3.1 Bacterial strains and growth conditions

Ministry of Agriculture, Forestry, and Fisheries (MAFF) strains of *X*. *axonopodis* pv. *citri*, *Xac* (Table 3.1) were obtained from the National Institute of Agrobiological

Sciences, Japan. Strain KC33 was obtained from the National Institute of Fruit Tree Science, the National Agriculture and Food Research Organization, Japan. All strains were stored at −80°C in 0.8% nutrient broth (NB) (BBL, Becton Dickinson and Co., Cockeysville, MD, USA) supplemented with 30% (v/v) glycerol. The strains were grown on nutrient agar (NA) medium (Difco, BBLBD, Cockeysville, MD, USA) at 28°C. For preparation of bacterial suspension, *Xac* strains were cultured for 24 h at 28°C with shaking at 220 rpm in NB medium.

For time course experiments, phage-infected and uninfected cells were grown overnight in 5 mL of NB media. Then, 0.5 mL of the cell suspensions (10^8 cfu/mL) were transferred into 100-mL flasks containing 30 mL of NB medium. Cultures were grown at 28°C with agitation at 200 rpm, and OD_{600nm} measurements were taken every 3 h over the course of 48 h using a spectrophotometer. Three replicates were included at each time point. The experiments were repeated twice (Li and Wang, 2011).

Table 3.1. Bacterial Strains used in this study[a]

Strain	Host (Citrus species)	XacF1 Sensitivity	Source
X.axonopodis pv. *Citri*			
MAFF 301077	*C. limon*	-	NIAS[b]
MAFF 301080	*C. sinensis*	+	NIAS
MAFF 311130	*C. iyo*	-	NIAS
MAFF 302102	*Citrus* sp.	+	NIAS
MAFF 673001	*C. natsudaidai*	+	NIAS
MAFF 673010	*Citrus* sp.	+	NIAS
MAFF 673011	*C. limon*	-	NIAS
MAFF 673013	*Citrus* sp.	+	NIAS
MAFF 673018	*Citrus* sp.	+	NIAS
MAFF 673021	*C. limon*	-	NIAS
KC33	*C. iyo*	+	Shiotani et al. (2007).
Phages			
XacF1			This study

[a] All strains originated in Japan

[b] NIAS, National Institute of Agrobiological sciences, Japan.

3.3.2. Bacteriophage isolation, purification, and characterization

The presence of filamentous phages in collected soil samples from cropping fields in Japan was detected by the spot test and plaque-forming assay technique (Yamada et al., 2007). Approximately 10 g of soil was placed in a sterile 50 mL conical centrifuge tube that then was filled to the top with tap water, and allowed to stand for 20 min with periodic inversions. The tubes were then centrifuged at 15000 ×g for 20 min and

the supernatant was passed through a membrane filter (0.45-µm pore size) (Millipore Corp., Bedford, MA, USA). One-hundred-microliter aliquots of the soil filtrate were subjected to spot test and plaque-forming assay with strains of *Xac* (Table 3.1) as host on NB plates containing 1.5% (w/v) agar. Phages were propagated and purified from single-plaque isolates. An overnight culture of bacteria grown in NB medium (1 mL) was diluted 100-fold with 100 mL of fresh NB medium in a 500 mL flask. To collect a sufficient amount of phage particles, a total of 2 L of bacterial culture was grown. When the cultures reached an OD_{600} of 0.2, bacteriophage was added at a multiplicity of infection (moi) of 0.001–1.0. After further growth for 12–24 h, the cells were removed by centrifugation in a Hitachi Himac CR21E centrifuge with an R12A2 rotor at 8000 × *g* for 15 min at 4°C. The supernatant was passed through a 0.45-µm-pore membrane filter followed by precipitation of the phage particles in the presence of 0.5 M NaCl and 5% (v/v) polyethylene glycol 6000 (Kanto Chemical Co., Tokyo, Japan). The pellet was collected by centrifugation in a Hitachi Himac CR21E centrifuge with an RPR20-2 rotor at 15 000 × *g* for 30 min at 4°C, and was dissolved in SM buffer (50 mM Tris/HCl at pH 7.5, 100 mM NaCl, 10 mM $MgSO_4$ and 0.01% gelatin (w/v)). Phages were stored at 4°C in complete darkness. Phage titers were determined by serial dilution and subsequent plaque-forming assays (Yamada et al., 2007). The purified phage (10^{13} pfu/mL was stained with sodium phosphotungstate prior to observation in a Hitachi H600A electron microscope, according to the methods of Dykstra (1993).

3.3.3. Phage susceptibility and adsorption assays

The phage susceptibility assays were based on a standard agar overlay method with dilution series of phage preparations (Yamada et al., 2007; Ahmad et al., 2014). Small turbid plaques, typical of Ff-phages, always appeared at reasonable frequencies

depending on input phage titers (usually 300–600 pfu/plate), if the bacterial strain was sensitive to the phage. No spontaneous phages (induced prophages) appeared from either strain tested under usual plaque assay conditions. In the phage adsorption assay, exponentially growing cells (OD_{600} 0.1) of the test strain were mixed with XacF1 phage at moi of 0.1, and the mixture was incubated for 0 min (no adsorption) and 30 min at 28°C to allow binding of the phage to the cell surface. Following centrifugation at 15,000 ×g for 5 min at 4°C in a Sakuma SS-1500 microcentrifuge (Sakuma Seisakusho, Tokyo, Japan), the phage titer in the supernatant was determined by a standard plaque assay with the indicator strain (MAFF301080). *Escherichia coli* JM109 was used as a negative control.

3.3.4. DNA isolation and manipulation

Standard molecular biological techniques for DNA isolation, digestion with restriction enzymes and other nucleases, and construction of recombinant DNAs were followed, according to Sambrook and Russell (2001). Phage DNA was isolated from the purified phage particles by phenol extraction. In some cases, extrachromosomal DNA was isolated from phage-infected *Xac* cells by the minipreparation method (Ausuble et al., 1995). Replicative-form (RF) DNA for sequencing was isolated from host bacterial cells infected with XacF1 phage, treated with S1 nuclease, and then shotgun-sequenced by Hokkaido System Science Co. (Sapporo, Japan) using a Roche GS Junior Sequence System. The draft assembly of the obtained sequences was assembled using GS *De Novo* Assembler v2.6. The analyzed sequences corresponded to 156 times the final genome size of XacF1 (7325 bp). Computer-aided analysis of the nucleotide sequence data was performed using DNASIS v3.6 (Hitachi Software Engineering Co., Tokyo, Japan). Potential ORFs larger than 80 bp were identified using the online program ORF Finder (http://www.ncbi.nlm.nih.gov/gorf/gorf.html)

and the DNASIS program. Sequence alignment was performed using the ClustalW (Larkin et al., 2007) program. To assign possible functions to the ORFs, DDBJ/EMBL/GenBank databases were searched using the FASTA, FASTX, BLASTN, and BLASTX programs (Altschul et al., 1997)

3.3.5. Determination of *att*L and *att*R sequences in *Xac* MAFF673010

Chromosomal DNA was extracted from *Xac* MAFF673010 after infection with XacF1 and subjected to PCR to amplify fragments containing left and right attachment sites (*att*L and *att*R*)*. The *att*L was amplified using a 29-base forward primer, 5'-TGC GAT CGA GCA GCT TCC CAG TTG GCG AT-3' (primer P1) and a 30-base reverse primer, 5'-TTC GAT GGT CAC GGT GCC TGT AGT AGA GGC-3' (primer P2), while *att*R was amplified using a 30-base forward primer, 5'-ATA ATT TGC TTG ACA CCG TGC GCA AGT CGT 3' (primer P3) and a 28-base reverse primer, 5'-CCT TGA CCG TCA GGG ACT GCA TCA GCC T-3' (primer P4). The primer sequences were based on the *dif* (*att*B*)* region sequence of *Xanthomonas citri* subsp. *citri* Aw12879 (DDBJ accession no. CP003778.1). The PCR products were purified from an agarose gel and subjected to sequencing.

3.3.6 Southern hybridization

Genomic DNA from bacterial cells was prepared by the minipreparation method according to Ausubel et al. (1995) Following digestion with restriction enzyme *Hin*cII, DNA fragments were separated by agarose gel electrophoresis, blotted onto a nylon membrane (Piodyne; Pall Gelman Laboratory, Closter, NJ, USA), hybridized with a probe (the entire XacF1 DNA digested by *Eco*RI), labeled with fluorescein (Gene Images Random Prime labeling kit; Amersham Biosciences, Uppsala, Sweden), and detected with a Gene Images CDP-Star detection module (Amersham Biosciences). Hybridization was performed in buffer containing 5× SSC (0.75 M

NaCl, 0.075 M sodium citrate), 0.1% (w/v) sodium dodecyl sulfate (SDS), 5% liquid block, and 5% (w/v) dextran sulfate for 16 h at 65°C. The filter was washed at 60°C in 1× SSC and 0.1% (w/v) SDS for 15 min and then in 0.5× SSC and 0.1% (w/v) SDS for 15 min with agitation, according to the manufacturer's protocol. The hybridization signals were detected by exposing X-ray film (RX-U; Fuji Film, Tokyo, Japan) to the filter.

3.3.7. EPS assay

EPS in bacterial culture supernatants was determined quantitatively as described previously (Guo et al., 2010). Briefly, bacterial strains were grown in NB supplemented with 2% (w/v) D-glucose for 24 h at 28°C with shaking at 200 rpm. A 10-mL portion of the culture was collected, and the cells were removed by centrifugation (5000 × *g* for 20 min). The supernatant was mixed with three volumes of 99% ethanol and the mixture was kept at 4°C for 30 min. To determine the dry weights of EPS, the precipitated EPS was collected by centrifugation and dried at 55°C overnight prior to measurement. Three replicates were used for each strain and the test was repeated three times.

3.3.8 Motility assay

Swimming and swarming motilities were examined on NB containing 0.3% (w/v) and 0.7% (w/v) agar (Difco, Franklin Lakes, NJ, USA), respectively. Overnight cultures of bacteria grown in NB were centrifuged at 8000 × *g* for 2 min at 4°C, washed twice with ddH_2O, and resuspended in ddH_2O (OD_{600}=1.0). Two microliters of the suspension were spotted onto NA plates (diameter, 90 mm; containing 20 mL of NA) and incubated at 28°C. The migration zones were measured, and used to evaluate the motility of *Xac* cells (Li and Wang, 2011; Addy et al., 2012). For twitching motility assays, overnight bacterial culture in NB were centrifuged at 8000 × *g* for 2 min at

4°C, washed twice with ddH_2O, resuspended in ddH_2O (OD_{600}=1.0), and spotted on minimal medium (MM) plates (Addy et al., 2012). Plates were incubated at 28°C, and the morphology of the colony edge was observed under a light microscope (100× magnification).

3.3.9. Bacterial surface appendages

Cells of *Xac* MAFF301080 were streaked heavily onto MM plates and incubated for 48 h. The colonies were suspended in a small volume of 10 mM Tris-HCl buffer at pH 8, and the cell suspension (same cell density in each sample) was forced five times through a 25- gauge hypodermic needle (Clough *et al*., 1994). Bacterial cells were removed by centrifugation at 8,000 × *g* for 20 min at 4°C. The bacterial surface appendages were collected by centrifugation at 136,000 × *g* for 60 min. Precipitated materials were subjected to Tris-Tricine sodium dodecyl sulfate polyacrylamide gel electrophoresis (SDS- PAGE) according to Schagger and von Jagow (Schagger *et al*., 1987). The identification of PilA was done according to Addy et al. (2012).

3.3.10. Pathogenicity assay

After careful washing with tap water, immature fully expanded lemon leaves were sterilized by soaking for 2 min in sodium hypochlorite, followed by rinsing in sterilized water. Leaves were placed on the surface of filter paper with abaxial surfaces facing upwards. Lemon leaves were inoculated with bacterial suspension of Xac phage-uninfected and phage-infected strains (108 cfu/mL in sterile water) using an infiltration or a needle pricking method. The infiltration method was conducted by pushing a needleless syringe containing the bacterial suspension against the surface of a citrus leaf supported by a finger on the opposite side of the leaf. The treated areas were immediately marked following inoculation (Chen et al., 2012). Needle-prick

inoculation was performed by pricking the leaves, and droplets (10 μL) of bacterial suspensions were applied to each inoculation site. In both methods, the inoculated leaves were covered with a plastic bag for 48 h to facilitate the infection. Leaves were incubated in a growth chamber at 28°C with a photoperiod of 12 h light and 12 h dark for 4 weeks (Verniere et al., 1998; Li and Wang, 2011; Malamud et al., 2012).

3.3.11 Phage stability test

We used *Xac* strain MAFF301080 because it was free from a XacF1 sequence in the genome. After infection with XacF1, a single colony was isolated and confirmed for its production of phage particles, the presence of XacF1 DNA in the cells by miniprep, and no integration of XacF1 DNA in the chromosome by PCR with a primer set of chromosomal sequences, 5'-ACT CGC TTT GCA TGA AAT TCG CTA GCG AT-3' (forward) and 5'-TTC GAT GGT CAC GGT GCC TGT AGT AGA GGC (reverse). After cultivation in NB at 28˚C for several generations, random colonies spread on NA plates were picked and subjected to plaque assay, miniprep for XacF1 DNA, and PCR to detect lysogeny with the same primers as above.

3.3.12. Nucleotide sequence accession number. The sequence of the XacF1 genome has been deposited in the DDBJ under accession no. AB910602.

3.4. Results

3.4.1. Isolation, morphology, and host range of XacF1

A total of 20 phages were isolated from soil samples collected from citrus fields in Japan using a plaque assay on *Xac* strains (see Experimental Procedures), one of which formed small and turbid plaques (designated XacF1). A single plaque of this phage was picked for propagation, purification, and further experiments. Electron micrographs using highly purified phage particles (10^{13} pfu/mL) showed that XacF1 virions have typical filamentous phage features, with a long fibrous shape

approximately 600 nm in length (Fig. 3.1A). To determine the host range of the phage, *Xac* strains infecting different citrus species were tested for phage susceptibility (Table 3.1). The host range of the XacF1 phage was relatively wide, infecting 7 out of 11 *Xac* strains tested in this study (Table 3.1).

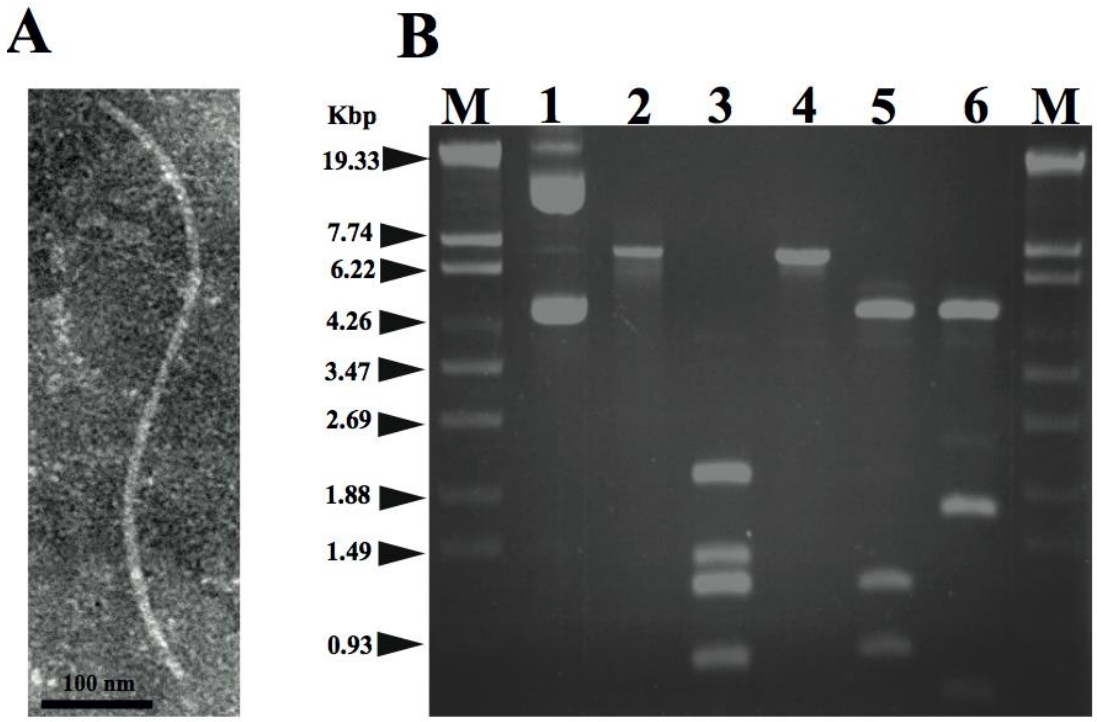

Figure 3.1. (A) Morphology of the XacF1 phage. The purified particles of XacF1 were negatively stained with phosphotungstate and examined by transmission electron microscopy. A filamentous structure was observed (approximately 1000 nm in length and 7 nm in width). (B) Restriction patterns of the replicative form of the XacF1 genomic DNA. Lanes: 1, undigested XacF1 DNA (RF); 2, digested with S1 nuclease; 3, *Hin*cII; 4, *Eco*RI; 5, *Eco*RV; 6, *Cla*I; M, λ *Sty*I marker.

3.4.2 Nucleotide sequence and genomic organization of XacF1

The genomic DNA of XacF1 was obtained as a replicative form (RF) from MAFF301080 as a host. XacF1 phage genomic DNA was digested using several restriction enzymes; *Eco*RI digestion produced a single band corresponding to approximately 7.3 kb on an agarose gel (Fig. 3.1B, lane 4). The genomic DNA isolated from phage particles was completely digested by S1 nuclease treatment (data not shown), suggesting that the XacF1 genome is a circular single stranded DNA, like those of all other filamentous phages.

To determine the entire nucleotide sequence of XacF1, DNA was shotgun-sequenced. The results showed that the complete genome was 7325 nucleotides long, with a G+C content of 57.8%, which was significantly lower than that of the host genome (i.e. 64.7% for strain 306, accession no. NC_003919). There were 13 putative open reading frames (ORFs), of which 11 were located on the same strand and two were on the opposite strand (Table 3.2 and Fig. 3.2). When databases were searched for sequences homologous to the XacF1 DNA sequence using BLAST and BLASTX programs, nine ORFs showed high similarity to ORFs previously reported for other filamentous phages, especially to ORFs of *X*. *campestris* pv. *citri* phage Cf1c (Kuo *et al*., 1991) (accession no. NC_001396), *X*. *campestris* pv. *vesicatoria* Cf1 phage (YP_364205.1), and *X*. *campestris* pv. *campestris* phi-Lf phage (X70328) (Table 3.2). XacF1 ORFs could be arranged in a similar modular structure to that of previously characterized filamentous phages of the Ff group (Model and Russel 1988; Marvin 1998), as shown in Fig. 3.2 Within the putative replication module (Fig. 3.2), we identified ORF1 and ORF2. The peptide encoded by ORF1 was homologous to filamentous phage phi-Lf replication initiation protein II (98% amino acid sequence identity) (Table 3.2). This gene encodes the pII protein, which is necessary for

rolling-circle replication of phage genomes (Model and Russel, 1988). The deduced amino acid sequence encoded by ORF2 was homologous to peptides that mapped at the same position as the ssDNA binding protein (gV gene) of Ff phages, and its size was similar to that of this binding protein (Fig. 3.2 and Table 3.2). Within the putative structural module of XacF1, we predicted five ORFs. ORF3 showed similarity to a hypothetical *Xanthomonas* protein (Table 3.2), with 32% amino acid sequence identity to a transmembrane motif (WP_005416529), supporting the hypothesis that ORF3 belongs to the module of structural genes (Fig. 3.2). Moreover, ORF4, ORF5, and ORF7 (Fig. 3.2 and Table 3.2) were the same size and in the same position as genes encoding the coat proteins of Ff phages. Another possible ORF included in this module was ORF6 (with similarity to coat protein Cf1c phage cp3, Kuo *et al*., 1991), which was similar in both size and location to *gIII* of the Ff phage. *gIII* encodes *p*III, a minor coat protein that recognizes and interacts with receptors and coreceptors on the host cells (Armstrong et al., 1981; Lubkowski *et al*., 1999; Heilpern and Waldor, 2003) (Fig. 3.2 and Table 3.2). It also showed 28% amino acid sequence identity to phage adsorption protein of *Xanthomonas citri* subsp. *citri* (YP_007649573). Therefore, ORF6 could be a homolog of g*III* in XacF1. In the third putative module of XacF1, the assembly module, we found that ORF8 showed the highest homology to the cp4 protein of Cf1c phage (Fig. 3.2 and Table 3.2), and to the zot protein of *Xanthomonas vesicatoria* (WP_005997731), with 59% amino acid sequence identity. Also, based on its size and position, it seems that ORF8 is a homolog of *p*I. XacF1 does not encode a *p*IV homolog, hence like many filamentous phages it must use a host encoded *p*IV homolog, outer membrane protein of the secretin family. Interestingly, we found that ORF12 might encode a regulator gene similar to those found in several filamentous phages, because amino acids encoded by this ORF

exhibited similarity to several putative transcriptional regulators and DNA-binding helix-turn-helix proteins of phages (e.g., Cp8 of *X*. *campestris* pv. *citri* phage Cf1c (99% amino acid identity) (Shieh *et al*., 1991); phage repressor of *Vibrio parahaemolyticus* V-223/04, exhibiting 45% amino acid identity, EVU16279, E-value = 0.71). ORFs 9, 10, 11, and 13 had homology to hypothetical proteins of phages and bacteria, but did not appear to belong to any of the previously described modules.

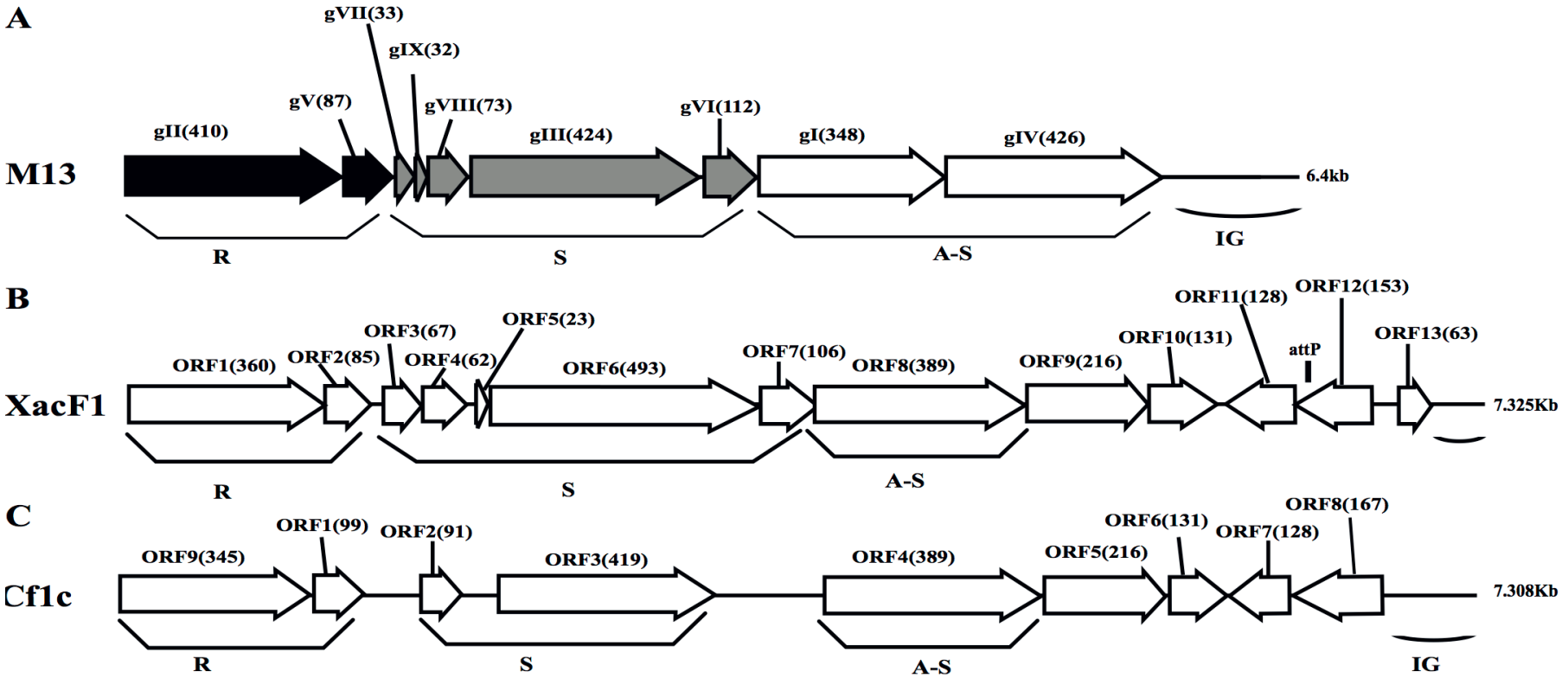

Figure 3.2. Genomic organization of bacteriophage XacF1. Linear genomic maps of *E. coli* phage M13 (A), XacF1 (B), and Cf1c (C) are compared. Arrows oriented in the direction of transcription represent ORFs or genes. The functional modules for replication (R), structure (S), and assembly-secretion (A-S) are indicated according to the M13 model (Marvin, 1998). Map for Cf1c was drawn according to the genomic sequence (accession no. NC_001396, Kuo et al., 1991). ORF sizes (in amino acids) are in parentheses. IG (intergenic region), and *att*P are also shown.

Table 3.2. Predicted ORFs found in the XacF1 genome.

Coding Sequence	Strand	Position 5` to 3`	GC Content (%)	Length of Protein (aa)	Molecular mass (Kda)	Amino acid sequence identity/similarity to best homologs (no. of amino acid identical; % identity)	E value	Accession no
ORF1	+	1-1080	57.7	360	40.5	Filamentous phage phiLf replication initiation protein II (340; 98)	0.0	YP_005637352
ORF2	+	1077-1373	57.3	99	9.1	V protein *Xanthomonas* phage Cf1c (73; 99)	2e-46	NP_536673
ORF3	+	1405-1605	51.4	67	7.2	Hypothetical protein- *Xanthomonas* (65; 98)	2e-40	WP_010378728
ORF4	+	1611-1868	60.5	62	8.4	B coat protein -Xanthomonas phage Cf1c (62; 100)	6e-33	Q38618
ORF5	+	1928-1995	55	23	5.9	No significant similarity	-	
ORF6	+	1996-3474	55.8	493	51.7	A coat protein -*Xanthomonas* phage Cf1c (383; 96)	0.0	Q38619
ORF7	+	3474-3791	54.2	106	11.5	Hypothetical protein - *Xanthomonas campestris* (103; 98)	5e-67	WP_010378725
ORF8	+	3788-4954	59.0	389	42.8	Hypothetical protein Cf1cp4 *Xanthomonas* phage Cf1c (388; 100)	0.0	NP_040477
ORF9	+	4954-5601	59.4	216	23.5	Hypothetical protein Cf1cp5 -*Xanthomonas* phage Cf1c (214; 99)	4e-148	NP_536676
ORF10	+	5617-6009	56.6	131	14.4	Hypothetical protein Cf1cp6 -*Xanthomonas* phage Cf1c (130; 100)	4e-88	NP_536677
ORF11	-	6047-6430	59.7	128	14.4	Hypothetical protein Cf1cp7 - *Xanthomonas* phage Cf1c (127; 100)	1e-86	NP_536678
ORF12	-	6427-6885	57.6	153	16.4	- Filamentous phage Cf1 protein -*Xanthomonas campestris* pv. *vesicatoria* str. 85-10 (146; 90) - 18.2K protein -*Xanthomonas* phage Cf1c (164; 99)	3e-88 5e-113	YP_364205 NP_536679
ORF13	+	7015-7203	54.8	63	6.8	Hypothetical protein- *Xanthomonas axonopodis* (59; 95)	6e-32	WP_017171337

3.4.3. XacF1 uses host XerCD recombinases to integrate into the *Xanthomonas* genome

Homology searches of the DDBJ/EMBL/GenBank databases for the XacF1 sequence revealed similar sequences in the genomes of some *Xanthomonas* species. This result suggested possible integration of this kind of phage into the host genome. To test this possibility, we performed genomic Southern blot analysis of 11 strains of *Xac* using a XacF1 DNA probe. The results, shown in Fig. 3.3A, indicated that eight of the 11 strains contained hybridizing bands and, among them, seven strains showed similar hybridization patterns with variations in signal intensity. Therefore, XacF1 likely has a lysogenic cycle and integrates frequently into the host genome. Regarding the integration mechanism of XacF1, we could not find any genes or ORFs that encode a phage integrase in the genome (Table 3.2). In several cases, involvement of the host recombination system by XerC/D in integration of filamentous phages into host genomes has been established, including *Vibrio cholerae* phage CTXϕ (Huber and Waldor, 2002; Das *et al*., 2011). In CTXϕ integration, the *dif* site of the host genome (*att*B) forms a recombination complex with *dif*-like sequences on the phage genome (*att*P) (Val *et al*., 2005). We therefore looked for a possible *dif*-like sequence for *att*P on the XacF1 sequence and found a 15-bp *dif* core sequence of 5`-TAT ACA TTA TGC GAA (XacF1 positions 6504–6518). This sequence showed a high degree of homology to *att*P sequences of phages Cf1c (accession no. NC_001396) (Kuo *et al*., 1991), Cf16-v1 (M23621), ϕLf (X70328), CTXϕ (AΦ220606), and ϕVGJ (AY242528) (Fig. 3.3B). It was also reported that Cf1c, Cf1t, Cf16v1, and ϕLf phages of *X. campestris* use the XerCD recombinases of their host to integrate into the *dif* locus of the bacterial genome (Campos et al., 2003; de Mello Varani et al., 2008 Askora et al., 2012; Das et al., 2013). These results suggested that the filamentous

phage XacF1 uses the host XerC/D system for integration into the host genome. To confirm this, we obtained both *att*L and *att*R fragments by PCR from newly established XacF1-lysogenic cells of *X*. *axonopodis* pv. *citri* strain MAFF673010. The *att*L and *att*R sequences are aligned with XacF1 *att*P and *dif* of *X*. *axonopodis* pv. *citri* strain 306 (accession no. AE008923.1, Jalan *et al*., 2011) in Fig. 3C. From these results, we predicted XerCD binding sites according to Das et al. (2011) as shown in Fig. 3.3D. However, XacF1 *att*P is located within the coding region of ORF12, so following integration into *att*B of the host chromosome, ORF12 may be split into two portions. This change in ORF12 may affect XacF1 functions because ORF12 encodes a possible phage regulator, as described above.

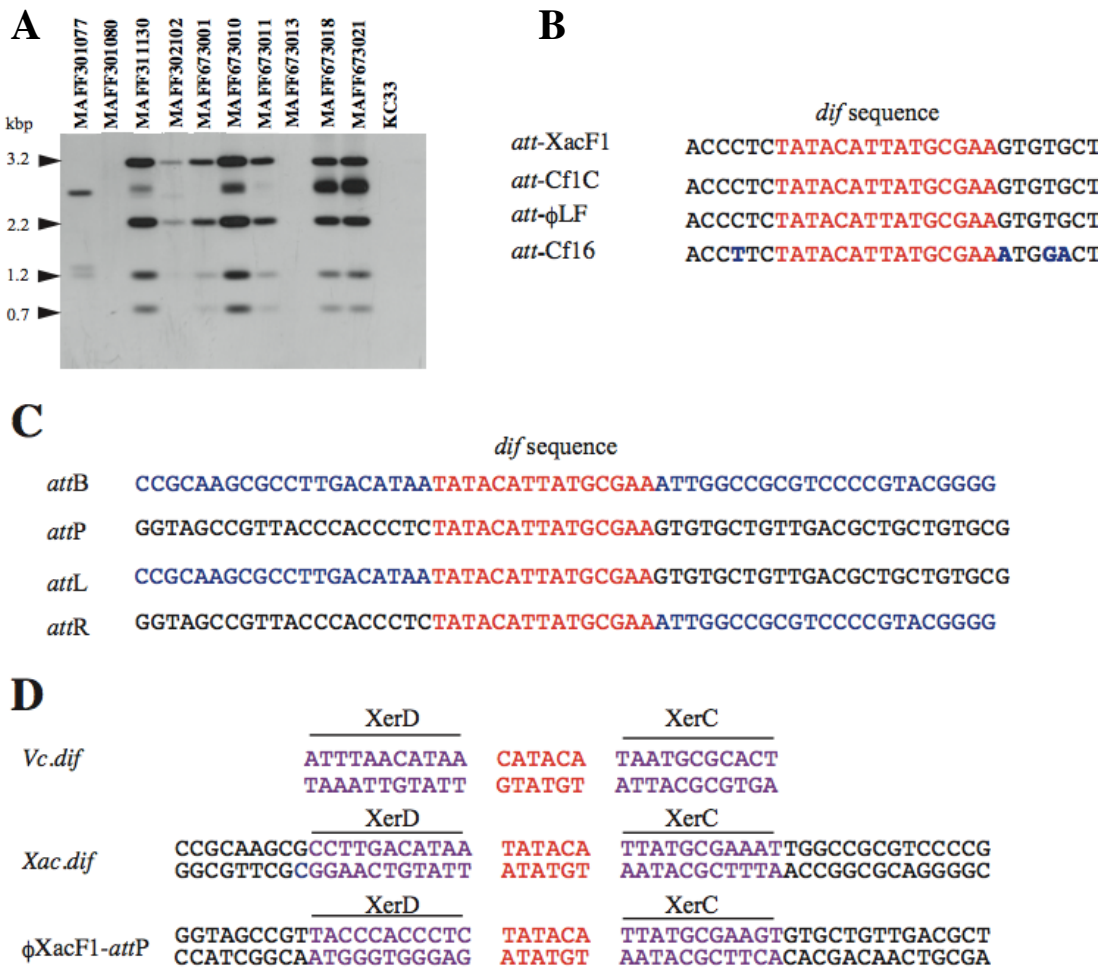

Figure 3.3. Site-specific integration of XacF1 DNA into the chromosome of *Xac*. (A) Southern blot hybridization analysis showing integration of the XacF1 phage into *Xac* host chromosomes. Genomic DNA of *X. axonopodis* pv. *citri* strains was digested with *Hin*cII and hybridized with a probe (the entire XacF1 phage genomic DNA digested with *Eco*RI). (B) The *att*P sequence indicated for XacF1 is compared with *att*P sequences (putative in some cases) of filamentous phages, including Cf1c (accession no. NC_001396), Cf16-v1 (M23621), and Lf (X70328) phages of *X. campestris*. The *dif* core sequences are shown in red. (C) Alignment of *att* sequences in the XacF1 integration system. The *att*L and *att*R sequences were determined for a lysogenic strain newly established with *Xac* MAFF673010 infected with XacF1. The *att*B sequence (*dif*) of *X. axonopodis* pv. *citri* 306 was obtained from the genome database (accession no. AE008923.1, Jalan *et al*., 2011). Common 15 bases are shown in red and chromosomal sequences are in blue. (D) Putative XerC, XerD binding sites of the XacF1 system are compared with those of *Vibrio cholerae dif*1.

3.4.3. Effects of XacF1 infection on the growth rate of *X. axonopodis* pv. *citri*

Unlike other bacterial viruses, the Ff phages do not kill their hosts, but establish a persistent coexistence in which new virions are continually released (Model and Russel, 1988). Because of this non-lytic mode of viral replication, it is possible to grow high-titer cultures of the virus. Similarly, infection by XacF1 did not cause lysis of host cells, but established a persistent association between the host and phage, releasing phage particles from the growing host cells**.** Although cells infected with XacF1 could continue to grow and divide indefinitely, the process caused the infected cells to grow at a significantly lower rate than uninfected cells (Fig. 3.4A).

3.4.4. Effect of XacF1 infection on host EPS production

EPS production was compared between uninfected and XacF1-infected cells of strain MAFF301080. The XacF1-infected cells used in this experiment were confirmed to be free from prophage by plaque assay of the culture supernatant, Southern hybridization (Fig. 3.3A), and PCR. The amount of EPS produced by the infected cells was significantly lower than that of the wild-type cells. We observed that following centrifugation, the culture pellets of the infected cells turned white, reflecting a low production of xanthan, which is the major component of EPS and is responsible for the yellow color of *Xanthomona*s culture in the media (Fig. 3.4B). Our prediction was confirmed by an EPS quantitation assay, which showed that the XacF1-infected cells had significantly lower EPS production (0.6 mg/ 10^{10} cfu) than uninfected cells (3.35 mg/ 10^{10} cfu).

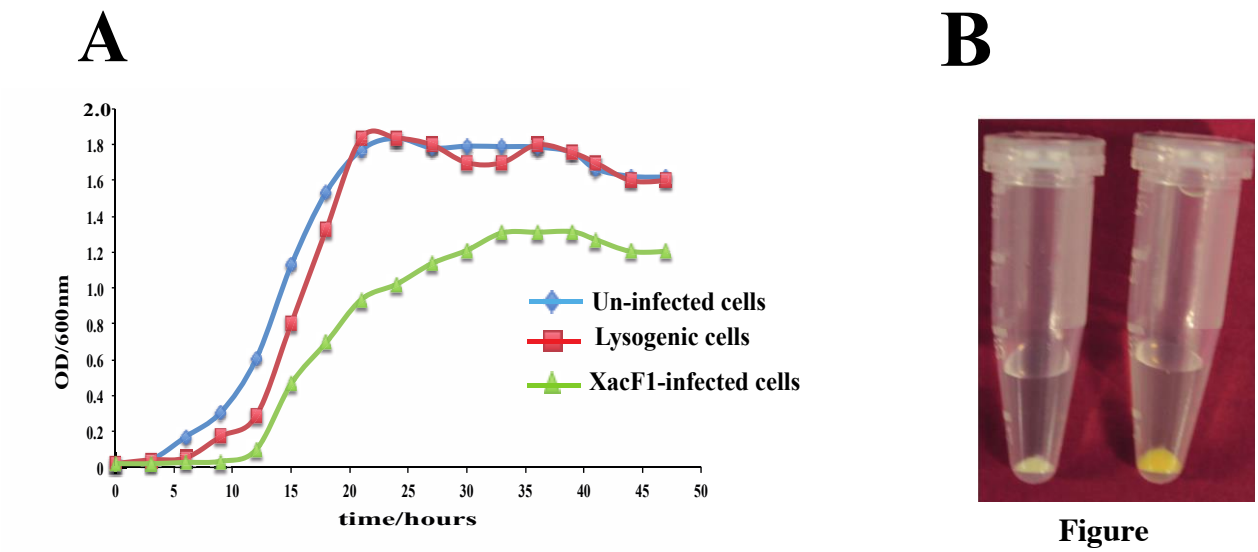

Figure

3.4. (A) Effects of XacF1 infection on the growth of *X. axonopodis* pv. *citri* (MAFF301080). (B) Effects of XacF1 infection on EPS production. The pellet of uninfected *Xac* MAFF301080 cells (right) was yellow, while the pellet of XacF1-infected cells (left) was white, indicating a defect in xanthan production.

3.4.5. Effect of XacF1 infection on host motility

Swimming, swarming, and twitching motilities of uninfected and XacF1-infected cells of strain MAFF301080 were compared. A significant reduction in swimming and swarming motility was observed in XacF1-infected cells (Fig. 3.5 A, B, C, D). When visualized with a microscope, the colony margin of uninfected cells had a highly irregular shape, indicating proficient twitching motility, whereas the colony edge of XacF1-infected cells was smooth (Fig. 3.5E), suggesting a decrease or loss of twitching motility. Because twitching motility is the surface movement associated with type IV pili (Marques et al., 2002; Meng et al., 2005), XacF1 infection may have affected the type IV pilus structures and/or functions of the host cells. We examined whether cell surface structural components were affected by XacF1 infection. Cell surface structure proteins were prepared by passing bacterial cells through a hypodermic needle, separated by SDS-PAGE, and compared between XacF1-infected and uninfected cells. XacF1-infected cells had considerably decreased levels of PilA, the major component of type IV pili, and decreased levels of FilC, flagellin (supplemental Fig. 3.6).

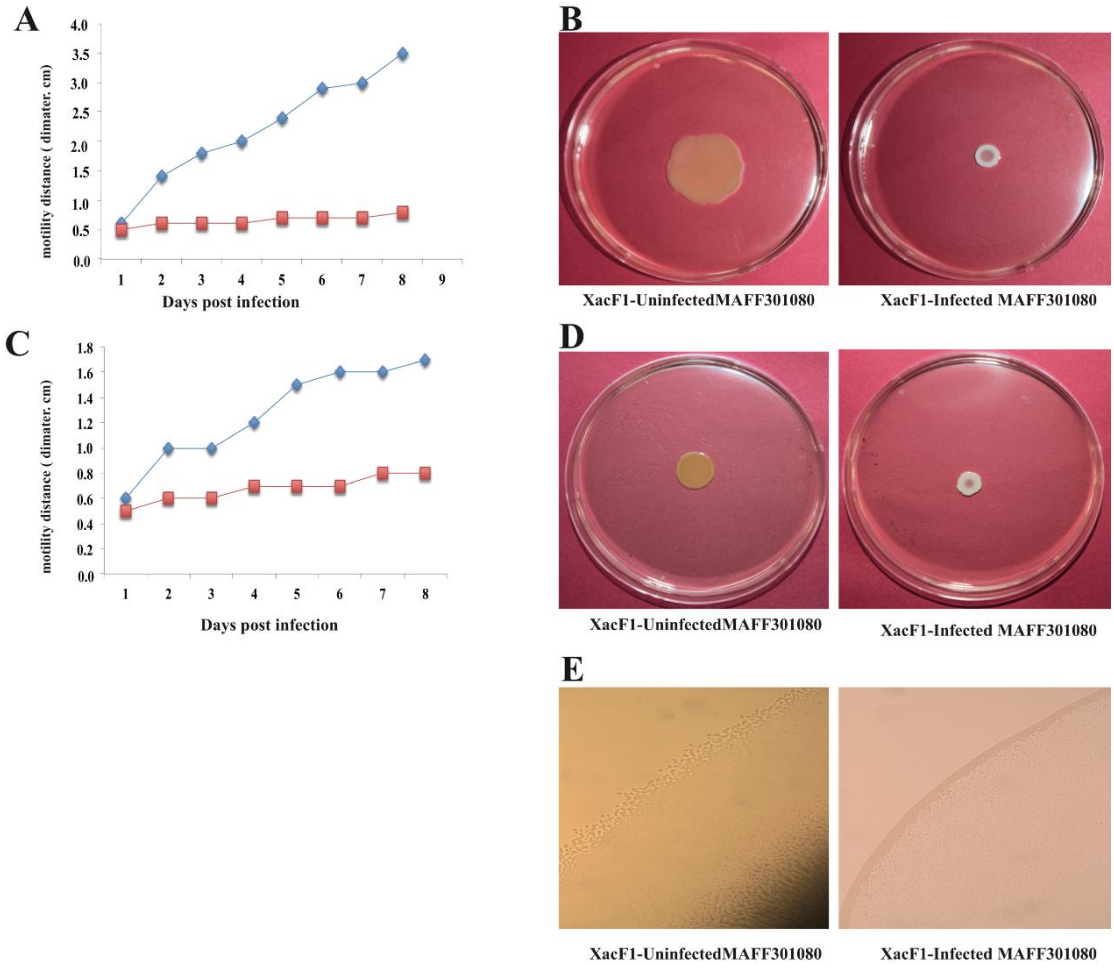

Figure 3.5. Impact of XacF1 infection on the motility of *Xac* MAFF301080 cells. Two microliters of bacterial solution (10^8 colony forming units (CFU)/mL) were inoculated in the swimming assay (0.3% (w/v) agar) (A, B), swarming assay (0.7% (w/v) agar) (C, D), and twitching motility assay (minimal agar medium) (E). The movement of bacterial cells was photographed 5 and 8 days post-inoculation (dpi) on the swimming and swarming plates, respectively. Twitching motility of bacteria was observed under a microscope 5 dpi on the twitching plates.

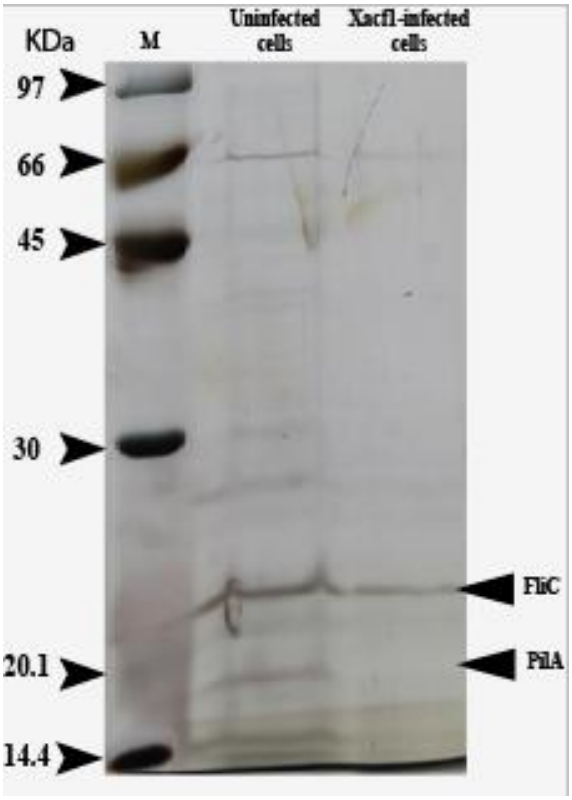

Figure 3.6. Comparison of proteins from cell surface structures. Cell surface appendages were released by passing bacterial cells through a hypodermic needle and their protein components were solubilized, separated by sodium dodecyl sulfate polyacrylamide gel electrophoresis, and stained with Coomassie blue. Molecular size of each marker protein (from Amersham LMW gel filtration kit) is indicated on the left. FliC, PilA, proteins were identified by their N-terminal amino acid sequence (Addy et al., 2012).

3.4.6. Effects of XacF1 infection on virulence of *X. axonopodis* pv. *citri*

Wild-type cells of strain MAFF301080 caused infection symptoms 4 days post-infection, and formed clear cankers 1 week post-inoculation (Fig. 3.6A). Starting from 2 weeks post-infection, the lesion became brown in color and its center became raised and spongy or corky, typical canker symptoms (Graham et al., 2004) that reflected the aggressive virulence of this strain. In contrast, the symptoms of XacF1-infected MAFF301080 cells were relatively weak, and no mature canker symptoms were observed up to 4 weeks post-infection, except for marginal lesions formed around the pricking site (Fig. 3.6A). To be more precise, we measured lesion size (Fig. 3.6B), which showed that in uninfected cells, the lesions were large with a smooth center, spongy raised top, and their distribution around the infected area reached more than 6.5 mm in width 4 weeks post-infection. In contrast, the lesions formed by XacF1-infected cells remained weak and dry, and they did not expand more than 1 mm in width. Another inoculation method, in which we infiltrated the bacterial suspension into the lemon leaves, showed that XacF1-uninfected MAFF301080 cells incurred water soaking at the inoculation site 3 days post-infection, and then an erumpent tissue reaction was obvious 1 week after inoculation. The erumpent tissue expanded to an aggressive canker area on both sides of the leaf, and then the lesions became dark and decayed with a yellow halo at the inoculation site 4 weeks post-infection (Fig. 3.6C). However, in XacF1-infected cells, a slight water-soaking area on the leaf surface was only visible 2 weeks after inoculation, and weak canker symptoms could be seen 4 weeks post-infection. In all cases, leaves inoculated with ddH_2O showed no canker symptoms.

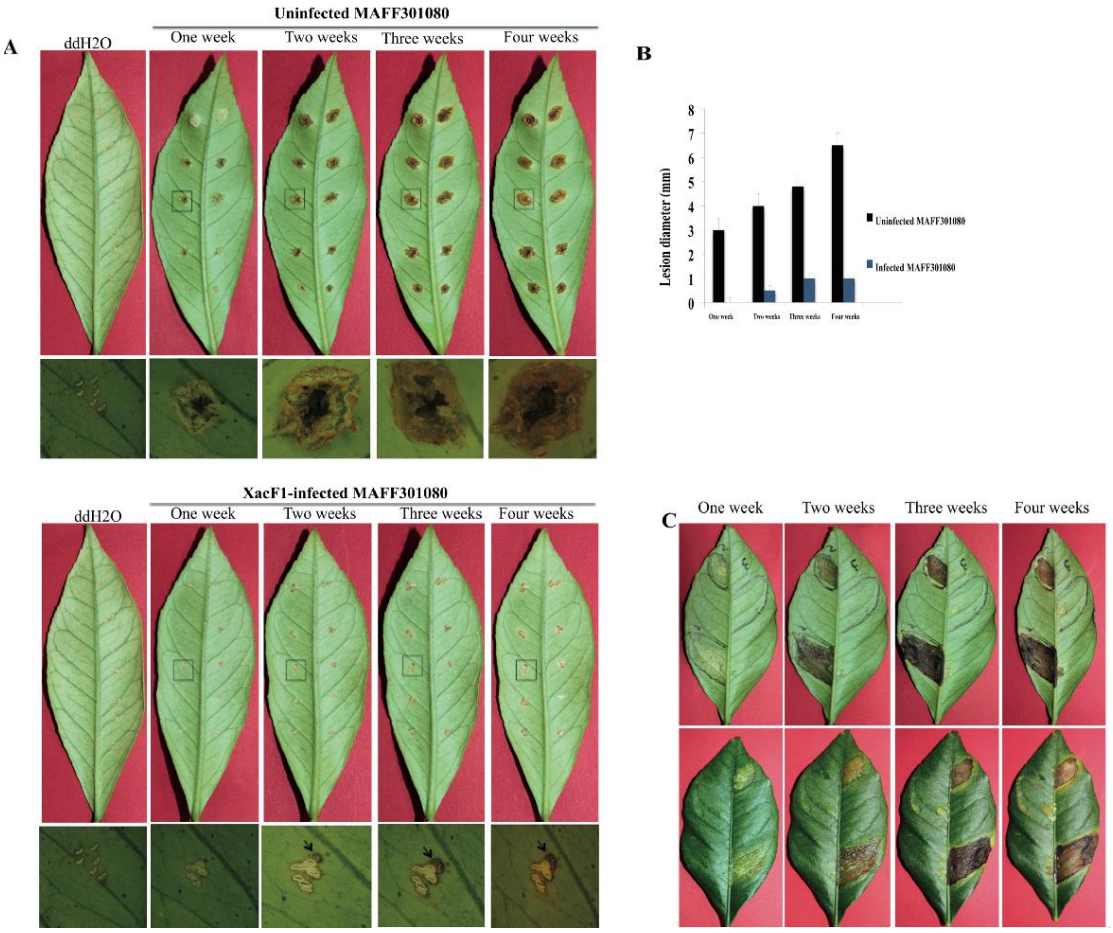

Figure 3.7. Lesions on detached lemon leaves inoculated with cells of *Xac* MAFF301080. (A) Canker symptoms that had developed on leaves 1, 2, 3 and 4 weeks post-infection by the needle-pricking method. Leaves were inoculated with uninfected cells (upper panels) or XacF1-infected cells (lower panels). Leaf areas shown by a square were examined by photomicroscopy and the microscopic images are shown under each corresponding leaf. Characteristic canker lesions occurred with uninfected cells, while no obvious cankers developed on XacF1-infected cells. (B) Comparison of the size of lesions formed on lemon leaves. (C) Lesions formed on lemon leaves by infiltration of bacterial cells. Uninfected MAFF301080 cells were applied to two areas of the leaf (left half of the abaxial side), and XacF1-infected cells were similarly applied to the right side (upper panels). Lesions on the adaxial side are also shown in lower panels. Lesions on both lower and upper surfaces of leaves inoculated with the uninfected cells showed severe symptoms, expanding with time. No lesions formed on either surface of the leaves infected with XacF1-infected cells.

3.5. Discussion

In this study, we isolated and characterized a filamentous phage, named XacF1, that infects *X. axonopodis* pv. *citri* strains. The isolated phage had a relatively wide range of host bacterial strains. Of particular interest, this study showed that along with the phage infection, the infected cells had decreased ability to form citrus cankers and a loss of virulence. We demonstrated that the canker symptoms of XacF1-infected lemon leaves were dramatically mitigated up to 4 weeks post-infection using both pricking and infiltration methods of inoculation (Fig. 6 A, B, C). The significant reduction in EPS (xanthan) production caused by XacF1 phage could be one of the reasons for such a dramatic decrease in canker formation. Virulence of numerous phytopathogenic bacteria, particularly various *Xanthomonas* species, is correlated with their ability to produce EPS (Bellemann and Geider, 1992; Chou et al., 1997; Dharmapuri and Sonti, 1999; Dolph et al., 1998; Kao et al., 1992; Katzen et al., 1998; Kemp et al., 2004; Yu et al., 1999). The multiple functions of EPS in virulence include protection of bacteria from toxic plant compounds, reduction of bacterial contact with plant cells to minimize host defense responses, promotion of bacterial multiplication by prolonging water soaking of tissues, and supporting invasion or systemic colonization of bacterial cells (Denny, 1999). Another possible role of EPS is to confer epiphytic fitness. It was previously suggested that EPS functions during both epiphytic and pathogenic phases of infection in *X. campestris* pv. *campestris* (Poplawsky and Chun, 1998; Rigano et al., 2007). As significant differences in virulence were observed between wild type and xanthan-deficient mutant strains of other *Xanthomonas* species, Dunger et al. (2007) proposed that in citrus canker, xanthan supports epiphytic survival in citrus canker, but is not required for colonizing nearby tissue. Without xanthan the bacteria were unable to retain water and could not

withstand abiotic stress and, thus, could not survive on the leaf surface. Therefore, xanthan works in two ways: to enhance bacterial virulence and to block the host defense. The drastic reduction in host EPS production caused by XacF1 infection may explain why the XacF1-infected cells showed dramatically decreased virulence.

Another major finding is the significant reduction in the swimming, swarming, and twitching motilities of *Xac* cells following infection by XacF1. Bacteria use a variety of motility mechanisms to colonize host tissues. These mechanisms include flagella-dependent swimming and swarming for movement in liquid surfaces, and flagella-independent twitching, gliding, and sliding for movement on solid surfaces (O'Toole and Kolter, 1998; Mattick, 2002; Harshey, 2003). Recent reports propose that bacterial adhesion and motility are required in the initial stages of *Xac* biofilm formation, whereas lipopolysaccharide and EPS play important roles in the establishment of mature biofilms (Li and Wang, 2011). The reduction in motility of XacF1-infected cells may be because filamentous phages such as XacF1 assemble on the host cell membrane and protrude from the cell surface, and so the nature of the host cell surface may change drastically during phage production (Addy et al., 2012). As shown in Fig. 3.6 XacF1-infected cells had considerably decreased levels of PilA, the major component of type IV pili.

Frequent protrusion of XacF1 particles from the infected cell surface may somehow compete with the formation of type four pili (Tfp). As reported by Kang et al. (2002), Tfp is responsible for twitching motility and adherence to multiple surfaces and is required for virulence. Interestingly, ORF 9 of the XacF1 phage (Table 3.2) showed significant homology to a TraX family protein (H8FlE6, E-value = 1e−70) and a putative F pilin acetylation protein (Q3BsT0, E-value = 4e−70), involved in pilus modification. Therefore, the loss of virulence in the XacF1-infected cells seems

to be, at least partly, caused by the reduction or modification of Tfp formation and decrease in swimming, swarming, and twitching motilities.

Several works have described the use of phages for control of bacterial citrus canker caused by *X. campestris* pv. *citri* (Balogh et al., 2010). In those cases, the bacteriophages used for foliar plant diseases interacted with the target bacteria on the leaf surface, the phylloplane. The phylloplane is a constantly changing environment: there are changes in temperature, sunlight irradiation, leaf moisture, relative humidity, osmotic pressure, pH, microbial flora, and, in the case of agricultural plants, chemical compounds (Jones et al., 2012). These factors may be harmful to bacteriophages to varying extents. Sunlight irradiation, especially in the UVA and -B range, is mainly responsible for eliminating bacteriophages within hours of application (Jones et al., 2012). To avoid quick inactivation of XacF1, we propose the application of XacF1-infected cells instead of XacF1 phage alone. The XacF1-infected cells can grow and continue to produce infectious phage, so the XacF1 phage may serve as an efficient long-lasting tool to control citrus canker by decreasing the virulence of the pathogen. Concerning the stability of XacF1-infected cells, we observed relatively high stability of "a free phage state" in the infected cells. After several bacterial generations, 100% cells contained XacF1 and more than 70% of them were at the state of producing free phages without integration into the host chromosome (confirmed by PCR)(data not shown). Even if once prophage states were established, we observed frequent spontaneous excision and production of phage particles.

Another possible way to use XacF1 for biological control may be given as a phage cocktail with other lytic phages, such as Cp1 and Cp2, originating from Japan, which can infect more than 97% of *Xac* strains and was recently characterized by Ahmad et al. (2014).

Chapter 4

General discussion

4.1. General discussion

Bacteria cause a number of economically important plant diseases. Bacterial outbreaks are generally problematic to control due to lack of effective bactericides and resistance development. As those plant diseases continue to have a serious impact on food production worldwide, new approaches for control are sought. This has seen resurgence of studies into the use of phage for prophylaxis and treatment of phytopathogens (Rebekah et al., 2012). Bacteriophages have recently been evaluated for control of several bacterial plant diseases. Phages have given great promising results and showed several characteristic results that make them potentially attractive biocontrol agents. However, there are some disadvantages for bacteriophages that limit their success and there are many challenges facing their use.

The first goal of this study was full characterization of Cp1 and Cp2, the historical *Xanthomonas* phages originated from Japan. This would be very useful for understanding the nature of these phages and bacterial-phage interaction, which may improve the using of bacteriophage as biocontrol agents against plant diseases .This also provides an appropriate explanation for the host selection by the Cp1 and Cp2. The strains of *Xac*, the causative agent of citrus canker, are historically classified based on bacteriophage (phage) sensitivity. Nearly all *Xac* strains isolated from different regions in Japan are lysed by either phage Cp1 or Cp2; Cp1-sensitive ($Cp1^s$) strains have been observed to be resistant to Cp2 ($Cp2^r$) and vice versa. In this study, genomic and molecular characterization was performed for the typing agents Cp1 and Cp2. Morphologically, Cp1 belongs to the *Siphoviridae*. Genomic analysis revealed that its genome comprises 43,870-bp double-stranded DNA (dsDNA), with 10-bp 3'-extruding cohesive ends, and contains 48 open reading frames (ORFs). The genomic organization was similar to that of *Xanthomonas* phage phiL7, but it lacked a group I

intron in the DNA polymerase gene. Cp2 resembles morphologically *Escherichia coli* T7-like phages of *Podoviridae*. The 42,963-bp linear dsDNA genome of Cp2 contained terminal repeats. The Cp2 genomic sequence has 40 open reading frames, many of which did not show detectable homologs in the current databases. By proteomic analysis, a gene cluster encoding structural proteins corresponding to the class III module of T7-like phages was identified on the Cp2 genome. Therefore, Cp1 and Cp2 were found to belong to completely different virus groups. In addition, we found that Cp1 and Cp2 use different molecules on the host cell surface as phage receptors and that host selection of *Xac* strains by Cp1 and Cp2 is not determined at the initial stage by binding to receptors. Moreover, we found that both Cp1 and Cp2 phages could inject their DNA into the *Xac* resistant cells as well as in the sinsitive cells, reavealed by SYBR gold-labeled phage infection experiments.

Further molecular studies are needed to deeply understand the molecular mechanism of host selection by these phages. Notably, the sensitivity of *Xac* strains to Cp1 and Cp2 is associated with differences in their physiological features and canker aggressiveness. Concerning Cp1 and Cp2, the following issues are of particular interest: (A) the phage receptors on the host cell surface are different between Cp1 and Cp2; (B) Cp1 can attach to and inject its genome into the cells of Cp1-resistance strain and this is also the case for Cp2 (Ahmed et al., 2014). These results suggest some host selection mechanisms after DNA injection. I hypothesize that the clustered regularly interspaced short palindromic repeat (CRISPR), which is a bacterial immunity system that requires a perfect sequence match between the CRISPR cassette spacer and a protospacer in invading DNA for exclusion of foreign genetic elements, may be involved in the host selection by Cp1 and Cp2 phages. CRISPR cassettes are hypervariable, possibly reflecting different exposure of strains of the same species to

foreign genetic elements (Dupuis et al., 2013). Actually many CRISPR sets were detected in *Xanthomonas* species. To confirm specific digestion of phage DNA after injection into resistant host cells, SYBR gold-labeled phage DNA needs to be monitored by using a high-resolution fluorescence microscopy system (For example, BIOREVO BZ-900 Keyence). As results, DNA-degradation timing and patterns will be revealed. To further confirm involvement of CRISPR in Cp1/Cp2 host selection, isolation of CRISPR cassette sequences of both phage-sensitive and phage-resistance strains of *Xac* by PCR would be useful. Bioinformatics identification of a conserved sequence motif adjacent to *Xac* phages protospacers, and determination of DNA cleavage by CRISPR-Cas during phage infection will make it clear if the CRISPR is the main mechanism of Cp1/Cp2 host selection or not.

Treatment of lemon leaves with a mixture of Cp1 and Cp2 before the inoculation by *Xac* cells decrease the canker severity even with the Cp1 and Cp2 resistance strain (data not shown). This preliminary results need to be confirmed under open filed conditions and with a large-scale experiment.

In this study (chapter 3), a filamentous phage XacF1, which can infect *Xac* strains, was isolated and characterized. Electron microscopy showed that XacF1 is a member of the family *Inoviridae* and is about 600 nm long. The genome of XacF1 is 7,325 nucleotides in size, containing 13 predicted open reading frames (ORFs). Infection with the XacF1 phage did not cause host cell lysis but established a persistent association between the host and phage. Upon infection by XacF1 the host cells showed some abnormal behaviors such as lower levels of extracellular polysaccharide production, reduced motility, slower growth rate, and a dramatic reduction in virulence. This case of loss of virulence is very interesting. Using such phage as a biological control agent against citrus canker disease may solve the

problems of phage instability in the plant environments where naked phages are easily inactivated by sunlight UV irradiation. Molecular basis of loss of virulence by XacF1 infection should be deeply cahracterized. I hypothesize that XacF1-infection somehow decreased the expression level of some *Xac* virulence-related genes. The preliminary results from the comparative studies on the expression levels of some *Xac* virulence genes by using qRT-PCR (Jalan et al., 2013) showed that, in the case of the XacF1-infected cells, there was a reduction in the expression of several genes, especially the *nlxA* gene, the virulence related gene which is involved in the production of lipopolysaccharide and extracellular polysaccharide, motility, biofilm formation and stress resistance (Yan et al, 2012).

Moreover, changes occurred on the cell surface may be examined by electron microscopy. Changes on the cell surface induced by the infection and production of XacF1 particles may result in inactivation of quorum sensing activity of the host cells. Another possibility is direct repression of virulence genes by the phage-encoded repressor. We have already identified an ORF (ORF12) encoding 153-aa putative phage repressor located upstream of ORF11 on the XacF1 genome (DDBJ accession # AB910602). This ORF will be connected to *Xanthomonas* specific vector downstream of the constitutive *lac* promoter and introduced into MAFF 301080. Then transformants will be analyzed for changes in expression levels of several virulence-related genes. Frequently, XacF1-like prophage was found to be integrated in the genome of *Xac* strains. This integration occurred at the host *dif* site (*att*B) and was mediated by the host XerC/D recombination system. The *att*P sequence was identical to that of *Xanthomonas* phage Cf1c. Mutagenesis of *dif* site may show the effect of an integrated form and a free replicating form on the virulence. Results from these experiments will reveal the molecular basis of loss of virulence caused by infection

with filamentous phage XacF1. After the deletion of ORF 12, no integration occurred and the phage was only obtained as an episomic from the transformed *Xac* cells (data not shown). The twitching motility of the transformed cells was also decreased (unpublished results).

References

Ackermann, H. W. (2007). 5500 phages examined in the electron microscop. *Arch*. *Virol*. 152,227-243

Addy, H. S., Askora, A., Kawasaki, T., Fujie, M., and Yamada, T. **(2012).** Loss of virulence of the phytopathogen *Ralstonia solanacearum* through infection by ϕRSM filamentous phages. *Phytopathology* 102, 469-477.

Ahamd, M. H., and Morgan, V. (1994). Characterization of a cowpea (*Vigna undulata*) rhizobiophage and its effects on cowpea nodulation and growth. *Biol Fertil Soils* 18, 297-301.

Ahmad, A. A., Ogawa, M., Kawasaki, T., Fujie, M., and Yamada, T. (2014). Characterization of bacteriophages Cp1 and Cp2, the strain typing agents for *Xanthomonas axonopodis* pv. *citri*. *Appl*. *Environ*. *Microbiol*. 80, 77-85.

Altschul, S. F., Madden, T. L., Schaffer, A. A., Zhang, Z., Miller, W., and Lipman, D. J. (1997). Gapped BLAST and PSI-BLAST: a new generation of protein database search programs. *Nucleic Acids Res*. 25, 3389–3402.

Anitei, S. (2007). Where did citrus fruits originate from? *Softpedia*. Available from: http://news.softpedia.com/news/Where-Did-Citrus-Fruits-Originate-From 67365.shtml. Accessed 2011 June.

Arai, K., Shimo, H., Doi, Y., and Yora, K. (1974). Electron microscopy of *Xanthomonas citri* phages CP1 and CP2 infection. *Ann*. *Phytopath*. *Soc*. *Jpn*. 40, 98-102.

Armstrong, J., Perharm, R. N., and Walker, J. E. (1981). Domain structure of bacteriophage fd adsorption protein. *FEBS Lett*. 135, 167–172.

Askora, A., Abdel-Haliem, M. E., and Yamada, T. (2012). Site-specific recombination systems in filamentous phages. *Mol*. *Genet*. *Genomics* 287, 525–530.

Askora, A., Kawasaki, T., Usami, S., Fujie, M., and Yamada, T. (2009). Host recognition and integration of filamentous phage ϕRSM in the phytopathogen, *Ralstonia solanacearum*. *Virology* 384, 69–76.

Ausubel, F., Brent, R., Kjngston, R. E., Moore, D. D., Seidman, J. G., Smith, J. A., and Struhl, K. (1995). Short protocols in molecular biology, 3rd ed. John Wiley & Sons, Inc., Hoboken, NJ.

Balogh, B. (2002). Strategies for improving the efficacy of bacteriophages for controlling bacterial spot of tomato, MS thesis, University of Florida, Gainesville, FL, USA.

Balogh, B. (2006). Characterization and use of bacteriophages associated with citrus bacterial pathogens for disease control. PhD Dissertation, Gainesville, FL: University of Florida.

Balogh, B., Canteros, B. I., Stall, R. E., and Jones, J. B. (2008). Control of citrus canker and citrus bacterial spot with bacteriophages. *Plant Dis*. 92, 1048-1052.

Balogh, B., Jones, J. B., Iriarte, F. B., and Momol, M. T. (2010). Phage therapy for plant disease control. *Curr*. *Pharm*. *Biotechnol*. 11, 48-57

Balogh, B., Jones, J. B., Momol, M. T., Olson, S. M., Obradovic, A., King, P., and Jackson, L. E. (2003). Improved efficacy of newly formulated bacteriophages for management of bacterial spot on tomato. *Plant Dis*. 87:949-954.

Balogh, B., Jones, J. B, Iriarte, F. B., and Momol, M. T. (2010). Phage therapy for plant disease control. *Curr*. *Pharm*. *Biotechnol*. 11, 48–57.

Bartholomew, E. T., Sinclair, W. B. (1952). The lemon fruit. University of California, Berkeley. Berkeley, CA.

Belasque, J., Parra-Pedrazzoli, A. L., Rodrigues Neto, J., Yamamoto, P. T., Chagas, M. C. M., Parra, J. R. P., Vinyard, B. T., and Hartung, J. S. (2005). Adult citrus leafminers (*Phyllocnistis citrella*) are not efficient vectors for *Xanthomonas axonopodis* pv. *citri*. *Plant Dis*. 89, 590-594.

Bellemann, P., and Geider, K. (1992). Localization of transposon insertions in pathogenicity mutants of *Erwinia amylovora* and their biochemical characterization. *J*. *Gen*. *Microbiol*. 138, 931–940.

Bergamin, F. A., and Kimati, H. (1981). Estudos sobre um bacteriofago isolado de *Xanthomonas campestris*. II. Seu emprego no controle de *X*. *campestris* e *X*. *vesicatoria*. *Summa Phytopathol*. 7, 35–43.

Brunings, A., and Gabriel, D. (2003). *Xanthomonas citri*: breaking the surface. *Mol*. *Plant Pathol*. 4, 141–157.

Byrne, J. M., Dianese, A. C., Ji, P., Campbell, H. L., Cuppels, D. A., Louws, F. J., Miller, S. A., Jones, J. B., and Wilson, M. (2005). Biological control of bacterial spot of tomato under field conditions at several locations in North America. *Biol*. *Control* 32, 408-418.

Campos, J., Martinez, E., Suzarte, E., Rodriguez, B.L, Marrero, K., Silva, Y., Ledon T., del Sol, R., and Fando, R. (2003). VGJϕ, a novel filamentous phage of *Vibrio cholerae*, integrates into the same chromosomal site as CTXϕ. *J*. *Bacteriol*. 185, 5685–5696.

Carlson, K. (1994). Single-step growth, p 434 – 437. In: Karam J., Drake, J. W., Kreuzer , K. N., Mosig, G., Hall, D. H., Eiserlig, F. A., Black, L. W., Spicer, E. K., Kutter, E., Carlson, K., Miller, E. S. (ed), Molecular biology of bacteriophage T4. ASM Press, Washington, DC.

Ceyssens, P. J., Lavigne, R., Mattheus, W., Chibeu, A., Hertveldt, K., Mast, J., Robben, J., and Volckaert, G. (2006). Genomic analysis of *Pseudomonas aeruginosa* phages LKD16 and LKA1: establishment of the ϕKMV subgroup within the T7 subgroup. *J. Bacteriol*. 188, 6924-6931.

Cheetham, G. M., Jeruzalmi, D., Steiz, T. A. (1999). Structural basis for initiation of transcription from an RNA polymerase-promoter complex. *Nature* 399, 80-83.

Chen, P. S., Wang, L. Y., Chen Y. J., Tzeng, K. C., Chang, S. C., Chung, K. R., and Lee, M. H. (2012). Understanding cellular defence in kumquat and calamondin to citrus canker caused by *Xanthomonas citri* subsp. *citri*. *Physiol*. *Mol*. *Plant Pathol*. 79, 1–12.

Chou, F. L., Chou, H. C., Lin, Y.S ., Yang, B. Y., Lin, N. T., Weng, S. F., and Tesng, Y. H. (1997). The *Xanthomonas campestris gum*D gene required for synthesis of xanthan gum is involved in normal pigmentation and virulence in causing Black rot. *Biochem*. *Biophys*. *Res*. *Commun*. 23, 265-269.

Civerolo, E. (1984). Bacterial canker disease of citrus. *J*. *Rio Grande Val*. *Hortic*. *Soc*. 37, 127–146.

Civerolo, E. L., and Keil, H. L. (1969). Inhibition of bacterial spot of peach foliage by *Xanthomonas pruni* bacteriophage. *Phytopathology* 12, 1966-1967.

Cook, A. A. (1988). Association of citrus canker pustules with leafminer tunnels in North Yemen. *Plant Dis*. 72, 546.

Crosse, J. E., and Hingorani, M. K. (1958). A method for isolating *Pseudomonas mors-prunorum* phages from the soil. *Nature* 181, 60-61.

Das, B., Bischerour, J., Barre, F. X. (2011). VGJϕ integration and excision mechanisms contribute to the genetic diversity of *Vibrio cholerae* epidemic strains. *Proc*. *Natl*. *Acad*. *Sci*. *USA* 108, 2516–2521.

Das, B., Martínez, E., Midonet, C., and Barre, F. X. (2013). Integrative mobile elements exploiting *Xer* recombination. *Trends Microbiol*. 21 , 23–30.

de Mello Varani, A., Souza, R. C., Nakaya, H. I, de Lima, W. C., de Almeid, P., Watabnabe-Kitajima, E., Chen, J., Civerelo, E., Vasconceliss, A. T. R., and Van Sluys, M. A. (2008). Origins of the *Xylella fastidiosa* prophage- like regions and their impact in genome differentiation. *PLoS ONE* 3(12), e4059.

Delcher, A. L., Harmon, D., Kasif, S., White, O., and Salzberg, S. L. (1999). Improved microbial gene identification with GLIMMER. *Nucleic Acids Res*. 27, 4636-4641.

Denny, T. P. (1999). Autoregulator-dependent control of extracellular polysaccharide production in phytopathogenic bacteria. *Eur*. *J*. *Plant Pathol*. 105, 417–430.

Dharmapuri, S., and Sonti, R. V. (1999). A transposon insertion in the *gum*G homologue of *Xanthomonas oryzae* pv. *oryzae* causes loss of extracellular polysaccharide production and virulence. *FEMS Microbiol*. 179, 53–59.

Dolph, P. J., Majerczak, D. R., and Coplin, D. L. (1988). Characterization of a gene cluster for exopolysaccharide biosynthesis and virulence in *Erwinia stewartii*. *J*. *Bacteriol*. 170, 865–871.

Dunger, G., Relling, V. M., Tondo, M. L., Barreras, M., Ielpi, L., Orellano, E. G. and. Flaherty, J. E., Jones, J. B., Harbaugh, B. K., Somodi, G. C., and Jackson, L. E. (2000). Control of bacterial spot on tomato in the greenhouse and field with H-mutant bacteriophages. *HortScience*. 35, 882-884.

Dunn, J. J., and Studier, F. W. (1983). Complete nucleotide sequence of bacteriophage T7 DNA and the locations of T7 genetic elements. *J*. *Mol*. *Biol*. 166**,** 477–535.

Dupuis, M. E., Villion, M., Magadan, A. H., Moineau, S. (2013). CRISPR-Cas and restriction-modification systems are compatible and increase phage resistance. *Nat*. *Commun*. 4, 2087.

Dykstra, M. J. (1993). A manual of applied technique for biological electron microscopy, Plenum Press, New York, USA.

FAO. (1967). The state of food and agriculture. Rome, Italy.

FAO. (2012). http://faostat.fao.org/site/567/DesktopDefault.aspx?PageID=567#ancor

Frampton, R. A., Pitman, A. R., and Fineran, P. C. (2012). Advances in bacteriophage-mediated control of plant pathogens. *Int*. *J*. *Microbiol*. 326452 10.1155/2012/326452

Flaherty J. E., Harbaugh B. K., Jones J. B., Somodi G. C., and Jackson L. E. (2001). H-mutant bacteriophages as a potential biocontrol of bacterial blight of geranium. *HortScience* 36, 98– 100.

Fujiwara, A., Fujisawa, M., Hamasaki, R., Kawasaki, T., Fujie, M., and Yamada, T. (2010). Biocontrol of *Ralstonia solanacearum* by treatment with lytic bacteriophages. *Appl*. *Environ*. *Microbiol*. 77, 4155-4162.

Gabriel, D. W. (2001). Citrus canker. In: Encyclopedia of Plant Pathology (Maloy, O.C. and Murray, T.D., eds), pp. 215 – 217. New York: John Wiley & Sons.

Gill, J. J., and Abedon, S. T. **(2003)**. Bacteriophage ecology and plants. *APSnet* November. http://www.apsnet.org/online/feature/phages/.

Gill, J. J., Svircev, A. M., Smith, R., and Castle, A. J. (2003). Bacteriophages of *Erwinia amylovora*. *Appl*. *Environ*. *Microbiol*. 69, 2133-2138.

Gmitter, F. G., and Hu, X. L. (1990). The possible role of Yunnan, China, in the origin of contemporary citrus species (rutaceae). *Econ Bot*. 44:267–77.

Goodridge, L., and Abedon, S. T. (2003). Bacteriophage biocontrol and bioprocessing: Application of phage therapy to industry. *Society for Industrial Microbiology News* 53: 254-262

Goto, M. **(1962).** Studies on citrus canker. I. Bull. *Fac*. *Agri*. Shizuoka University 12: 3-72.

Goto, M. (1992). Fundamentals of bacterial plant pathology. Academic Press, Inc., San Diego, California.

Goto, M., Serizawa, S., and Morita, M. (1971). Studies on citrus canker disease. II. Leaf infiltration technique for detection of *Xanthomonas citri* (Hasse) Dowson, with special reference to comparison with phage method. hizuoka Daigaku Nogakubu Kenkyu Hokoku = Bulletin of the Faculty of Agriculture, Shizuoka University 20 pp. 1-19; 21-29

Goto, M., Takahashi, T., and Messina, M. A. (1980). A comparative study of the strains of *Xanthomonas campestris* pv. *citri* isolated from citrus canker in Japan and cancrosis B in Argentina. *Ann*. *of the Phytopathol*. *Soc*. *Japan*. 46, 329-338.

Gottwald, T. R., and Graham, J. H. (1992). A device for precise and nondisruptive stomatal inoculation of leaf tissue with bacterial pathogens. *Phytopathology* 82, 930-935.

Gottwald, T. R., Hughes, G., Graham, J. H., Sun, X., and Riley, T. (2001). The citrus canker epidemic in Florida: The scientific basis of regulatory eradication policy for an invasive species. *Phytopathology* 91, 30-34.

Gottwald, T., Graham, J., and Schubert, T. (**2002**) **[a].** Citrus canker: The pathogen and its impact. Online. Plant Health Progress doi: 10.1094/PHP-2002-0812-01-RV. St. Paul, MN: *American Phytopathological Society*.

Gottwald, T., Sun, X., Riley, T., Graham, J., Ferrandino, F., and Taylor, E. (2002)[b]. Georeferenced spatiotemporal analysis of the urban citrus canker epidemic in Florida. *Phytopathology*. 92, 362–377.

Graham, J. H., and Leite, R. P. Jr. (2004). Lack of control of citrus canker by induced systemic resistance compounds. *Plant Dis*. 88, 745-750.

Graham, J. H., Gottwald, T. R., Riley, T. D., and Achor, D. (1992). Penetration through leaf stomata and strains of *Xanthomonas campestris* in citrus cultivars varying in susceptibility to bacterial diseases. *Phytopathology* 82, 1319-1325.

Graham, J.H., Gottwald, T.R., Cubero, J., and Achor, D.S. (2004). *Xanthomonas axonopodis* pv. *citri*: factors affecting successful eradication of citrus canker. *Mol*. *Plant*. *Pathol*.5, 1–15.

Greer, G. G. (2005). Bacteriophage control of foodborne bacteria. *J Food Prot* 68, 1102-1111.

Guo, Y., Sagaram, U. S., Kim, J. S., and Wang, N. (2010). Requirement of the galU gene for polysaccharide production by and pathogenicity and growth in planta of *Xanthomonas citri* subsp. *citri*. *Appl*. *Environ*. *Microbiol*. 76, 2234– 2242.

Hadas, H., Einav, M., Fishov, I., and Zaritsky, A. (1997). Bacteriophage T4 development depends on the physiology of its host *Escherichia coli*. *Microbiology* 143, 179-185.

Hardies, S. C., Comeau, A. M., Serwer, P., and Suttle, C. A. (2003). The complete sequence of marine bacteriophage VpV262 infecting *Vibrio parahaemolyticus*

indicates that an ancestral component of a T7 viral supergroup is widespread in the marine environment. *Virology* 310:359-371.

Harshey, R.M. (2003). Bacterial motility on a surface: many ways to a common goal. *Annu*. *Rev*. *Microbiol*. 57, 249–273.

He, S.Y. (1998). Type III protein secretion systems in plant and animal pathogenic bacteria. *Annu*. *Rev*. *Phytopathol*. 36, 363 – 392.

Heilpern, A. J., and Waldor, M. K. (2003). pIIICTX , a predicted CTX phi minor coat protein, can expand the host range of coliphage fd to include *Vibrio cholerae*. *J*. *Bacteriol*. 185, 1037–1044.

Heppner, J. (1993). Citrus leafminer, Phyllocnistis citrella, (Lepidoptera: Gracillariidae: Phyllocnistinae) in Florida. Tropical Lepidoptera 4, 49–64.

Higashiyama, T., and Yamada, T. (1991). Electrophoretic karyotyping and chromosomal gene mapping of Chlorella. Nucleic Acids Res. 19, 6191-6195.

Hiroshi, M., Junichi, K., and Satochi, W. (1980). Filamentous phages released from Xanthomonas campestris pv. citri. Japanese Journal of Phytopathology. 46(4), 526-532.

Hogg, D. R. (1985). Citrus canker in Argentina: A case history. Pages 8-10 in: Citrus Canker: An International Perspective. L. W. Timmer, ed. Citrus Research & Education Center, University of Florida, Lake Alfred**.**

Huber, K.E., and Waldor, M.K. (2002). Filamentous phage integration requires the host recombinases XerC and XerD. Nature 417, 656–659.

Hung, C. H., Yang, C. F., Yang, C. Y., and Tseng, Y. H. (2003). Involvement of tonB-exbBD1D2 operon in infection of *Xanthomonas campestris* phage phiL7. *Biochem*. *Biophys*. *Res*. *Commun*. 302, 878-884.

Inoue, Y., Matsuura, T., Ohara, T., Azekami, K. (2006). Bacteriophage OP_1, lytic for *Xanthomonas oryzae* pv. *oryzae*, changes its host range by duplication and deletion of the small domain in the deduced tail fiber gene. *J*. *Gen*. *Plant Pathol*. 72: 111-118**.**

Iriarte, F. B., Balogh, B., Momol, M. T., Smith, L. M., Wilson, M., and Jones, J. B. (2007). Factors affecting survival of bacteriophage on tomato leaf surfaces. *Appl*. *Environ*. *Microbiol*. 73, 1704–11. doi: 10.1128/AEM.02118-06.

Iriarte, F. B., Obradovic, A., Wernsing, M. H., Jason, A., Hong, M., Momol, T., Jones, J. B., and Vallad, G. E. (2012). Soil-based systemic delivery and phyllosphere in vivo propagation of bacteriophages: two possible strategies for improving bacteriophage persistence for plant disease control. *Bacteriophage*. 4, 215–224.

Jalan, N., Aritua, V., Kumar, D., Yu, F., Jones, J. B., Graham, J. H., Setubal, J. C., and Wang, N. (2011). Comparative genomic analysis of *Xanthomonas axonopodis* pv. *citrumelo* F1, which causes citrus bacterial spot disease and related strains provides insights into virulence and host specificity. *J*. *Bacteriol*. 14, 6342–6357. doi: 10.1128/JB.05777-11.

Jalan, N., Kumar, D., Andrade, M. O., Yu, F., Jones, J. B., Graham, J. H., White, F. F., Setubal, J. C., and Wang, N. (2013). Comparative genomic and transcriptome analyses of pathotypes of *Xanthomonas citri* subsp. *citri* provide insights into mechanisms of bacterial virulence and host range. *BMC Genomics*. 14, 551, doi:10.1186/1471-2164-14-551

Ji, P., Campbell, H. L., Kloepper, J. W., Jones, J. B., Suslow, T. V., and Wilson, M. (2006). Integrated biological control of bacterial speck and spot of tomato under

field conditions using foliar biological control agents and plant growth-promoting rhizobacteria. *Biol*. *Control*. 36, 358-367.

Ji, P., Momol, M. T., Pradhanang, P. M., Olson, S. M., Mayfield, J. L., and Jones, J. B. (2004). Acibenzolar-S-methyl enhanced host resis- tance in tomato against *Ralstonia solanacearum*. (Abstr.) *Phytopathology* 94, S46.

Johnson, K. B. (1994). Dose-response relationships and inundative biological control. *Phytopathology* 84,780-784.

Jones, J. B., Jackson, L. E., Balogh, B., Obradovich, A., Iriarte, F. B., and Momol, M. T. (2007). Bacteriophages for plant disease control. *Annu*. *Rev*. *Phytopathol*. 45, 245-262

Jones, J. B., Vallad, G. E., Iriarte, F. B., Obradovic, A., Wernsing, M. H., Jackson, L. E., Balogh, B., Hong, J. C., and Momol, M. T. (2012). Considerations for using bacteriophages for plant disease control. *Bacteriophage* 2 (4), 208-214.

Jun, S. R., Sims, G. E., Wu, G. A., and Kim, S. H. (2010). Whole-proteome phylogeny of prokaryotes by feature frequency profiles: an alignment-free method with optimal feature resolution. *Proc*. *Natl Acad*. *Sci*. USA 107, 133–138.

Kang, Y., Liu, H., Genin, S., Schell, M. A., and Denny, T. P. (2002). *Ralstonia solanacearum* requires type 4 pili to adhere to multiple surfaces and for natural transformation and virulence. *Mol*. *Microbiol*. 46, 427-437.

Kang, Y., Liu, H., Genin, S., Schell, M. A., and Denny, T. P. (2002). *Ralstonia solanacearum* requires type 4 pili to adhere to multiple surfaces and for natural transformation and virulence. *Mol*. *Microbiol*. 2, 427 – 437.

Kao, C. C., Barlow, E., and Sequeira. L. (1992). Extracellular polysaccharide is required for wild-type virulence of *Pseudomonas solanacearum*. *J*. *Bacteriol*. 174, 1068–1071.

Katzen, F., Ferreiro, D., Oddo, C., Ielmini, M. V., Becker, A., Puhler, A., and Ielpi, L. (1998). *Xanthomonas campestris* pv. *campestris* gum mutants: effects on xanthan biosynthesis and plant virulence. *J. Bacteriol*.180, 1607–1617.

Kawasaki, T., Shimizu, M., Satsuma, H., Fujiwara, A., Fujie, M., Usami, S., and Yamada, T. (2009). Genomic characterization of *Ralstonia solanacearum* phage ϕRSB1, a T7-like wide-host-range phage. *J. Bacteriol*. 191: 422-427.

Kemp, B. P., Horne, J., Bryant, A., and Cooper, R. M. (2004). *Xanthomonas axonopodis* pv. *manihotis gum*D gene is essential for EPS production and pathogenicity and enhances epiphytic survival on cassava (Manihotesculenta). *Physiol. Mol. Plant Pathol*. 64, 209–218.

Koizumi, M. (1977). Relation of temperature to the development of citrus canker lesions in the spring. *Proc. Int. Soc. Citriculture* 3:924-928.

Koizumi, M. (1985). Citrus canker: The world situation. Pages 2-7 in: Citrus Canker: An International Perspective. L. W. Timmer, ed. Citrus Research & Education Center, University of Florida, Lake Alfred.

Kuhara, S. (1978). Present epidemic status and control of the citrus canker disease (*Xanthomonas citri* (Hasse) Dowson) in Japan. *Rev. Plant Prot. Res*. 11:132-142.

Kuo, T. T., Tan, M. S., Su, M. T., and Yang, M. K. (1991). Complete nucleotide sequence of filamentous phage Cf1c from *Xanthomonas campestris* pv. *citri*. *Nucleic Acids Res*. 19, 2498.

Kutateladze, M., and Adamia R. (2010). Bacteriophages as potential new therapeutics to replace or supplement antibiotics, *Trends Biotechnol*. 28, 591-595

Kutter, E. Bacteriophage Therapy: Past and Present, 258-266, In: Moselio Schaechter (Ed.), Encyclopedia of Microbiology, Elsevier, Oxford,

Laemmli, U. K. (1970). Cleavage of structural proteins during the assembly of the head of bacteriophage T4. *Nature* 227, 680-685.

Lang, J. M., Gent, D. H., and Schwartz, H. F. (2007). Management of *Xanthomonas* leaf blight of onion with bacteriophages and a plant activator. *Plant Dis*. 91, 871-878.

Larkin, M. A., Blackshields, G., Brown, N. P., Chenna, R., McGettigan, P. A., McWilliam, H., Valentin, F., Wallace, I. M., Wilm, A., Lopez, R., Thompson, J. D., Gibson, T. J., and Higgins, D. G. (2007). Clustal W and Clustal X version 2.0. *Bioinformatics* 23, 2947-2948.

Lee, C. N., Hu, R. M., Chow, T. Y., Lin, J. W., Chen, H. Y., Tseng, Y. H., and Weng, S. F. (2007). Comparison of genomes of three *Xanthomonas oryzae* bacteriophages. *BMC Genomics* 8, 442-453.

Lee, C. N., Lin, J. W., Weng, S. F., and Tseng, Y. H. (2009). Genomic characterization of the intron- containing T7-like phage phiL7 of *Xanthomonas campestris*. *Appl*. *Environ*. *Microbiol*. 75, 7828-7837.

Leite, R. P. Jr. (2005). Integrated management of citrus canker in Southern Brazil. Second international citrus canker and huanglongbing research workshop; Orlando, Florida.

Leite, R. P. Jr., (1990). Citrus canker: Prevention and control in the state of Parana. Fundacao IAPAR, Circular Instituto Agronomico do Paraná. No. 61.

Leite, R.P. Jr., and Mohan, S. K. **(1990).** Integrated management of the citrus bacterial canker disease caused by *Xanthomonas campestris* pv. *citri* in the State of Paraná, Brazil. *Crop Protection*. 9, 3-7.

Leite, R.P. Jr., Mohan, S. K., Pereira, A. L. G., and Campacci, C. A. (1987). Integrated control of citrus canker: Effect of genetic resistance and application of bactericides. *Fitopatologia-Brasileira*. 12, 257-263.

Li, J., and Wang, N. (2011). The *wxac*O gene of *Xanthomonas citri* ssp. *citri* encodes a protein with a role in lipopolysaccharide biosynthesis, biofilm formation, stress tolerance and virulence. *Mol*. *Plant*. *Pathol*. 1, 381–396.

Liu, Y. Q., Heying, E., and Tanumihardjo, S. A. (2012). History, global distribution, and nutritional importance of citrus fruits. *Comprehensive Reviews in Food Science and Food Safety* 11, 530–545

Louws, F. J., Fulbright, D. W., Stephens, C. T., and de Bruijn, F. J. (1994). Specific genomic fingerprints of phytopathogenic *Xanthomonas* and *Pseudomonas* pathovars and strains generated with repetitive sequences and PCR. *Appl*. *Environ*. *Microbiol*. 60,2286-2295.

Louws, F. J., Wilson, M., Campbell, H. L., Cuppels, D. A., Jones, J. B., Shoemaker, P. B., Sahin, F., and Miller, S. A. (2001). Field control of bacterial spot and bacterial speck of tomato using a plant activator. *Plant Dis*. 85, 481-488.

Lubkowski, J., Hennecke, F., Puckthun, A., and Wlodawer. A. (1999). Filamentous phage infection: crystal structure of g3p in complex with its coreceptor, the C-terminal domain of TolA. *Structure* 7, 711–722.

Malamud, F., Conforte, V. P., Rigano, L. A., Castagnaro, A. P., Marano, M. R., Morais do Amaral, A., and Vojnov, A. A. (2012). *hrpM* is involved in glucan biosynthesis, biofilm formation and pathogenicity in *Xanthomonas citri* ssp. *citri*. *Mol*. *Plant Pathol*. 13, 1010–1018.

Marco, G. M., and Stall, R. E. (1983). Control of bacterial spot of pepper initiated by strains of *Xanthomonas campestris* pv. *vesicatoria* that differ in sensitive to copper, *Plant Dis* . 67, 779–781

Marques, L. L. R., Ceri, H., Manfio, G. P., Reid, D. M., and Olsen, M. E. (2002). Characterization of biofilm formation by *Xylella fastidiosa* in vitro. *Plant Di*s. 86, 633-638.

Marvin, D. A., and Hohn, B. (1998). Filamentous phage structure, infection and assymply. *Curr*. *Opin*. *Struct*. *Biol*. 8, 150-158.

Mattick, J. S. (2002). Type IV pili and twitching motility. *Annu*. *Rev*. *Microbiol*. 56, 289-314.

Maxson-Stein, K., and He, S. Y., Hammerschmidt, R., and Jones, A. L. (2002). Effect of treating apple trees with acibenzolar-S-methyl on fire blight and expression of pathogenesis-related protein genes. *Plant Dis*. 86, 785-790.

McNeil, D. L., Romero, S., Kandula, J., Stark, C., Stewart, A., and Larsen, S. (2001). Bacteriophages: A potential biocontrol agent against walnut blight (*Xanthomonas campestris* pv. *juglandis*). *N Z Plant Prot*. 54, 220-224.

Meng, Y., Li, Y., Galvani, C.D., Hao, G., Turner, J.N., Burr, T.J., and Hoch, H.C. (2005). Upstream migration of *Xylella fastidiosa* via pilus-driven twitching motility. *J*. *Bacteriol*. 187, 5560-5567.

Model, P., and Russel, M. (1988). Filamentous bacteriophage, pp. 375–456. In: R. Calendar (ed.), The bacteriophages, vol. 2. Plenum Publishing Corpora- tion, New York, N.Y.

Molineux, I. J. (1999). T7-like phages (*Podoviridae*). pp. 1722-1729. In: Encyclopedia of Virology. A. Granoff, and R. Webster (eds). Academic Press. Ltd. London, United Kingdom.

Mosier-Boss, P. A., Lieberman, S. H., Andrews JM, Rohwer FL, Wegley LE, Breitbart M. (2003). Use of fluorescently labeled phage in the detection and identification of bacterial species. *Appl*. *Spectrosc*. 57, 1138-1144.

Mosig, G., Hall, D. H., Eiserlig, F. A., Black, L. W, Spicer, E. K., Kutter, E., Carlson, K., and Miller, E. S. (eds), Molecular biology of bacteriophage T4. ASM Press, Washington, D. C., USA.

Nagy, S., and Attaway, J. A., (1980). Citrus nutrition and quality. Washington, D.C.: American Chemical Society.

O'Toole, G. A., and Kolter, R. (1998). Flagellar and twitching motility are necessary for *Pseudomonas aeruginosa* biofilm development. *Mol*. *Microbiol*. 30, 295-304.

Obata, T. (1974). Distribution of *Xanthomonas citri* strain in relation to the sensitivity to phage CP1 and CP2. *Annu*. *Phytopathol*. *Soc*. *Jpn*. 40, 6-13.

Obradovic, A., Jones, J. B., Momol, M. T., Balogh, B. and Olson, S. M. (2004). Management of tomato bacterial spot in the field by foliar applications of bacteriophages and SAR inducers. *Plant Dis*. 88, 736-740.

Obradovic, A., Jones, J. B., Momol, M. T., Olson, S. M., Jackson, L. E., Balogh, B., Guven, K., and Iriarte, F. B. (2005). Integration of biological control agents and systemic acquired resistance inducers against bacterial spot on tomato. *Plant Dis*. 89, 712-716.

Okabe, N., and Goto, M. (1963). Bacteriophages of plant pathogens. *Annu Rev Phytopathol* 1, 397-418.

Osumi-Davis, P. A., de Aguilera, M. C., Woody, R. W., and Woody, A. Y. (1992). Asp537, Asp812 are essential and Lys631,His811 are catalytically significant in bacteriophage T7 RNA polymerase activity. *J*. *Mol*. *Biol*. 226, 37-45.

Poplawsky, A.R., and Chun, W. (1998). *Xanthomonas campestris* pv. *campestris*

requires a functional *pigB* for epiphytic survival and host infection. *Mol*. *Plant–Microbe Interact*. 11, 466–475.

Ramana, K. V. R., Govindarajan, V. S., Ranganna, S. **(1981).** Citrus fruits varieties, chemistry, technology, and quality evaluation. Part I: Varieties, production, handling, and storage. *Crit Rev Food Sci Nutr*. 15, 353–431.

Rigano, L. A., Payette, C., Brouillard, G., Marano, M. R., Abramowicz, L., Torres, P. S., Yun, M., Castagnaro, A. P., Oirdi, M. E., Dufour, V., Malamud, F., Dow, J. M., Bouarab, K., and Vojnov, A. (2007). Bacterial cyclic beta-(1,2)-glucan acts in systemic suppression of plant immune responses. *Plant Cell* 19, 2077– 2089.

Rodrigues, J. C. V., Rossetti, V., Machado, M. A., Sobrinho, J. T., and de Lima-Nogueira, N. **(1998).** Citrus leafminer: A factor for increase of pests and citrus canker. *Laranja*. 19, 49-60.

Ryan, R. P., and Dow, J. M. (2011). Communication with a growing family: DSF signaling in bacteria. *Trends Microbiol*. 19, 145–152.

Rybak, M. A. (2005). Genetic determinants of host range specificity of the Wellington strain of *Xanthomonas axonopodis* pv. *citri* [dissertation]. Gainesville, Florida: University of Florida.

Sambrook, J., and Russell, D. W. (2001). Molecular cloning: a laboratory manual, 3rd ed. Cold Spring Harbor Laboratory Press, Cold Spring Harbor, NY.

Schnabel, E. L., Fernando, W. G. D., Meyer, M. P., Jones, A. L., and Jackson, L. E. (1999). Bacteriophage of *Erwinia amylovora* and their potential for biocontrol. *Acta Hortic*. 489, 649–54.

Schubert, T. S., Rizvi, S. A., Sun, X., Gottwald, T. R., Graham, J. H., and Dixon, W. N. (2001). Meeting the challenge of eradicating citrus canker in Florida Again. *Plant Dis*. 85, 340-356.

Scora, R. W. (1975). On the history and origin of citrus. *Bull Torrey Bot Club* 102, 369–75.

Semenova, E., Djordjevie, M., Shraiman, B., and Severinov, K. (2005). The tale of two RNA polymerases: transcription profiling and gene expression strategy of bacteriophage Xp10. *Mol. Microbiol*. 55, 764-777.

Shieh, G. J., Charng, Y. C., Yang, B. C., Jenn, T., Bau, H. J. and Kuo, T. T. (1991). Identification and nucleotide sequence analysis of an open reading frame involved in high-frequency conversion of turbid to clear plaque mu- tants of filamentous phage Cf1t. *Virology* 185, 316–322.

Shiotani, H. (2007). Dissertation, The United Graduate School of Agricultural Science, Gifu University. Gifu, Japan.

Shiotani, H., Fujikawa, T., Ishihara, H., Tsuyumu, S., and Ozaki, K. (2007). A *pthA* homolog from *Xanthomonas axonopodis* pv. *citri* responsible for host-specific suppression of virulence. *J*. *Bacteriol*. 189, 3271-3279.

Shiotani, H., Tsuyumu, S., and Ozaki, K. (2000). Pathogenic interactions between *Xanthomonas axonopodis* pv. *citri* and cultivars of Pummelo (*Citrus grandis*). *Phytopathology* 90, 1383-1389.

Sinclair, W. B. (1961). The orange. Berkeley, Calif.: University of California, Berkeley.

Sinha, M. K., Batra, R. C., and Uppal, D. K. (1972). Role of citrus leaf-miner (Phyllocnistis citrella Staintan (sic) on the prevalence and severity of citrus canker [*Xanthomonas citri* (Hasse) Dowson]. *Madras Agr*. *J*. 59,240-245.

Skerker, J. M., and Berg, H.C. (2001). Direct observation of extension and retraction of type IV pili. *Proc*. *Natl Acad*. *Sci*. USA, 98, 6901 – 6904.

Slopek S., Weber-Dabrowska B., Dabrowski M., and Kucharewica-Krukowska A. (1987). Results of bacteriophage treatment of suppurative bacterial infections in the years 1981–1986, *Arch*. *Immunol*. *Ther*. *Exp*. 35, 569–583

Sohi, G. S., and Sandhu, M. S. (1968). Relationship between citrus leafminer (Phyllocnistis citrella Stainton) injury and citrus canker [(*Xanthomonas citri* (Hasse) Dowson] incidence on citrus leaves. *J*. *Res*. *Punjab Agric*. University (Ludhiana) 5, 66-69.

Stall, R. E., and Civerolo, EL. (1991). Research relating to the recent outbreak of citrus canker in Florida. *Annu*. *Rev*. *Phytopathol*. 29, 399-420.

Stall, R. E., and Seymour, C. P. (1983). Canker: a threat to citrus in the Gulf Coast states. *Plant Dis*. 67, 581-585.

Stall, R. E., Civerolo, E. L., Ducharme, E. P., Krass, C. J., Poe, S. R., Miller, J. W., and Schoulties, C. L. **(1987).** Management of citrus canker by eradication of *Xanthomonas campestris* pv. *citri*. pp. 900-905 In: Plant Pathogenic Bacteria, Current Plant Science and Biotechnology in Agriculture. E. L. Civerolo, A Collmer, R. E. Davis, and A. G. Gillaspie, (eds). Martinus Nijhoff Publishers, Dordrecht, The Netherlands.

Stall, R. E., Miller, J. W., Marco, G. M., and Canteros de Echenique, B. I. (1980). Population dynamics of *Xanthomonas citri* causing cancrosis of citrus in Argentina. *Proc*. *Fla*. *Hort*. *Soc*. 93, 10-14.

Stein, B., Ramallo, J., Foguet, L., and Morandini, M. (2005). Chemical control of citrus canker in lemons (Citrus limon, (L.) Burm. f) in Tucuman, Argentina (Abstr.). Second international citrus canker and huanglongbing research workshop; November 7-11, 2005; 25.

Sulakvelidze, A., Alavidze Z., and Morris J.G. Jr. (2001). Bacteriophage therapy, *Antimicrob*. *Agents Ch*. 45, 649-659

Summers W.C. (2001). Bacteriophage therapy, *Ann*. *Rev*. *Microbiol*. 55: 437-451

Summers W.C. (2005). Bacteriophage research: Early history. pp. 5-27, In: Kutter E., Sulakvelidze A., (eds.), Bacteriophages: Biology and Applications, CRC Press, Boca Raton, FL.

Svircev, A. M., Lehman, S. M., Kim, W. S. , Barszcz, E., Schneider, K. E., and Castle, A. J. **(2005).** Control of the fire blight pathogen with bacteriophages. pp. 259-261) *In: Zeller W, Ullrich C (eds)*. *Proc 1st Int Symp Biol Control Bact Plant Dis*, October 23–26, 2005. Berlin, Germany: Die Deutsche Bibliothek – CIP-Einheitsaufnahme.

Swarup, S., Yang, Y., Kingsley, M. T., and Gabriel, D. W. (1992). An *Xanthomonas citri* pathogenicity gene, phcA, pleiotropically encodes gratuitous avirulence on nonhosts. *Mol*. *Plant-Microbe Interact*. 5, 204-213.

Szurek, B., Rossier, O., Hause, G., and Bonas, U. (2002). Type III dependent translocation of the *Xanthomonas* AvrBs3 protein into the plant cell. *Mol*. *Microbiol*. 46, 13–23.

Tanaka, H., Negishi, H., and Maeda, H. (1990). Control of tobacco bacterial wilt by an avirulent strain *of Pseudomonas solanacearum* M4S and its bacteriophage. *Ann Phytopathological Soc Jpn*. 56, 243- 246. doi: 10.3186/jjphytopath.56.243.

Timmer, L. W. (2000). Inoculum production and epiphytic survival of *Xanthomonas campestris* pv. *citri*. (Abstr.) In: Proceedings of the International Citrus Canker Research Workshop, Ft. Pierce FL, June 20-22, 2000. Online. Division of Plant Industry, Florida Department of Agriculture and Consumer Services.

UniProt Consortium., (2007). The Universal Protein Resource (UniProt). *Nucleic Acids Res*. 35, D193-D197.

United Nations Conference on Trade and Development (UNCTAD). (2004). Market Information in the Commodities Area: Information on citrus fruit. Available from: http://r0.unctad.org/infocomm/anglais/orange/ sitemap.htm. Accessed 2011 June.33, 301-310.

Val, M. E., Bouvier, M., Campos, J., Sherratt, D., Cornet, F., Mazel, D. and Barre, F. X. (2005). The single-stranded genome of phage CTX is the form used for integration into the genome of *Vibrio cholerae*. *Mol*. *Cell* 19, 559–565.

Vernière, C., Hartung, J. S., Pruvost, O. P., Civerolo, E. L., Alvarez, A. M., Maestri, P., and Luisetti, J. (1998). Characterization of phenotypically distinct strains of *Xanthomonas axonopodis* pv. *citri* from Southwest Asia. *Eur*. *J*. *Plant Pathol*. 104, 477– 487.

Vidaver, A. K. (1976). Prospects for control of phytopathogenic bacteria by bacteriophages and bacteriocins. *Ann*. *Rev*. *Phytopathol*. 14, 451–65

Vojnov, A. A., Morais do Amaral, A., Dow, J. M., Castagnaro, A. P., and Marano, M. R. (2010). Bacteria causing important diseases of citrus utilise distinct modes of pathogenesis to attack a common host. *Appl*. *Microbiol*. *Biotechnol*. 87, 467–477.

Wakimoto, S. (1967). Some characteristics of citrus canker bacteria, *Xanthomonas citri* . *Ann*. *Phytopath*. *Soc*. *Japan*. 33, 301-310

Wakimoto, S. (1981). Effect of the infection with filamentous phage xf 2 on the properties of *Xanthomonas campestris var oryzae*. *Ann Phytopathol*. *Soc*. *Japan*. 627-636.

Webber, H. J. (1967). History and development of the citrus industry. In: Reuther, W., Webber, H. J., and Batchelor, L. D. editors. The citrus industry. Vol. 1. History, world distribution, botany and varieties. Berkeley, Calif.: University of California, Berkeley, Division of Agricultural Sciences. pp. 1–39.

Wheeler, D. L., Barrett, T., Benson, D. A., Bryant, S. H., Canese, K., Chetvrnin, V., Church, D. M., DiCuccio, M., Edgar, E., Federhen, S., Geer, L. Y., Kapustin, Y., Khovayko, O., Landsman, D., Lipman, D. J., Madden, T. L., Maglott, D. R., Ostell, J., Miller, V., Pruitt, K. D., Schuler, G. D., Sequeira, E., Sherry, S. T., Sirotkin, K., Souvorov, A., Starchenko, G., Tatusov, R. L., Tatusova, T. A., Wagner, L., and Yaschenko, E. (2007). Database resources of the National Center for Biotechnology Information. *Nucleic Acids Res*. 35, D5-D12.

Wu, W. C. (1972). Phage-induced alterations of cell disposition, phage adsorption and sensitivity, and virulence in *Xanthomonas citri*. *Ann Phytopath Soc Japan*. 38,333-341.

Wu, W. C., Lee, S. T., Kuo, H. F., and Wang, L. Y. (1993). Use of phages for identifying the citrus canker bacterium *Xanthomonas campestris*pv. *citri*in Taiwan. *Plant Patho*l. 42, 389-395

Yamada, T. (2009). Bacteriophage biocontrol: The *Ralstonia solanacearum* case. In: Contemporary Trends in Bacteriophage Research (Adams, H. T. ed.), Nova Science Publishers, Inc, pp. 375-390.

Yamada, T., Kawasaki, T., Nagata, S., Fujiwara, A., Usami, S., and Fujie, M. (2007). New bacteriophages that infect the phytopathogen *Ralstonia solanacearum*. *Microbiology* 153, 2630-2639.

Yan, Q., Hu, X., and Wang, N. (2012). The novel virulence-related gene nlxA in the lipopolysaccharide cluster of *Xanthomonas citri* ssp. *citri* is involved in the

production of lipopolysaccharide and extracellular polysaccharide, motility, biofilm formation and stress resistance. *Mol*. *Plant Pathol*. 13(8), 923–934.

Yu, J., Penaloza-Vazquez, A., Chakrabarty, A. M., and Bender, C. L. (1999). Involvement of the exopolysaccharide alginate in the virulence and epiphytic fitness of *Pseudomonas syringae* pv. *syringae*. *Mol*. *Microbiol*. 33, 712–720.

Yuzenkova, J., Nechaev, S., Berlin, J., Rogulja, D., Kuznedelov, K., Inman, R., Mushegian, A., and Severinov, K. (2003). Genome of *Xanthomonas oryzae* bacteriophage XP10: an odd T-odd phage. *J*. *Mol*. *Biol*. 330: 735-748.

Thesis Summary

Asiatic citrus canker (ACC), which is caused by the phytopathogenic bacterium *Xanthomonas axonopodis* pv. *citri* (*Xac)* , is one of the biggest problems in citrus production worldwide. Given the difficulties in controlling this disease using conventional methods, considerable efforts have been made to find alternative strategies. Recently, biological controlling agents, especially bacteriophages, have been successfully used in several plant diseases and are also promising candidates for control of ACC. However there may be many challenges that are facing and limiting the success of bacteriophages as biological control agent. These include the narrow host range and high specificity, which put phages at a disadvantage against other anti-bacterial materials such as antibiotics. Furthermore, the emergency of resistance mutants is a practical problem, which significantly limits the use of bacteriophages as abiocotrol agent. Other major affecting factors are the environmental effects such as temperature, pH, host physiology and inactivation by UV light. These environmental factors have great negative impact on the ability of phage to infect the target pathogen as well as on the persistence of phages in both phyllosphere and rizosphere. Molecular characterization and studies of the biology and ecology of phages are very important to understand the phage host interaction and to figure out the most effective way of bacteriophage utilization as biological control agents.

The first subject of this study was to make a full characterization of the historical *Xanthomonas* Cp1 and Cp2 phages. Nearly *all Xac* strains isolated from different regions in Japan are lysed by either of phage Cp1 or Cp2; Cp1-sensitive ($Cp1^S$) strains have been observed to be resistant to Cp2 ($Cp2^R$) and *vice versa*. Morphologically, Cp1 belonged to the *Siphoviridae*. Both Cp1 and Cp2 form clear plaques with various *Xac* strains. The infection cycle of Cp1 showed that the latent period was ~ 60 min, followed by a raise period of 20-30 min, giving an entire cycle of 80-90 min with average burst size of ~20 plaque forming unit per infected cell. For Cp2 replication, the infection cycle showed that the latent period was ~90 min, with a 60 min raise period, taking 150-180 min per cycle with burst size of ~100 plaque forming unit per infected cell. Genomic analysis revealed that its genome comprised 43,870-bp dsDNA, with 10-bp 3'-extruding cohesive ends, and contained 48 open reading frames (ORFs). The genomic organization was similar to that of *Xanthomonas* phage phiL7, but it lacked a group-I intron in the DNA polymerase

gene. Cp2 resembled morphologically *Escherichia coli* T7-like phages of *Podoviridae*. The 42,963-bp linear dsDNA genome of Cp2 contained terminal repeats. The Cp2 genomic sequence had 40 ORFs, many of which did not show detectable homologs in the current databases. By proteomic analysis, a gene cluster encoding structural proteins corresponding to the Class III module of T7-like phages was identified on the Cp2 genome**.** Therefore, Cp1 and Cp2 were found to belong to completely different virus groups. In addition, I found that Cp1 and Cp2 used different molecules on the host cell surface as phage receptors and that host-selection of *X*. *axonopodis* pv. *citri* strains by Cp1 and Cp2 was not determined at the initial stage by binding to receptors. Further investigation was done to examine the fate of the phage DNA after cell attachment to non-host strains. This was conducted by adding the SYBR-gold labeled phages to cells of *Xac* then the movement of SYBR Gold-phage DNA was monitored. The result showed that the DNA of Cp1 and Cp2 was injected into the host cells as well as into the non-host cells. Thus, further molecular studies are needed to deeply understand the molecular mechanism of host selection by these phages.

My second goal was to find a better solution that may contribute to solving the major challenge associated with the use of phages, mainly instability of phages during treatment of field crop plants. XacF1, which can infect *Xanthomonas axonopodis* pv. *citri* (*Xac*) strains, was isolated and characterized. Electron microscopy showed that XacF1 was a member of the family *Inoviridae* and was about 600 nm long. The genome of XacF1 was 7,325 nucleotides in size, containing 13 predicted ORFs, some of which showed significant homology to Ff-like phage proteins such as ORF1 (pII), ORF2 (pV), ORF6 (pIII), and ORF8 (pVI)**.** XacF1 showed a relatively wide host range, infecting seven out of 11 strains tested in this study. Frequently, XacF1 was found to be integrated into the genome of *Xac* strains. This integration occurred at the host *dif* site (*att*B) and was mediated by the host XerC/D recombination system. The *att*P sequence was identical to that of *Xanthomonas* phage Cf1c**.** Preliminary results of the deletion mutant of XacF1 lacking ORF12 (□XacF1) showed that XaCF1could not integrated into the host genome and solely replicated as episomic forms. Interestingly, infection by XacF1 phage caused several physiological changes to the bacterial host cells, including lower levels of extracellular polysaccharide production, reduced motility, slower growth rate, and a dramatic reduction in virulence. In particular, the reduction in virulence suggested possible utilization of XacF1 as a

biological control agent against citrus canker disease. The *Inovirus* nature of XacF1 establishing a coexisting state with the host cells ensures long-lasting effects of this phage. This is an advantage of filamentous phages to solve the problem of bacteriophages easily inactivated by sunlight UV irradiation and other environmental factors.

This research provides valuable information and new insight into the molecular mechanism of host selection between Cp1 and Cp2; the historical problem in phytopathology as well as the molecular basis of loss of virulence caused by XacF1 infection. They may open a new strategy of phage therapy, solve many of the problems, which are associated with phage application including the weak persistence of phage in the environment, and bring an ecofriendly sustainable way for next generation agriculture or food production.

ACKNOWLEDGEMENTS

I am thankful to Almighty Allah, most Gracious, who in his infinite mercy has guided me to complete this PhD work.

I am thankful to my premotor Professor Takashi Yamada who gave me the opportunity to work under his supervision. He is the most talented person I have ever met. I can not sum up the experience I have had with Professor Yamada over the past four years in a phrase or saying, but I would like to express my gratitude and appreciate him for guiding me during the course of my research work with his unique style of "gradually increasing the level of criticism", and for him never hesitating help me despite his busy agenda. He always provides me with encouragement, advice and support at all levels.

I am using this opportunity to express my gratitude to Professor Juinichi Kato, Department of Molecular Biotechnology, graduate School of Advanced Sciences of Matter (ADSM), Hiroshima University, and professor Nobukazu Tanaka, Center for gene Science, Natural Science Center for Basic Research and Development, Hiroshima University for their help, support and their valuable reviewing of this thesis.

I would also like to acknowledge the assistance of Dr. Makoto Fujie and Dr. Takeru Kawasaki, Department of Molecular Biotechnology, Graduate School of Advanced Sciences of Matter (ADSM), Hiroshima University, for their valuable suggestions, discussion, and help during this study.

I express my warm thanks to all my family members including my lovely wife (Hagar), my sweet daughters (Tasneem and Reem), and my beloved son (Omar). They have supported me all the time, understood my work duties, and have been very nice and patient during the course of this research. My heartily and special thanks are to my lovely wife, who has inspired me and provided constant encouragement during the entire process. I also would like to thank my parents for all the support they have provided me over the years. I extend my thanks to my brothers and my sisters for their continuous help, love, and support.

I appreciate to all lab members as well as to all members of student support office of the Graduate School of Advanced Sciences of Matter (ADSM) for their kindness, help and the cooperation during this study.

Finally, I would like to acknowledge my gratefulness to my government (Egypt) through the Ministry of Higher Education and Scientific Research for the support and granting me scholarship for this study. Really, it was great chance to have this opportunity to study in Japan. My thanks are also to all of my professors at the Department of Plant pathology, Faculty Agriculture, Minia University, Egypt, for their support, help, and advice over the years.

All praise and glory belong to almighty Allah, the sustainer of the universe.

Abdelmonim Ali

公表論文
(Articles)

AEM
Journals.ASM.org

Characterization of Bacteriophages Cp1 and Cp2, the Strain-Typing Agents for *Xanthomonas axonopodis* pv. citri

Abdelmonim Ali Ahmad, Megumi Ogawa, Takeru Kawasaki, Makoto Fujie, Takashi Yamada

Department of Molecular Biotechnology, Graduate School of Advanced Sciences of Matter, Hiroshima University, Higashi-Hiroshima, Japan

The strains of *Xanthomonas axonopodis* pv. citri, the causative agent of citrus canker, are historically classified based on bacteriophage (phage) sensitivity. Nearly all *X. axonopodis* pv. citri strains isolated from different regions in Japan are lysed by either phage Cp1 or Cp2; Cp1-sensitive ($Cp1^s$) strains have been observed to be resistant to Cp2 ($Cp2^r$) and *vice versa*. In this study, genomic and molecular characterization was performed for the typing agents Cp1 and Cp2. Morphologically, Cp1 belongs to the *Siphoviridae*. Genomic analysis revealed that its genome comprises 43,870-bp double-stranded DNA (dsDNA), with 10-bp 3′-extruding cohesive ends, and contains 48 open reading frames. The genomic organization was similar to that of *Xanthomonas* phage phiL7, but it lacked a group I intron in the DNA polymerase gene. Cp2 resembles morphologically *Escherichia coli* T7-like phages of *Podoviridae*. The 42,963-bp linear dsDNA genome of Cp2 contained terminal repeats. The Cp2 genomic sequence has 40 open reading frames, many of which did not show detectable homologs in the current databases. By proteomic analysis, a gene cluster encoding structural proteins corresponding to the class III module of T7-like phages was identified on the Cp2 genome. Therefore, Cp1 and Cp2 were found to belong to completely different virus groups. In addition, we found that Cp1 and Cp2 use different molecules on the host cell surface as phage receptors and that host selection of *X. axonopodis* pv. citri strains by Cp1 and Cp2 is not determined at the initial stage by binding to receptors.

Citrus canker, caused by *Xanthomonas axonopodis* pv. citri (syn., *Xanthomonas campestris* pv. citri or *Xanthomonas citri*), is a widespread disease in citrus-producing areas of the tropical and subtropical world (1, 2). Different types of citrus canker, corresponding to different pathotypes of *X. axonopodis* pv. citri, have been reported (3). The Asiatic type, caused by *X. axonopodis* pv. citri pathotype A, is the most widespread and the most economically important citrus canker. The host range of pathotype A strains is wider than that of the other pathotypes, including most citrus varieties (3). *X. axonopodis* pv. citri pathotype A strains are separated into two groups based on their sensitivity to phages Cp1 and Cp2 (4, 5). Phage typing with Cp1 and Cp2 was first demonstrated by Wakimoto (4). Wakimoto found that nearly all strains isolated from different regions in Japan were lysed by either Cp1 or Cp2 and that Cp1-sensitive ($Cp1^s$) strains were resistant to Cp2 ($Cp2^r$) and *vice versa*. Cp1 and Cp2 phages were morphologically different: Cp1 showed a head-tail structure, whereas Cp2 consisted of a polyhedral head without tail (4). In a larger survey, Obata found that $Cp1^r/Cp2^s$ strains predominated in major citrus-producing regions in Japan, with the exception of Hiroshima Prefecture, where $Cp1^s/Cp2^r$ strains predominated (5). Two different strain types can occur in a mixture on the same single leaf of a tree, but one single lesion usually consists of a single strain.

Notably, the sensitivity of *X. axonopodis* pv. citri strains to Cp1 and Cp2 is associated with differences in their physiological features and canker aggressiveness. *X. axonopodis* pv. citri strains that are $Cp1^s/Cp2^r$ can assimilate mannitol, while $Cp1^r/Cp2^s$ strains cannot (6). All strains that are $Cp1^r/Cp2^s$ are canker aggressive to the citrus variety "Otachibana," whereas all the strains with $Cp1^s/Cp2^r$ are weakly aggressive (7). The $Cp1^r/Cp2^s$ strains generate a 1.8-kbp-specific fragment by repetitive sequence-based PCR (rep-PCR) (8) using enterobacterial repetitive intergenic consensus (ERIC) primers. The 1.8-kbp band corresponds to a region encompassing XAC1661 (Isxac3 transposase) and XAC1662 (*repA*) within an insertion element in the genomic sequence of *X. axonopodis* pv. citri strain 306 (9). Most strains with $Cp1^s/Cp2^r$ contain *hssB3.0*, a member of the *avrBs3* and *pthA* (avirulence and pathogenicity) gene family (10, 11), which is responsible for the suppression of virulence on a *Citrus grandis* cultivar; however, $Cp1^r/Cp2^s$ strains lack this gene (12). These results suggest some relatedness between Cp1/Cp2 sensitivity and the virulence and pathogenic features of *X. axonopodis* pv. citri strains.

In contrast to the large contribution toward characterization of host strains, very little information is available about the nature or identity of phages Cp1 and Cp2. Concerning Cp1 and Cp2, the following issues are of particular interest: (i) the virological identification and phylogenetic relationships of these phages, (ii) the origin of the above-mentioned 1.8-kbp sequence on the host genome and its possible association with a phage sequence, (iii) *hssB3.0* and its possible association with a phage sequence, and (iv) the molecular mechanism of host selection by these phages. As a first step toward exploring these issues, the present study performed genomic and molecular characterization of Cp1 and Cp2.

MATERIALS AND METHODS

Bacterial strains and phages. Ministry of Agriculture, Forestry and Fisheries (MAFF) strains of *X. axonopodis* pv. citri were obtained from the National Institute of Agrobiological Sciences, Japan. Strain KC33 (7) was obtained from the National Institute of Fruit Tree Science, National Agriculture and Food Research Organization (NAFRO), Japan. Their origins and sensitivity to Cp1 and Cp2 are listed in Table 1. Bacteriophages Cp1

Received 12 July 2013 Accepted 7 October 2013
Published ahead of print 11 October 2013
Address correspondence to Takashi Yamada, tayamad@hiroshima-u.ac.jp.
Supplemental material for this article may be found at http://dx.doi.org/10.1128/AEM.02310-13.

doi:10.1128/AEM.02310-13

TABLE 1 Bacterial strains and bacteriophages used in this study[a]

Strain	Host (*Citrus* species)	Phage type[b]	Source
X. axonopodis pv. citri			
MAFF 301077	*C. limon*	$Cp1^s/Cp2^r$	NIAS[c]
MAFF 301080	*C. sinensis*	$Cp1^s/Cp2^r$	NIAS
301080 R1		$Cp1^r/Cp2^r$	This study
MAFF 311130	*C. iyo*	$Cp1^r/Cp2^r$	NIAS
MAFF 302102	*Citrus* sp.	$Cp1^r/Cp2^s$	NIAS
MAFF 673001	*C. natsudaidai*	$Cp1^r/Cp2^s$	NIAS
MAFF 673010	*Citrus* sp.	$Cp1^r/Cp2^s$	NIAS
673010 R2		$Cp1^r/Cp2^r$	This study
MAFF 673011	*C. limon*	$Cp1^s/Cp2^r$	NIAS
MAFF 673013	*Citrus* sp.	CP_1^s/CP_2^r	NIAS
MAFF 673018	*Citrus* sp.	$Cp1^r/Cp2^s$	NIAS
MAFF 673021	*C. limon*	$Cp1^r/Cp2^s$	NIAS
KC33	*C. iyo*	$Cp1^s/Cp2^s$	Shiotani et al. (12)
Phages			
Cp1			Wakimoto (4)
Cp2			Wakimoto (4)

[a] All strains originated in Japan.
[b] Sensitivity to phages CP_1 and CP_2; s, sensitive; r, resistant.
[c] NIAS, National Institute of Agrobiological Sciences, Japan.

and Cp2 (4, 5) were obtained from the Yokohama Plant Protection Station, Japan. Strains MAFF 301080 and MAFF 673010 were used as hosts for routine propagation of Cp1 and Cp2, respectively. Bacterial cells were cultured in nutrient broth (NB) medium (BBL, Becton, Dickinson and Co., Cockeysville, MD, USA) at 28°C with shaking at 200 to 300 rpm. An overnight culture of bacterial cells grown in NB was diluted 100-fold with 100 ml fresh NB in a 500-ml flask. To collect sufficient phage particles, 1 liter of bacterial culture (10 × 100-ml cultures) was grown. When the cultures reached 0.2 units of optical density at 600 nm (OD_{600}), the phages were added at a multiplicity of infection (MOI) of 0.1. After further growth for 9 to 18 h, the cells were removed by centrifugation with an R12A2 rotor in a Hitachi heavy ion medical accelerator (HIMAC) CR21E centrifuge (Hitachi Koki Co. Ltd., Tokyo, Japan), at 8,000 × *g* for 15 min at 4°C. The supernatant was passed through a 0.45-μm membrane filter, and phage particles were precipitated by centrifugation with a P28S rotor in a Hitachi XII100β centrifuge at 40,000 × *g* for 1 h at 4°C and dissolved in SM buffer (50 mM Tris-HCl at pH 7.5, 100 mM NaCl, 10 mM $MgSO_4$, and 0.01% gelatin). Purified phages were stored at 4°C until use. Bacteriophage particles purified by CsCl gradient ultracentrifugation (with a P28S rotor in a Hitachi XII100β ultracentrifuge) (13) were stained with Na-phosphotungstate before observation in a Hitachi H600A electron microscope, according to the method of Dykstra (14). λ phage particles were used as an internal standard marker for size determination. For host range determination, standard plaque-forming assays (15) or lysis zone formation spot tests (16) were performed.

Single-step growth experiment. Single-step growth experiments were performed as previously described (17, 18), with some modifications. Strains MAFF 301080 and MAFF 673010 were used as hosts for Cp1 and Cp2, respectively. Cells (0.1 U of OD_{600}) were harvested by centrifugation and resuspended in fresh NB (ca. 1×10^8 CFU/ml) to a final culture volume of 10 ml. Phage was added at an MOI of 1.0 and allowed to adsorb for 10 min at 28°C. After centrifugation and resuspending in the initial volume of NB with decimal dilution to a final volume of 10 ml, the cells were incubated at 28°C. Samples were taken at intervals (every 10 min up to 3.5 h for Cp1 and every 30 min up to 5 h for Cp2), and the titers were determined by the double-layered agar plate method.

Phage adsorption test. Phage adsorption was assayed as follows: when fresh bacterial cultures (10 ml) reached 0.1 unit of OD_{600}, the phage (10 μl) was added at an MOI of 0.1. After incubation for 10 min at 28°C, the cells were removed by centrifugation with an R12A2 rotor in a Hitachi HIMAC CR21E centrifuge at 8,000 × *g* for 10 min at 4°C. The supernatant was subjected to a plaque assay, where strains MAFF 301080 and MAFF 673010 were used as the hosts for Cp1 and Cp2, respectively. *Escherichia coli* JM109 was used as a negative control in phage adsorption.

DNA manipulation and sequencing. Standard molecular biological techniques for DNA isolation, digestion with restriction enzymes and other nucleases, and construction of recombinant DNAs were followed, according to Sambrook and Russell (13). Phage DNA was isolated from the purified phage particles by phenol extraction. For genome size determination, the purified phage particles were embedded in 0.7% low-melting-point agarose (InCert agarose; FMC Corp., Philadelphia, PA, USA) and, after treatment with proteinase K (1 mg/ml; Merck Ltd., Tokyo, Japan) and 1% Sarkosyl, subjected to pulsed-field gel electrophoresis (PFGE) in a Chef Mapper electrophoresis apparatus (Bio-Rad Lab., Hercules, CA, USA) according to the method of Higashiyama and Yamada (19). Shotgun sequencing was performed at Hokkaido System Science Co., Ltd. (Sapporo, Japan), using the Roche GS Junior Sequence system. The draft assembly of the obtained sequences was assembled using GS *De novo* Assembler v2.6. The analyzed sequences corresponded to 94 and 40 times the final genome sizes of Cp1 (43,860 bp) and Cp2 (42,963 bp), respectively. Potential open reading frames (ORFs) larger than 150 bp (50 codons) were identified using Glimmer (20) and GeneMark. Homology searches were performed using BLAST/RPS-BLAST (21) against the UniProt sequence database (22) and the NCBI/CDD database (23), using an E value lower than e−4 as a cutoff for notable similarity. Multiple-sequence alignments were generated using the DNASIS program (version 3.6; Hitachi Software Engineering, Co., Ltd., Tokyo, Japan). For phylogenetic analysis of RNA polymerase (RNAP) proteins, the unrooted dendrogram was constructed with the Treeview tool using the maximum likelihood method based on a complete protein sequence alignment of RNAP proteins from other phages using ClustalX. The Cp1 cohesive ends (*cos*) sequence was determined as follows. A 6.8-kbp PstI fragment of Cp1 DNA was dissociated into two fragments (4.3 and 2.5 kbp) after heating at 70°C for 15 min. The dissociated bands were recovered from the agarose gel and treated with T4 DNA polymerase to form blunt ends. The nucleotide sequences of these bands were determined. By comparing the nucleotide sequences with each other and with the Cp1 genomic sequence, the *cos* sequence was determined according to the method of Fujiwara et al. (24).

Southern and dot blot hybridization. Genomic DNA from bacterial cells was prepared by the minipreparation method according to Ausubel et al. (25). After digestion with various restriction enzymes (EcoRI, EcoRV, HindIII, and HincII), DNA fragments were separated by agarose gel electrophoresis, blotted onto a nylon membrane (Biodyne; Pall Gelman Laboratory, Closter, NJ, USA), hybridized with probes (the entire Cp1 DNA by combining all the HincII fragments and the entire Cp2 DNA with all the HincII fragments), labeled with fluorescein (Gene Images Random Prime labeling kit; Amersham Biosciences, Uppsala, Sweden), and detected with a Gene Images CDP-Star detection module (Amersham Biosciences). Hybridization was performed in buffer containing 5× SSC (1× SSC is 0.15 M NaCl plus 0.015 M sodium citrate), 0.1% SDS, 5% liquid block, and 5% dextran sulfate for 16 h at 65°C. The filter was washed at 60°C in 1× SSC and 0.1% SDS for 15 min and then in 0.5% SSC and 0.1% SDS for 15 min with agitation, according to the manufacturer's protocol. The hybridization signals were detected by exposing the filter onto an X-ray film (RX-U; Fuji Film, Tokyo, Japan).

SDS-PAGE and LC-MS/MS analysis. Purified phage particles were subjected to SDS-polyacrylamide gel electrophoresis (SDS-PAGE) (10 to 12% [wt/vol] polyacrylamide) according to Laemmli (26). Protein bands were visualized by staining the gel with Coomassie brilliant blue, excised from the gel, digested with trypsin, and subjected to liquid chromatography-tandem mass spectrometry (LC-MS/MS) (LTQ Orbitrap XL; Thermo Fisher Scientific, Osaka, Japan) analysis at the Natural Science Center for Basic Research and Development, Hiroshima University.

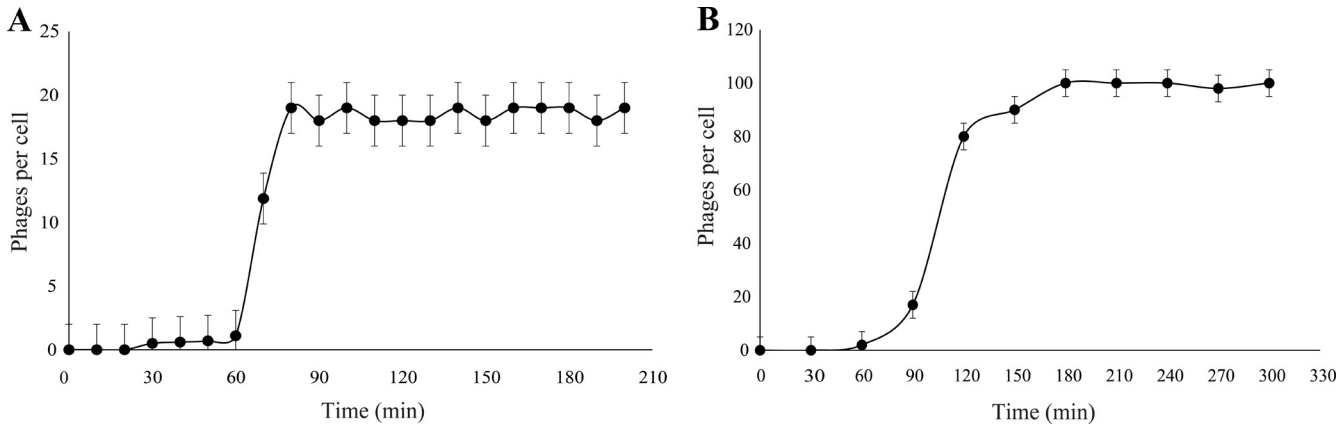

FIG 1 Single-step growth curves for Cp1 (A) and Cp2 (B). The PFU per infected cell in cultures of MAFF 301080 for Cp1 and MAFF 673010 for Cp2 at different times postinfection are shown. Samples were taken at intervals (every 10 min up to 3.5 h for Cp1 and every 30 min up to 5 h for Cp2). Error bars indicate standard deviations ($n = 3$).

Staining of bacterial cells by SYBR gold-labeled phages. Phage labeling and observation of phage-treated bacterial cells were performed according to Mosier-Boss et al. (27). To 100 ml of the phage lysate, 10 μl of $10^4\times$ SYBR gold (Molecular Probes, Inc., Eugene, OR, USA) in dimethyl sulfoxide (DMSO) was added. After 10 min, the labeled phage particles were precipitated by centrifugation with a P28S rotor in a Hitachi XII100β centrifuge at 40,000 × *g* for 1 h at 4°C. Three washes using 1× PBS were done to ensure the removal of excess SYBR gold. A 1-ml sample of an overnight culture of *X. axonopodis* pv. citri was mixed with 4 ml NB and allowed to grow until an OD_{600} of 0.5 was reached. To a 10-μl sample of the bacterial culture was added 10 μl SYBR gold-labeled phage, and the mixture was incubated for 10 to 60 min. As a control, a culture of *E. coli* JM109 was treated in the same way. After fixation of the mixture with 30 μl 4% paraformaldehyde in PBS, 5 ml double-distilled water (ddH_2O) was added, and the mixture was filtered through a membrane filter (0.2-μm pore size, Steradisc; Krabo, Osaka, Japan). The bacterial cells were observed under a fluorescence microscope system with filter sets (Olympus BH2 fluorescence microscope; Olympus, Tokyo, Japan). Microscopic images were recorded with a charge-coupled-device (CCD) camera (Kyence VB-6010; Osaka, Japan).

Nucleotide sequence accession numbers. The sequence data for the Cp1 and Cp2 genomes have been deposited in the DDBJ database under accession no. AB720063 and AB720064, respectively.

RESULTS AND DISCUSSION

Cp1 and Cp2 belong to different virus families. Morphology indicates that phages Cp1 and Cp2 belong to different virus families: Cp1 as a member of *Siphoviridae* and Cp2 as a member of *Podoviridae*. The purified particles of Cp1 and Cp2 were negatively stained and examined by transmission electron microscopy. Cp1 particles had an icosahedral capsid of 60 ± 5 nm in diameter with a long noncontractile tail of 135 ± 10 nm long by 12 ± 2 nm wide (see Fig. S1 in the supplemental material). This morphology was almost the same (though in smaller dimensions) as that reported preliminarily for CP1 particles replicated in strain N6101 as a host (28), indicating that, morphologically, Cp1 belongs to the family *Siphoviridae*. In contrast, Cp2 particles showed an icosahedral capsid of 60 ± 5 nm in diameter with a short tail of 15 ± 5 nm long (see Fig. S1 in the supplemental material), indicating that Cp2 has a structure typical of members of the family *Podoviridae*. In a preliminary work, this phage was reported to have larger polyhedral particles without a tail (28). These results raised the question of whether Cp1 and Cp2 are related to each other in infection and replication in host strains.

Comparison of infection cycles of Cp1 and Cp2. Both Cp1 and Cp2 form clear plaques with various *X. axonopodis* pv. citri strains, including those shown in Table 1, as hosts (4, 5). The infection cycle of each phage was characterized by a single-step growth experiment with appropriate hosts. The growth curves are shown in Fig. 1. In the case of Cp1 replication, the latent period was ~60 min, followed by a rise period of 20 to 30 min, giving an entire cycle of 80 to 90 min. The average burst size was 20 PFU per infected cell. For Cp2 replication, the latent period was ~90 min, with a 60-min rise period, taking 150 to 180 min for a single growth cycle. The burst size was approximately 100 PFU/cell. These results showed that Cp1 infected and replicated more rapidly than Cp2, but the burst size was much smaller than that of Cp2. These results contrasted with the observation that more than 600 progeny phages were formed in an infected bacterial cell for both Cp1 and Cp2, as detected by electron microscopy (28). The burst size of a phage may depend on the host strain, culture medium, culture conditions, cell age, and MOI (29). The net ratio of infective to noninfective phage particles in the progeny population and the frequent readsorption of phage particles onto cell debris may partly explain this discrepancy.

Genomic analyses of Cp1: gene organization and homology to other phages. The Cp1 genome was a linear double-stranded (ds) DNA of approximately 44 kbp, as determined by PFGE (data not shown). The nucleotide sequence of the Cp1 genome was determined using shotgun sequencing of DNA purified from phage particles. Sequences were assembled into a circular contig of 43,870 bp, suggesting the presence of terminal repeats. The exact termini of the Cp1 genome were determined to have a 10-nucleotide (nt) 3′-protruding *cos* site (5′-CCAGTTGTCT, corresponding to positions 43,861 to 43,870) at either end.

The Cp1 genome had a G+C content of 53.3%; this value was significantly lower than that of the host genome (e.g., 64.7% for strain 306, accession no. NC_003919). When the databases were searched using BLAST and BLASTX programs for sequences homologous to the Cp1 DNA sequence, extensive homologies were detected in the genome sequence of *X. campestris* phage phiL7 (accession no. EU717894), *X. oryzae* phage OP1 (accession no.

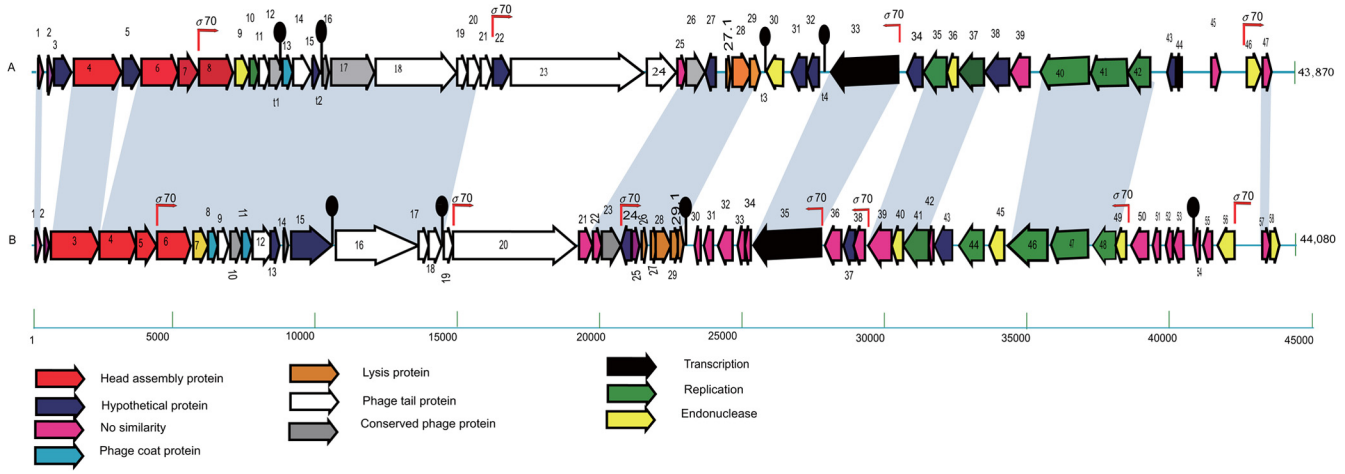

FIG 2 Genomic organization of phages Cp1 (A) and phiL7 (B). Colored arrows indicate the directions and categories of the genes. Broken arrows and black knobs indicate the σ^{70}-type promoters and predicted terminators for transcription, respectively. "No similarity" was determined using an E value lower than e−4 as a cutoff for notable similarity.

AP008979), and *Xanthomonas* phage Xp10 (accession no. AY299121). All these phages are siphoviruses infecting species of *Xanthomonas*, which is consistent with the Cp1 morphological features. An extended colinearity of the nucleotide sequence homology, with several short interspersed divergent islands, was detected throughout almost the entire genomic region between Cp1 and phiL7, which gave the highest similarity score (see Fig. S2 in the supplemental material).

Forty-eight potential ORFs comprising 50 or more codons, starting with ATG or GTG as the initiation codon, and with a Shine-Dalgarno ribosome-binding sequence preceding the initiation codon, were detected in the Cp1 genome. The genome was divided into left and right arms by the ORF29 and ORF30 intergenic region, with genes on the two arms transcribed convergently (Fig. 2). The 48 deduced proteins included (i) 27 proteins that had database homologs of known function, including phage structural proteins, DNA packaging proteins, and proteins involved in DNA replication, transcription, and lysis; (ii) 19 hypothetical proteins in the databases, including many phiL7 proteins; and (iii) 2 proteins with no similarities in the databases (see Table S1 in the supplemental material). The gene organization of Cp1 was compared with that of phiL7 (Fig. 2). This comparison showed that *p21*, *p25*, *p26*, *p30-p34*, *p36-p38*, *p42*, *p45*, *p49-p52*, *p55*, and *p56* of phiL7, most of which were without similarity in the databases, were missing from Cp1, and instead *orf3*, *orf5*, *orf30-orf32*, *orf34*, *orf44*, and *orf45* were inserted or replaced in the Cp1 genome. Some of these genes, such as *p45*, *p49*, and *p56* of phiL7 and *orf3*, *orf5*, and *orf30* of Cp1, encoded HNH endonuclease, GIY-YIG endonuclease, or group I intron endonuclease, suggesting their involvement in gene rearrangements, especially horizontal gene movements. However, the group I intron inserted in the DNA polymerase gene (*p44-p46*) in phiL7 (30) was missing from the corresponding region of the Cp1 gene (*orf40*).

Interestingly, Cp1 encodes a viral RNA polymerase (RNAP; ORF33) (a single-subunit RNAP similar to the T7-type enzymes). Sequence analysis showed that Cp1 ORF33 was 71.4% identical to phiL7 p35 (ACE75775.1) and 31.5% identical to T7 RNAP (NP_041960) (Fig. 3A). Cp1 ORF33 also showed 40 to 50% amino acid sequence identity with RNAPs of other *Xanthomonas* phages, such as Xp10 (AAP58699.1), OP1 (BAE72738.1), and Xop411 (ABK00180.1) (Fig. 3A). All important amino acid residues identified in T7 RNAP for structure and function (31, 32) were conserved among these RNAPs. Their phylogenetic relationship is shown in Fig. 3B. The siphovirus Xp10 was shown to rely on both host and phage RNAPs, and the shift from host to phage RNAP is regulated by phage protein p7 (33). Xp10 p7 (73 amino acids [aa]) is encoded by gene p45L, located after the replication module of the Xp10 genome. A similar regulation may work in Cp1 because ORF44, encoding 66 aa with a sequence similarity to inhibitors of transcriptional initiators and terminators (33% identical to Xp10 p45L; AAP58713.1), was located at the corresponding position on Cp1 DNA (Fig. 2). Like Xp10, the protein encoded by ORF44 may function to inhibit host RNAP and act as an antiterminator, allowing RNAP to pass through the intrinsic terminator for expression of the late genes (33).

Furthermore, we detected a homolog of the OP1 tail fiber protein (Tfb, OP1-ORF25), which was thought to be involved in host range determination, mediated by variation in the combination of repetitive motifs at the N terminus (34).

Genomic analyses of Cp2: gene organization and homology to other phages. The Cp2 genome was also a linear dsDNA of approximately 43.0 kbp, based on PFGE analysis (data not shown). The Cp2 DNA isolated from phage particles was subjected to shotgun sequencing. Sequences were assembled into a circular contig of 42,963 bp, also suggesting the presence of terminal repeats. The precise sequence of the repeat was not determined. The Cp2 genome had a G+C content of 66.7%, comparable with that of the host genome (ca. 64.7%). To find homologous sequences, nucleotide sequences from Cp2 were used to search sequence databases. Short-ranged homologies were found in the sequences of *Azospirillum brasilense* Sp245 plasmid (accession no. HE577328; E value, 2e−11 [84 bit]) and *Burkholderia pseudomallei* bacteriophage phi1026b (accession no. AY453853; E value, 5e−09 [76 bit]). Interestingly, a sequence in the genome of *X. axonopodis* pv. citri strain 306 also showed some homology to the Cp2 genome (accession no. AE008923; E value, 8e−08 [72 bit]). The homologous sequence corresponded to a single gene (*orf32* of Cp2, encoding a single-strand [ss] binding protein). However, the

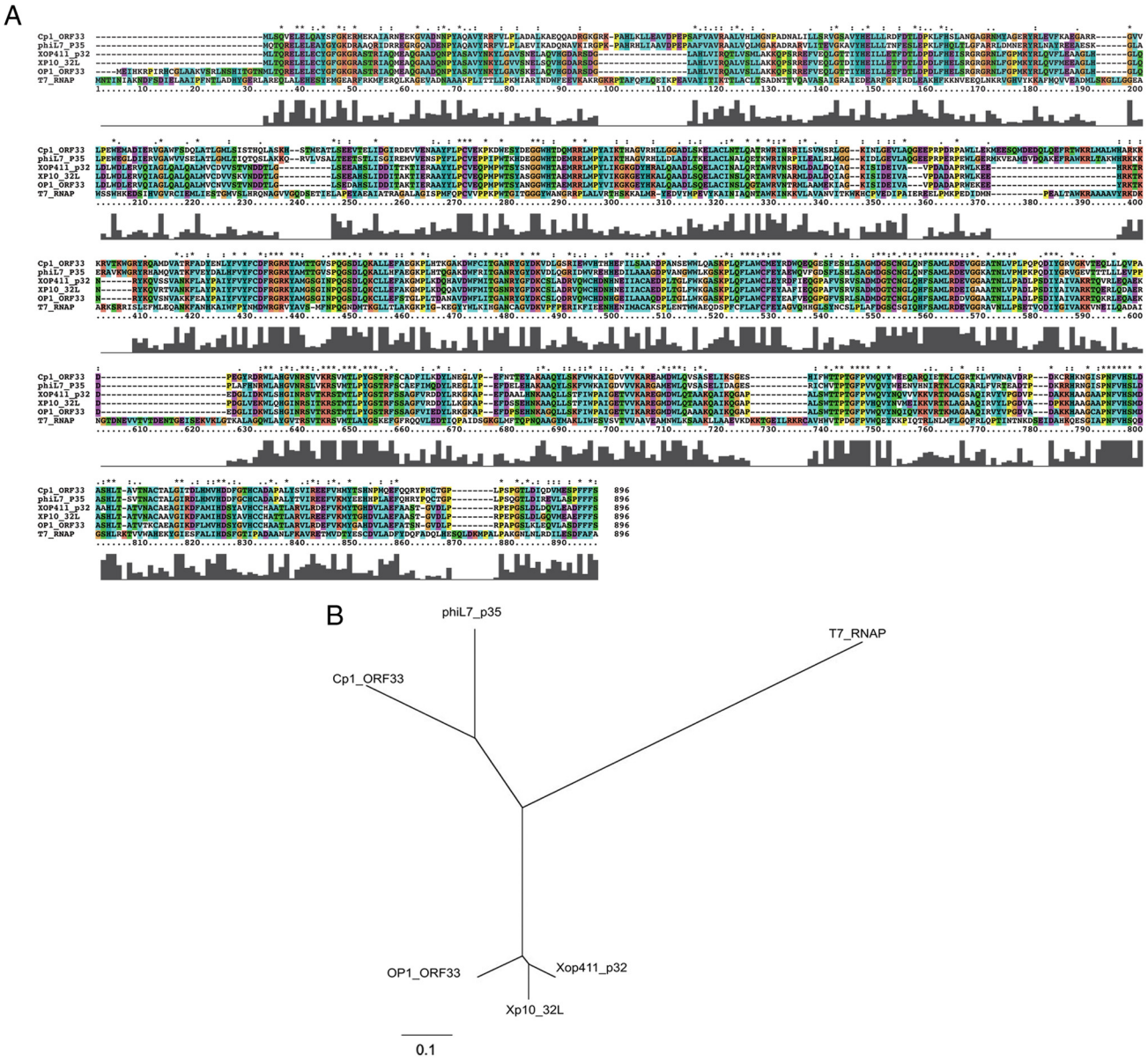

FIG 3 Comparison of amino acid sequences of RNA polymerases (RNAP) encoded by *Xanthomonas* phages. (A) The amino acid sequence of Cp1 ORF33 (AB720063) was aligned with those of phiL7 p35 (ACE75775.1)., Xop411 p32 (ABK00180.1), Xp10 32L (AAP58699.1), OP1 ORF33 (BAE72738.1), and coliphage T7 RNAP (NP_041960.1) using ClustalX. The ClustalX coloring scheme depends on both the residue type and the pattern of conservation within a column (http://www.cgl.ucsf.edu/chimera/docs/ContributedSoftware/multalignviewer/cxcolor.html). Conservation scores are drawn below the alignment. (B) The unrooted dendrogram was constructed with the Treeview tool using the maximum likelihood method based on a complete protein sequence alignment of RNAP proteins from other phages.

1.8-kbp region, including XAC1661 (Isxac3 transposase) and XAC1662 (*repA*) of strain 306, which was specifically amplified by rep-PCR for $Cp1^r/Cp2^s$ strains (9), did not show any sequence homology with the Cp2 genome. Forty potential ORFs were identified in the Cp2 genome. The 40 deduced proteins included (i) 20 proteins that had database homologs of known functions, including phage structural proteins, DNA processing proteins, and lysis proteins; (ii) 16 hypothetical proteins showing marginal similarities with unknown proteins of various origins; and (iii) four proteins with no similarities in the databases (see Table S2 in the supplemental material). The ORF map is shown in Fig. 4. Morphologically, Cp2 belongs to the family *Podoviridae*. The genome of coliphage T7, the representative of T7-like phages of the *Podoviridae*, generally consists of three functional gene clusters: one for early functions (class I), one for DNA metabolism (class II), and the other for structural proteins and virion assembly (class III) (35). For the Cp2 genome, the assignment of classes I to III was difficult because of the lack of sufficient information about each gene, especially about key genes, such as those encoding RNAP, DNA metabolism, and structural proteins. After identifying genes for structural proteins, we tentatively assigned the three functional modules according to the T7 gene arrangement (Fig. 4). In this

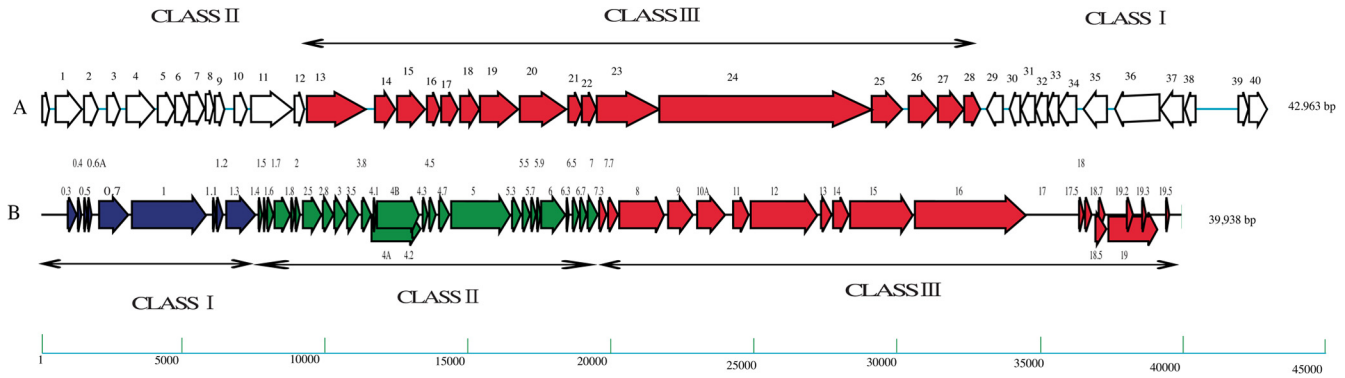

FIG 4 Genomic organization of phages of Cp2 (A) and *Escherichia coli* T7 (B). Arrows indicate the sizes and directions of the genes. The typical podovirus genome represented by T7 phage consists of three functional modules: class I, class II, and class III, as shown in panel B (35). Putative class I (white), class II (white), and class III (red) modules for Cp2 are shown in panel A.

Cp2 gene arrangement, the putative class I module contained ORF32 (with similarity to ssDNA-binding proteins), ORF33 (HNH endonuclease), ORF34 (YqaJ-like recombinase), and ORF35 (ERF family protein) (see Table S2 in the supplemental material). The Cp2 putative class II region contained ORF39 (with a marginal similarity to DNA polymerase gamma-1 subunit), ORF40 (pyocin-like), ORF3 (Holliday junction resolvase), and ORF5 (lysozyme) (see Table S2 in the supplemental material). The details for class III, consisting of ORF13 to ORF29, are described below.

We could not find a gene for RNAP in the Cp2 genome. In general, T7-like podoviruses use phage-encoded RNAP for predominant expression of phage genes (36). T7-RNAP encoded in the class I module (early expressed by host RNAP) specifically recognizes phage promoters of class II and class III genes for the shift of gene expression. However, several podoviruses that have the RNAP gene in the class II module showed a high dependency on the host RNAP for the expression of phage genes (18, 37). Marine phages VpV262 and SI01, which share extensive homology with T7, lack a phage RNAP (38), indicating absolute dependency on the host RNAP for the expression of phage genes. Therefore, the lack of an RNAP gene in the Cp2 genome is not surprising. Searching promoter sequences throughout the Cp2 genome using ORFinder revealed only typical σ^{70} promoters (data not shown). Notably, the siphovirus Cp1 contained an RNAP gene that is phylogenetically related to RNAP genes of T7-like phages. In the genomes of siphoviruses such as *Xanthomonas* phage Xp10, as well as Xop411 and OP1, a cluster of λ-like structural genes is connected to other gene clusters arranged in the reverse orientation, such as the T7-like class II and class I genes (39).

Proteomic analyses of Cp1 and Cp2 virions. Using SDS-PAGE in conjunction with LC-MS/MS, we identified virion proteins of Cp1 and Cp2. In the case of Cp1, at least 10 proteins, ranging from 13 kDa to ca. 120 kDa, were separated by SDS-PAGE (Fig. 5A). All these proteins were recovered, in-gel digested, and subjected to mass spectrometric analysis. The results are shown on the right side of Fig. 5A. The identified proteins include p5 (unknown protein), p6 (head portal protein), p8 (head protein), p14 (major tail protein), p18 (tail length tape major protein), p23 (tail fiber protein), p28 (lysozyme), p29 (hypothetical protein), and p31 (unknown protein). We observed oligomerization of two proteins. The major head protein (p8; calculated to be 41.7 kDa) was detected at a position corresponding to ~200 kDa by SDS-PAGE, suggesting oligomers consisting of five subunits. In addition, p5 (unknown protein) has a calculated molecular mass of 23.71 kDa but was observed at a position corresponding to 60 to 70 kDa, suggesting that this protein exists as a trimer. These subunits may be covalently linked in the phage particles. For other proteins, the observed size was close to the calculated size. In the Cp1 genomic analysis, we detected a homolog of the OP1 tail fiber protein (Tfb, OP1-ORF25), which was thought to be involved in host range determination, mediated by variation in the combination of repetitive motifs at the N terminus (33). However, the corresponding Cp1 ORF (ORF24) was much smaller (358 aa) than OP1-ORF25 (431 aa) and the similarity was limited to 42 aa at the N terminus (67% identity) without any following repetitive motifs. Indeed, this protein was not detected among the Cp1 structural proteins (Fig. 5A). It is unknown whether this protein is involved in host range determination. Instead, a large protein corresponding to ORF23 (1,574 aa residues) was detected (Fig. 5A), which showed significantly high similarity to tail fiber proteins of several phages: 22R of Xp10 (accession no. Q7Y5J5), p22 of Xop411 (accession no. YP_001285691) and p20 of phiL7 (accession no. YP_002922634). This protein might be involved in determining the host range, as suggested by Lee et al. (30, 40).

For Cp2 virions, at least 13 proteins, ranging from 16 kDa to ca. 300 kDa, were separated by SDS-PAGE (Fig. 5B). All of these proteins were recovered and subjected to mass spectrometric analysis as above. The results are shown on the right side of Fig. 5B. The proteins identified were from the cluster of ORFs 13 to 28 on the Cp2 map (Fig. 4), giving a putative structural module (class III) of T7-like phages. From this cluster, p14 (endoproteinase), p17 (unknown protein), and p21 (hypothetical protein) were not detected. The identified proteins included p13 (head-tail connecting protein), p15 (major capsid protein), p18 (tail tubular protein A), p23 (structural lysozyme), p24 (lysin-like protein), p25 (end-tail-spike protein), P26 (LysM domain protein), p27 (tail fiber protein), and p28 (tail fiber protein). Among these, p23 (structural lysozyme; calculated to be 79 kDa) gave three ladder bands around 80 to 130 kDa, which suggested processing and oligomerization of this protein.

Host selection by Cp1 and Cp2. As described above, phages Cp1 and Cp2, used practically for phage typing of *X. axonopodis*

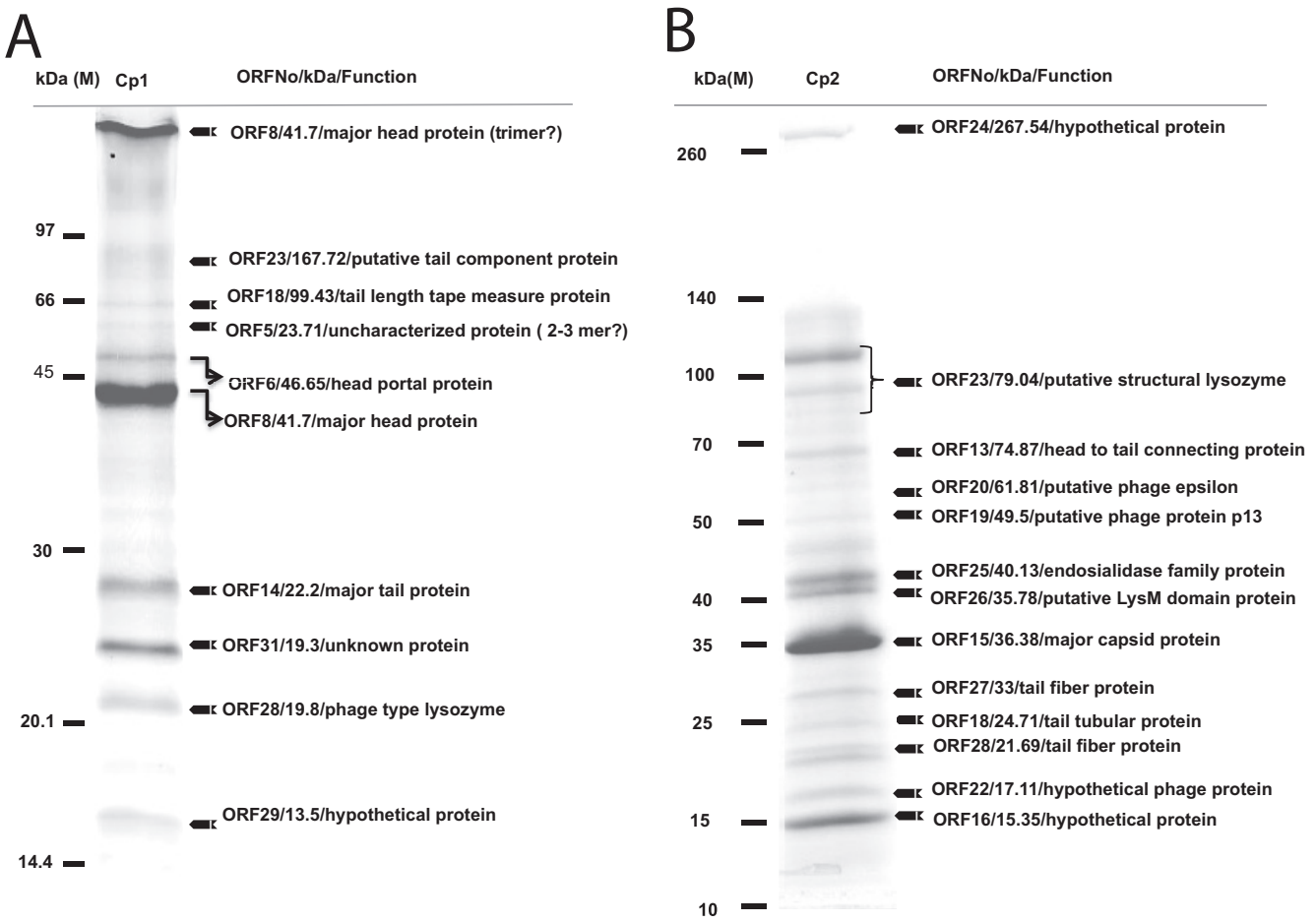

FIG 5 Proteomic analysis of Cp1 (A) and Cp2 (B) particles. Proteins of purified phage particles were separated in 10% (wt/vol) polyacrylamide gel by SDS-PAGE and stained with Coomassie brilliant blue. The protein bands were recovered, digested in gel, and subjected to LC-MS/MS analysis. On the right are the descriptions of the genes, their deduced molecular sizes based on the ORF sequences, and their possible functions. Positions of size markers are shown on the left. For some protein bands, possible oligomerization of the phage protein was observed.

pv. citri strains, were found to belong to completely different virus groups. This raises the question of how these phages discriminate host strains. The initial and essential event for a phage to succeed in infection is attachment of the phage particles to the host surface receptors. Therefore, differential adsorption of Cp1 and Cp2 to host cells was examined, according to the method described in Materials and Methods. The results shown in Table 2 indicated that both $Cp1^s/Cp2^r$ and $Cp1^r/Cp2^s$ strains (MAFF 301080 and MAFF 673010, respectively) adsorbed Cp1 and Cp2 efficiently. Even a $Cp1^r/Cp2^r$ strain (MAFF 31130) also adsorbed Cp1 and Cp2 almost equally. To further investigate the relationship between Cp1 and Cp2 infection, we isolated resistant mutants from the host strains. When a spontaneous mutant showing $Cp1^r$ from MAFF 301080 was subjected to phage adsorption assay, it did not adsorb Cp1 but did absorb Cp2, as did its wild type (Table 2). This mutant also showed $Cp2^r$. In the same way, a spontaneous mutant showing $Cp1^r/Cp2^r$ from MAFF 673010 did not adsorb Cp2 but did absorb Cp1 (Table 2). Moreover, when cells of MAFF 301080 ($Cp1^s/Cp2^r$) were first treated with Cp2 particles at an MOI of 5 and then subjected to plaque assay with Cp1, the number of plaques that appeared were almost the same as that with untreated cells (data not shown). Similar results were obtained for MAFF 673010 ($Cp1^r/Cp2^s$) cells with pretreated with Cp1 and assayed for Cp2 infection. Taken together, these results indicated that Cp1 and Cp2 use different molecules on the host cell surface as phage receptors and that discrimination of strains by Cp1 and Cp2 is not at the initial stage by binding to receptors, but at some stage(s) afterwards. Another question arose as to what happens to the phage DNA after cell attachment in the case of nonhost strains. To answer this question, SYBR gold-labeled phages were added to

TABLE 2 Adsorption of Cp1 and Cp2 to bacterial strains

Strain	Phage type	Phage adsorption (%)	
		Cp1	Cp2
X. axonopodis pv. citri			
MAFF 301080	$Cp1^s/Cp2^r$	100	>99
301080 R1	$Cp1^r/Cp2^r$	0	>99
MAFF 673010	$Cp1^r/Cp2^s$	>99	100
673010 R2	$Cp1^r/Cp2^r$	>99	0
MAFF 31130	$Cp1^r/Cp2^r$	>99	>99
E. coli JM109		0	0

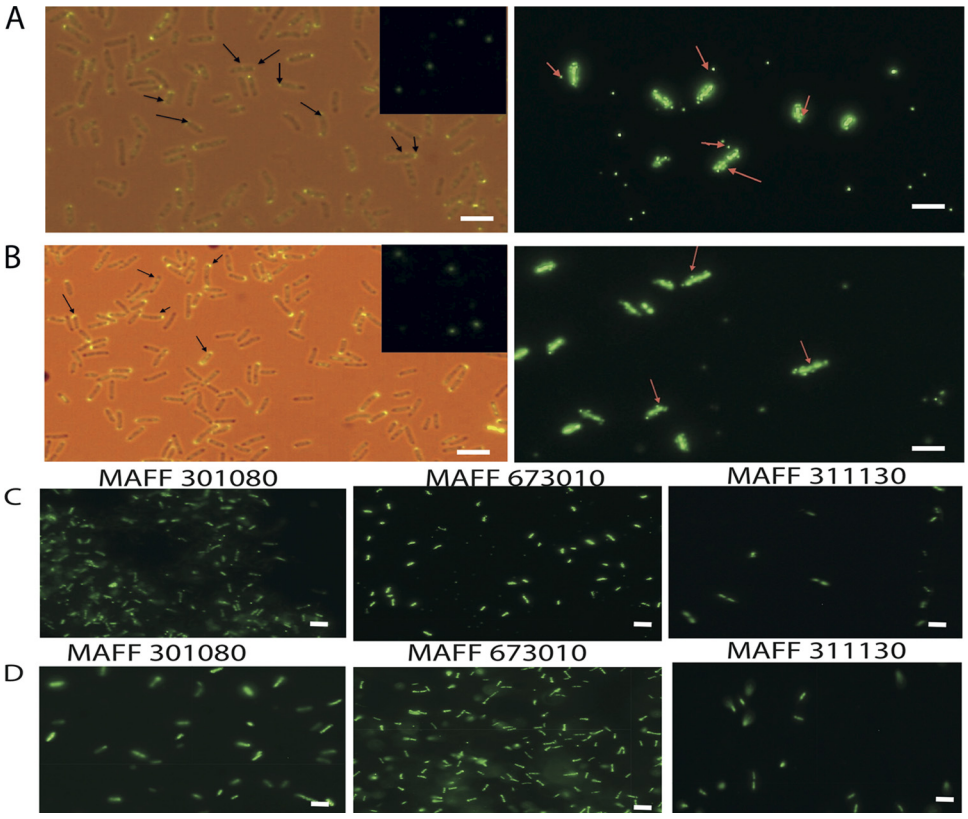

FIG 6 Attachment of SYBR gold-labeled phage particles to bacterial cells and staining of the cells by possible injection of phage DNA. (A) Cp1 particles were added to cells of host strain MAFF 301080; (B) Cp2 particles were added to cells of host strain MAFF 673010. Cells from panels A and B were observed under a fluorescence microscope at 10 min (MOI = 1, left panel) and 20 min (MOI = 10, right panel) postinfection. The attachment of the phage particles to the bacterial cell surface is shown. Phage particles appear as tiny spots (arrows). At 10 min postinfection, bacteria cell were not stained (bright and dark fields), while cells became stained at 20 min postinfection (dark field). Cp1 (C) and Cp2 (D) particles were also added to cells of MAFF 301080 ($Cp1^s/Cp2^r$), MAFF 673010 ($Cp1^r/Cp2^s$), and MAFF 311130 ($Cp1^r/Cp2^r$). Cells were observed under a fluorescence microscope at 30 min postinfection. Bacterial cells were stained by SYBR gold, indicating injection of phage DNA into the $Cp1^s/Cp2^r$ or $Cp1^r/Cp2^s$ as well as $Cp1^r/Cp2^r$ cells. Bar, 10 μm.

cells of *X. axonopodis* pv. citri strains and the movement of SYBR gold-labeled phage DNA was monitored. SYBR gold-labeled phage attached to host cells (observed after 10 to 20 min postinfection), and bacterial cells were not stained at 10 min postinfection (Fig. 6A and B, left panels), but some cells became stained at 20 min postinfection, possibly by injection of phage DNA (Fig. 6AB, right panels). As shown in Fig. 6C and D, after 30 min postinfection, Cp1 DNA seemed to be injected into most cells of MAFF 673010, MAFF 31130, and MAFF 301080. Similarly, Cp2 DNA seemed to be injected into most cells of MAFF 301080, MAFF 31130, and MAFF 673010. With cells of *E. coli* as the control, Cp1 and Cp2 did not attach to the cells and no injection of DNA occurred (data not shown). Once the phage DNA was introduced into cells, it was retained stably for a certain period. In the case of resistant strains, cell growth continued after phage addition. Host restriction/ modification systems may contribute to this host selection, but its importance is not clear because Cp1 and Cp2 progenies produced from strain KC33 ($Cp1^s/Cp2^s$) showed exactly the same host range as their original phages (data not shown). These results suggested that host selection by Cp1 and Cp2 may occur at or after immediate early expression of phage genes.

In the genome of hosts such as strain 306 (accession no. NC_603919), there are no sequence elements that showed significant homology with Cp1 or Cp2 sequences. The 1.8-kbp region containing a transposon that was specifically amplified by rep-PCR from genomic DNA of $Cp1^r/Cp2^s$ strains (9) and the region containing *avrBs3* and *pthA*, varying between $Cp1^s/Cp2^r$ and $Cp1^r/Cp2^s$ strains (9), did not show any nucleotide sequence homology with the Cp1 and Cp2 genomes. Dot blot and Southern blot hybridization of genomic DNA from 11 strains tested (Table 1) showed no significant hybridization signals with Cp1 DNA or Cp2 DNA as a probe (data not shown). Therefore, no direct connection between the host genome and Cp1/Cp2 genomes was detected.

Conclusion. Bacteriophages Cp1 and Cp2, traditionally used as phage-typing agents for *X. axonopodis* pv. citri strains, were found to belong to completely different virus groups. Cp1 was characterized as a phiL7-like siphovirus, but without a group I intron in the genome, and Cp2 was classified as a new podovirus with genes lacking detectable homologs in the current databases. The host *hssB3.0* and XAC1661-XAC1662 sequences were not related to either Cp1 or Cp2 sequences. Both Cp1 and Cp2 efficiently attached to host cells, even if those were resistant strains.

ACKNOWLEDGMENTS

We thank H. Shiotani of the National Institute of Fruit Tree Science, NAFRO, for *X. axonopodis* pv. citri strain KC33 and helpful suggestions about the strains, H. Ogata of Tokyo Institute of Technology for Cp2 gene

annotation, and M. Nakano of ADSM, Hiroshima University, for her technical guidance on LC-MS/MS analysis.

REFERENCES

1. **Civerelo EL.** 1984. Bacterial canker disease of citrus. J. Rio. Grande Val. Hort. Soc. **37:**127–145.
2. **Gottwald TR, Graham JH, Schubert TS.** 2002. Citrus canker: the pathogen and its impact. Plant health progress. http://www.plantmanagementnetwork.org/pub/php/review/citruscanker/.
3. **Stall RE, Civerolo EL.** 1991. Research relating to the recent outbreak of citrus canker in Florida. Annu. Rev. Phytopathol. **29:**399–420.
4. **Wakimoto S.** 1967. Some characteristics of citrus canker bacteria, Xanthomonas citri (Hasse) Dowson, and the related phages isolated from Japan. Ann. Phytopathol. Soc. Jpn. **33:**301–310.
5. **Obata T.** 1974. Distribution of *Xanthomonas citri* strain in relation to the sensitivity to phage CP1 and CP2. Ann. Phytopathol. Soc. Jpn. **40:**6–13.
6. **Goto M, Takahashi T, Messina MA.** 1980. A comparative study of the strains of *Xanthomonas campestris pv. citri* isolated from citrus canker in Japan and cancrosis B in Argentina. Ann. Phytopathol. Soc. Jpn. **46:**329–338.
7. **Shiotani H, Tsuyumu S, Ozaki K.** 2000. Pathogenic interactions between *Xanthomonas axonopodis pv. citri* and cultivars of Pummelo (*Citrus grandis*). Phytopathology **90:**1383–1389. http://dx.doi.org/10.1094/PHYTO.2000.90.12.1383.
8. **Louws FJ, Fulbright DW, Stephens CT, de Bruijn FJ.** 1994. Specific genomic fingerprints of phytopathogenic *Xanthomonas* and *Pseudomonas* pathovars and strains generated with repetitive sequences and PCR. Appl. Environ. Microbiol. **60:**2286–2295.
9. **Shiotani H.** 2007. Dissertation. The United Graduate School of Agricultural Science, Gifu University, Gifu, Japan.
10. **Swarup S, Yang Y, Kingsley MT, Gabriel DW.** 1992. An *Xanthomonas citri* pathogenicity gene, phcA, pleiotropically encodes gratuitous avirulence on nonhosts. Mol. Plant Microbe Interact. **5:**204–213.
11. **Szurek B, Rossier O, Hause G, Bonas U.** 2002. Type III dependent translocation of the *Xanthomonas* AvrBs3 protein into the plant cell. Mol. Microbiol. **46:**13–23. http://dx.doi.org/10.1046/j.1365-2958.2002.03139.x.
12. **Shiotani H, Fujikawa T, Ishihara H, Tsuyumu S, Ozaki K.** 2007. A *pthA* homolog from *Xanthomonas axonopodis pv. citri* responsible for host-specific suppression of virulence. J. Bacteriol. **189:**3271–3279. http://dx.doi.org/10.1128/JB.01790-06.
13. **Sambrook J, Russell DW.** 2001. Molecular cloning: a laboratory manual, 3rd ed. Cold Spring Harbor Laboratory Press, Cold Spring Harbor, NY.
14. **Dykstra MJ.** 1993. A manual of applied technique for biological electron microscopy. Plenum Press, New York, NY.
15. **Yamada T, Kawasaki T, Nagata S, Fujiwara A, Usami S, Fujie M.** 2007. New bacteriophages that infect the phytopathogen *Ralstonia solanacearum*. Microbiology **153:**2630–2639. http://dx.doi.org/10.1099/mic.0.2006/001453-0.
16. **Hung CH, Yang CF, Yang CY, Tseng YH.** 2003. Involvement of tonB-exbBD1D2 operon in infection of *Xanthomonas campestris* phage phiL7. Biochem. Biophys. Res. Commun. **302:**878–884. http://dx.doi.org/10.1016/S0006-291X(03)00255-9.
17. **Carlson K.** 1994. Single-step growth, p 434–437. *In* Karam J, Drake JW, Kreuzer KN, Mosig G, Hall DH, Eiserlig FA, Black LW, Spicer EK, Kutter E, Carlson K, Miller ES (ed), Molecular biology of bacteriophage T4. ASM Press, Washington, DC.
18. **Kawasaki T, Shimizu M, Satsuma H, Fujiwara A, Fujie M, Usami S, Yamada T.** 2009. Genomic characterization of *Ralstonia solanacearum* phage ϕRSB1, a T7-like wide-host-range phage. J. Bacteriol. **191:**422–427. http://dx.doi.org/10.1128/JB.01263-08.
19. **Higashiyama T, Yamada T.** 1991. Electrophoretic karyotyping and chromosomal gene mapping of *Chlorella*. Nucleic Acids Res. **19:**6191–6195.
20. **Delcher AL, Harmon D, Kasif S, White O, Salzberg SL.** 1999. Improved microbial gene identification with GLIMMER. Nucleic Acids Res. **27:**4636–4641.
21. **Altschul SF, Madden TL, Schaffer AA, Zhang Z, Miller W, Lipman DJ.** 1997. Gapped BLAST and PSI-BLAST: a new generation of protein database search programs. Nucleic Acids Res. **25:**3389–3402.
22. **UniProt Consortium.** 2007. The Universal Protein Resource (UniProt). Nucleic Acids Res. **35:**D193–D197. http://dx.doi.org/10.1093/nar/gkl929.
23. **Wheeler DL, Barrett T, Benson DA, Bryant SH, Canese K, Chetvrnin V, Church DM, DiCuccio M, Edgar E, Federhen S, Geer LY, Kapustin Y, Khovayko O, Landsman D, Lipman DJ, Madden TL, Maglott DR, Ostell J, Miller V, Pruitt KD, Schuler GD, Sequeira E, Sherry ST, Sirotkin K, Souvorov A, Starchenko G, Tatusov RL, Tatusova TA, Wagner L, Yaschenko E.** 2007. Database resources of the National Center for Biotechnology Information. Nucleic Acids Res. **35:**D5–D12. http://dx.doi.org/10.1093/nar/gkl1031.
24. **Fujiwara A, Fujisawa M, Hamasaki R, Kawasaki T, Fujie M, Yamada T.** 2011. Biocontrol of *Ralstonia solanacearum* by treatment with lytic bacteriophages. Appl. Environ. Microbiol. **77:**4155–4162. http://dx.doi.org/10.1128/AEM.02847-10.
25. **Ausubel F, Brent R, Kingston RE, Moore DD, Seidman JG, Smith JA, Struhl K.** 1995. Short protocols in molecular biology, 3rd ed. John Wiley and Sons, Inc., Hoboken, NJ.
26. **Laemmli UK.** 1970. Cleavage of structural proteins during the assembly of the head of bacteriophage T4. Nature **227:**680–685.
27. **Mosier-Boss PA, Lieberman SH, Andrews JM, Rohwer FL, Wegley LE, Breitbart M.** 2003. Use of fluorescently labeled phage in the detection and identification of bacterial species. Appl. Spectrosc. **57:**1138–1144. http://dx.doi.org/10.1366/00037020360696008.
28. **Arai K, Shimo H, Doi Y, Yira K.** 1974. Electron microscopy of *Xanthomonas citri* phages CP1 and CP2 infection. Ann. Phytopathol. Soc. Jpn. **40:**98–102.
29. **Hadas H, Einav M, Fishov I, Zaritsky A.** 1997. Bacteriophage T4 development depends on the physiology of its host *Escherichia coli*. Microbiology **143:**179–185.
30. **Lee CN, Lin JW, Weng SF, Tseng YH.** 2009. Genomic characterization of the intron-containing T7-like phage phiL7 of *Xanthomonas campestris*. Appl. Environ. Microbiol. **75:**7828–7837.
31. **Cheetham GM, Jeruzalmi D, Steiz TA.** 1999. Structural basis for initiation of transcription from an RNA polymerase-promoter complex. Nature **399:**80–83.
32. **Osumi-Davis PA, de Aguilera MC, Woody RW, Woody AY.** 1992. Asp537, Asp812 are essential and Lys631, His811 are catalytically significant in bacteriophage T7 RNA polymerase activity. J. Mol. Biol. **226:**37–45.
33. **Semenova E, Djordjevie M, Shraiman B, Severinov K.** 2005. The tale of two RNA polymerases: transcription profiling and gene expression strategy of bacteriophage Xp10. Mol. Microbiol. **55:**764–777. http://dx.doi.org/10.1111/j.1365-2958.2004.04442.x.
34. **Inoue Y, Matsuura T, Ohara T, Azekami K.** 2006. Bacteriophage OP_1, lytic for *Xanthomonas oryzae pv. oryzae*, changes its host range by duplication and deletion of the small domain in the deduced tail fiber gene. J. Gen. Plant Pathol. **72:**111–118. http://dx.doi.org/10.1007/s10327-005-0252-x.
35. **Dunn JJ, Studier FW.** 1983. Complete nucleotide sequence of bacteriophage T7 DNA and the locations of T7 genetic elements. J. Mol. Biol. **166:**477–535.
36. **Molineux IJ.** 1999. T7-like phages (*Podoviridae*), p 1722–1729. *In* Granoff A, Webster R (ed), Encyclopedia of virology. Academic Press, London, United Kingdom.
37. **Ceyssens PJ, Lavigne R, Mattheus W, Chibeu A, Hertveldt K, Mast J, Robben J, Volckaert G.** 2006. Genomic analysis of *Pseudomonas aeruginosa* phages LKD16 and LKA1: establishment of the ϕKMV subgroup within the T7 subgroup. J. Bacteriol. **188:**6924–6931. http://dx.doi.org/10.1128/JB.00831-06.
38. **Hardies SC, Comeau AM, Serwer P, Suttle CA.** 2003. The complete sequence of marine bacteriophage VpV262 infecting *Vibrio parahaemolyticus* indicates that an ancestral component of a T7 viral supergroup is widespread in the marine environment. Virology **310:**359–371. http://dx.doi.org/10.1016/S0042-6822(03)00172-7.
39. **Yuzenkova J, Nechaev S, Berlin J, Rogulja D, Kuznedelov K, Inman R, Mushegian A, Severinov K.** 2003. Genome of *Xanthomonas oryzae* bacteriophage XP10: an odd T-odd phage. J. Mol. Biol. **330:**735–748. http://dx.doi.org/10.1016/S0022-2836(03)00634-X.
40. **Lee CN, Hu RM, Chow TY, Lin JW, Chen HY, Tseng YH, Weng SF.** 2007. Comparison of genomes of three *Xanthomonas oryzae* bacteriophages. BMC Genomics **8:**442–453. http://dx.doi.org/10.1186/1471-2164-8-442.

frontiers in
MICROBIOLOGY

ORIGINAL RESEARCH ARTICLE
published: 01 July 2014
doi: 10.3389/fmicb.2014.00321

The filamentous phage XacF1 causes loss of virulence in *Xanthomonas axonopodis* pv. *citri*, the causative agent of citrus canker disease

Abdelmonim Ali Ahmad[1], Ahmed Askora[1,2], Takeru Kawasaki[1], Makoto Fujie[1] and Takashi Yamada[1]*

[1] Department of Molecular Biotechnology, Graduate School of Advanced Sciences of Matter, Hiroshima University, Higashi-Hiroshima, Japan
[2] Department of Microbiology, Faculty of Science, Zagazig University, Zagazig, Sharkia, Egypt

Edited by:
Jasna Rakonjac, Massey University, New Zealand

Reviewed by:
Bhabatosh Das, Translational Health Science and Technology Institute, India
Anne Derbise, Pasteur Institut, France

***Correspondence:**
Takashi Yamada, Department of Molecular Biotechnology, Graduate School of Advanced Sciences of Matter, Hiroshima University, 1-3-1 Kagamiyama, Higashi-Hiroshima 739-8530, Japan
e-mail: tayamad@hiroshima-u.ac.jp

In this study, filamentous phage XacF1, which can infect *Xanthomonas axonopodis* pv. *citri* (*Xac*) strains, was isolated and characterized. Electron microscopy showed that XacF1 is a member of the family *Inoviridae* and is about 600 nm long. The genome of XacF1 is 7325 nucleotides in size, containing 13 predicted open reading frames (ORFs), some of which showed significant homology to Ff-like phage proteins such as ORF1 (pII), ORF2 (pV), ORF6 (pIII), and ORF8 (pVI). XacF1 showed a relatively wide host range, infecting seven out of 11 strains tested in this study. Frequently, XacF1 was found to be integrated into the genome of *Xac* strains. This integration occurred at the host *dif* site (*att*B) and was mediated by the host XerC/D recombination system. The *att*P sequence was identical to that of *Xanthomonas* phage Cf1c. Interestingly, infection by XacF1 phage caused several physiological changes to the bacterial host cells, including lower levels of extracellular polysaccharide production, reduced motility, slower growth rate, and a dramatic reduction in virulence. In particular, the reduction in virulence suggested possible utilization of XacF1 as a biological control agent against citrus canker disease.

Keywords: filamentous phage, loss of virulence, citrus canker, biocontrol

INTRODUCTION

Xanthomonas axonopodis pv. *citri*, *Xac* (syn. *Xanthomonas campestris* pv. *citri*), is the causative agent of Asiatic citrus canker disease (ACC), one of the most serious citrus plant diseases in the world (Civerolo, 1984; Graham et al., 2004). Under natural conditions, the bacterium can invade all aboveground parts of plants, entering through natural openings and wounds (Brunings and Gabriel, 2003; Vojnov et al., 2010). A characteristic symptoms include raised corky lesions surrounded by a water or oil-soaked margin on leaves, stems, and fruits, including defoliation, twigs dieback, general tree decline, blemished fruit, and premature fruit drop in severely infected trees (Graham et al., 2004). Management of ACC relies on an integrated approach that includes: (1) replacement of susceptible citrus species with resistant ones; (2) production of disease-free nursery stock; (3) reduction of pathogen spread by establishing windbreaks and fences around groves; (4) preventative copper sprays; and (5) application of insecticide to control Asian leafminer. Because of the limited effectiveness of the current integrated management strategies, citrus canker disease continues to be an economically serious problem for field-grown crops worldwide (Balogh et al., 2010). Hence, alternative control methods are necessary.

Bacteriophages have recently been evaluated for controlling a number of phytobacteria and are now commercially available for some diseases (Balogh et al., 2010). The use of phages for disease control is a fast expanding area of plant protection, with great potential to replace existing chemical control measures. Bacteriophages have been used effectively for controlling several diseases caused by *Xanthomonas* species, including, peach bacterial spot, caused by *X. campestris* pv. *pruni*, geranium bacterial blight, caused by *X. campestris* pv. *pelargonii*, tomato bacterial spot caused by *Xanthomonas euvesicatoria* and *Xanthomonas perforans*, and onion leaf blight caused by *X. axonopodis* pv. *allii* (Flaherty et al., 2000; Balogh et al., 2003; Obradovic et al., 2004, 2005; Lang et al., 2007). Major challenges of agricultural use of phages arise from the inherent diversity of target bacteria, high probability of resistance development, and weak phage persistence in the plant environment (Balogh et al., 2008, 2010). Very recently, utilization of filamentous phages as a disease management strategy has been investigated, and application will likely increase in the future (Askora et al., 2009; Addy et al., 2012). The filamentous ϕRSM phages have dramatic effects on the virulence of *Ralstonia solanacearum*. Infection of *R. solanacearum* cells with ϕRSM3 decreased their growth rate, twitching motility, movement in tomato plant stems, extracellular polysaccharide (EPS) production, and *phcA* expression, resulting in loss of virulence (Addy et al., 2012). This strategy using filamentous phage might be expanded to control various diseases, including citrus canker disease. In contrast to lytic phages, filamentous phages do not kill the host cells but establish a persistent association between the host and the phage (Askora et al., 2009; Addy et al., 2012). This is an advantage of filamentous phages to solve the problem of bacteriophages easily inactivated by sunlight UV irradiation (Balogh et al., 2010).

In the current study, we isolated and characterized a novel filamentous phage and showed that changes occurred at a cellular level in *X. axonopodis* pv. *citri* strains following infection. This filamentous phage might be a unique biological agent for use against bacterial citrus canker disease.

MATERIALS AND METHODS

BACTERIAL STRAINS AND GROWTH CONDITIONS

Ministry of Agriculture, Forestry, and Fisheries (MAFF) strains of *X. axonopodis* pv. *citri, Xac* (**Table 1**) were obtained from the National Institute of Agrobiological Sciences, Japan. Strain KC33 was obtained from the National Institute of Fruit Tree Science, the National Agriculture and Food Research Organization, Japan. All strains were stored at −80°C in 0.8% nutrient broth (NB) (BBL, Becton Dickinson and Co., Cockeysville, MD, USA) supplemented with 30% (v/v) glycerol. The strains were grown on nutrient agar (NA) medium (Difco, BBLBD, Cockeysville, MD, USA) at 28°C. For preparation of bacterial suspension, *Xac* strains were cultured for 24 h at 28°C with shaking at 220 rpm in NB medium.

For time course experiments, phage-infected and uninfected cells were grown overnight in 5 mL of NB media. Then, 0.5 mL of the cell suspensions (10^8 cfu/mL) were transferred into 100-mL flasks containing 30 mL of NB medium. Cultures were grown at 28°C with agitation at 200 rpm, and $OD_{600\,nm}$ measurements were taken every 3 h over the course of 48 h using a spectrophotometer. Three replicates were included at each time point. The experiments were repeated twice (Li and Wang, 2011).

BACTERIOPHAGE ISOLATION, PURIFICATION, AND CHARACTERIZATION

The presence of filamentous phages in collected soil samples from cropping fields in Japan was detected by the spot test and plaque-forming assay technique (Yamada et al., 2007). Approximately 10 g of soil was placed in a sterile 50 mL conical centrifuge tube that then was filled to the top with tap water, and allowed to stand for 20 min with periodic inversions. The tubes were then centrifuged at 15,000 × g for 20 min and the supernatant was passed through a membrane filter (0.45-μm pore size) (Millipore Corp., Bedford, MA, USA). One-hundred-microliter aliquots of the soil filtrate were subjected to spot test and plaque-forming assay with strains of *Xac* (**Table 1**) as host on NB plates containing 1.5% (w/v) agar. Phages were propagated and purified from single-plaque isolates. An overnight culture of bacteria grown in NB medium (1 mL) was diluted 100-fold with 100 mL of fresh NB medium in a 500 mL flask. To collect a sufficient amount of phage particles, a total of 2 L of bacterial culture was grown. When the cultures reached an OD_{600} of 0.2, bacteriophage was added at a multiplicity of infection (moi) of 0.001–1.0. After further growth for 12–24 h, the cells were removed by centrifugation in a Hitachi Himac CR21E centrifuge with an R12A2 rotor at 8000 × g for 15 min at 4°C. The supernatant was passed through a 0.45-μm-pore membrane filter followed by precipitation of the phage particles in the presence of 0.5 M NaCl and 5% (v/v) polyethylene glycol 6000 (Kanto Chemical Co., Tokyo, Japan). The pellet was collected by centrifugation in a Hitachi Himac CR21E centrifuge with an RPR20-2 rotor at 15 000 × g for 30 min at 4°C, and was dissolved in SM buffer [50 mM Tris/HCl at pH 7.5, 100 mM NaCl, 10 mM $MgSO_4$ and 0.01% gelatin (w/v)]. Phages were stored at 4°C in complete darkness. Phage titers were determined by serial dilution and subsequent plaque-forming assays (Yamada et al., 2007). The purified phage [10^{13} pfu/mL was stained with sodium phosphotungstate prior to observation in a Hitachi H600A electron microscope, according to the methods of Dykstra (1993)].

Table 1 | Bacterial strains used in this study[a].

Strain	Host (Citrus species)	XacF1 sensitivity	Source
X.axonopodis* pv. *citri			
MAFF 301077	*C. limon*	−	NIAS[b]
MAFF 301080	*C. sinensis*	+	NIAS
MAFF 311130	*C. iyo*	−	NIAS
MAFF 302102	*Citrus* sp.	+	NIAS
MAFF 673001	*C. natsudaidai*	+	NIAS
MAFF 673010	*Citrus* sp.	+	NIAS
MAFF 673011	*C. limon*	−	NIAS
MAFF 673013	*Citrus* sp.	+	NIAS
MAFF 673018	*Citrus* sp.	+	NIAS
MAFF 673021	*C. limon*	−	NIAS
KC33	*C. iyo*	+	Shiotani et al., 2007
Phages			
XacF1			This study

[a] *All strains originated in Japan.*

[b] *NIAS, National Institute of Agrobiological sciences, Japan.*

PHAGE SUSCEPTIBILITY AND ADSORPTION ASSAYS

The phage susceptibility assays were based on a standard agar overlay method with dilution series of phage preparations (Yamada et al., 2007; Ahmad et al., 2014). Small turbid plaques, typical of Ff-phages, always appeared at reasonable frequencies depending on input phage titers (usually 300–600 pfu/plate), if the bacterial strain was sensitive to the phage. No spontaneous phages (induced prophages) appeared from either strain tested under usual plaque assay conditions. In the phage adsorption assay, exponentially growing cells (OD_{600} 0.1) of the test strain were mixed with XacF1 phage at moi of 0.1, and the mixture was incubated for 0 min (no adsorption) and 30 min at 28°C to allow binding of the phage to the cell surface. Following centrifugation at 15,000 × g for 5 min at 4°C in a Sakuma SS-1500 microcentrifuge (Sakuma Seisakusho, Tokyo, Japan), the phage titer in the supernatant was determined by a standard plaque assay with the indicator strain (MAFF301080). *Escherichia coli* JM109 was used as a negative control.

DNA ISOLATION AND MANIPULATION

Standard molecular biological techniques for DNA isolation, digestion with restriction enzymes and other nucleases, and construction of recombinant DNAs were followed, according to Sambrook and Russell (2001). Phage DNA was isolated

from the purified phage particles by phenol extraction. In some cases, extrachromosomal DNA was isolated from phage-infected *Xac* cells by the minipreparation method (Ausubel et al., 1995). Replicative-form (RF) DNA for sequencing was isolated from host bacterial cells infected with XacF1 phage, treated with S1 nuclease, and then shotgun-sequenced by Hokkaido System Science Co. (Sapporo, Japan) using a Roche GS Junior Sequence System. The draft assembly of the obtained sequences was assembled using GS *De novo* Assembler v2.6. The analyzed sequences corresponded to 156 times the final genome size of XacF1 (7325 bp). Computer-aided analysis of the nucleotide sequence data was performed using DNASIS v3.6 (Hitachi Software Engineering Co., Tokyo, Japan). Potential ORFs larger than 80 bp were identified using the online program ORF Finder (http://www.ncbi.nlm.nih.gov/gorf/gorf.html) and the DNASIS program. Sequence alignment was performed using the ClustalW (Larkin et al., 2007) program. To assign possible functions to the ORFs, DDBJ/EMBL/GenBank databases were searched using the FASTA, FASTX, BLASTN, and BLASTX programs (Altschul et al., 1997).

DETERMINATION OF *att*L AND *att*R SEQUENCES IN *Xac* MAFF673010

Chromosomal DNA was extracted from *Xac* MAFF673010 after infection with XacF1 and subjected to PCR to amplify fragments containing left and right attachment sites (*att*L and *att*R). The *att*L was amplified using a 29-base forward primer, 5′-TGC GAT CGA GCA GCT TCC CAG TTG GCG AT-3′ (primer P1) and a 30-base reverse primer, 5′-TTC GAT GGT CAC GGT GCC TGT AGT AGA GGC-3′ (primer P2), while *att*R was amplified using a 30-base forward primer, 5′-ATA ATT TGC TTG ACA CCG TGC GCA AGT CGT 3′ (primer P3) and a 28-base reverse primer, 5′-CCT TGA CCG TCA GGG ACT GCA TCA GCC T-3′ (primer P4). The primer sequences were based on the *dif* (*att*B) region sequence of *Xanthomonas citri* subsp. citri Aw12879 (DDBJ accession no. CP003778.1). The PCR products were purified from an agarose gel and subjected to sequencing.

SOUTHERN HYBRIDIZATION

Genomic DNA from bacterial cells was prepared by the minipreparation method according to Ausubel et al. (1995). Following digestion with restriction enzyme *Hin*cII, DNA fragments were separated by agarose gel electrophoresis, blotted onto a nylon membrane (Piodyne; Pall Gelman Laboratory, Closter, NJ, USA), hybridized with a probe (the entire XacF1 DNA digested by *Eco*RI), labeled with fluorescein (Gene Images Random Prime labeling kit; Amersham Biosciences, Uppsala, Sweden), and detected with a Gene Images CDP-Star detection module (Amersham Biosciences). Hybridization was performed in buffer containing 5× SSC (0.75 M NaCl, 0.075 M sodium citrate), 0.1% (w/v) sodium dodecyl sulfate (SDS), 5% liquid block, and 5% (w/v) dextran sulfate for 16 h at 65°C. The filter was washed at 60°C in 1× SSC and 0.1% (w/v) SDS for 15 min and then in 0.5× SSC and 0.1% (w/v) SDS for 15 min with agitation, according to the manufacturer's protocol. The hybridization signals were detected by exposing X-ray film (RX-U; Fuji Film, Tokyo, Japan) to the filter.

EPS ASSAY

EPS in bacterial culture supernatants was determined quantitatively as described previously (Guo et al., 2010). Briefly, bacterial strains were grown in NB supplemented with 2% (w/v) D-glucose for 24 h at 28°C with shaking at 200 rpm. A 10-mL portion of the culture was collected, and the cells were removed by centrifugation (5000 × g for 20 min). The supernatant was mixed with three volumes of 99% ethanol and the mixture was kept at 4°C for 30 min. To determine the dry weights of EPS, the precipitated EPS was collected by centrifugation and dried at 55°C overnight prior to measurement. Three replicates were used for each strain and the test was repeated three times.

MOTILITY ASSAY

Swimming and swarming motilities were examined on NB containing 0.3% (w/v) and 0.7% (w/v) agar (Difco, Franklin Lakes, NJ, USA), respectively. Overnight cultures of bacteria grown in NB were centrifuged at 8000 × g for 2 min at 4°C, washed twice with ddH_2O, and resuspended in ddH_2O ($OD_{600} = 1.0$). Two microliters of the suspension were spotted onto NA plates (diameter, 90 mm; containing 20 mL of NA) and incubated at 28°C. The migration zones were measured, and used to evaluate the motility of *Xac* cells (Li and Wang, 2011; Addy et al., 2012). For twitching motility assays, overnight bacterial culture in NB were centrifuged at 8000 × g for 2 min at 4°C, washed twice with ddH_2O, resuspended in ddH_2O ($OD_{600} = 1.0$), and spotted on minimal medium (MM) plates (Addy et al., 2012). Plates were incubated at 28°C, and the morphology of the colony edge was observed under a light microscope (100× magnification).

PATHOGENICITY ASSAY

After careful washing with tap water, immature fully expanded lemon leaves were sterilized by soaking for 2 min in sodium hypochlorite, followed by rinsing in sterilized water. Leaves were placed on the surface of filter paper with abaxial surfaces facing upwards. Lemon leaves were inoculated with bacterial suspension of *Xac* phage-uninfected and phage-infected strains (10^8 cfu/mL in sterile water) using an infiltration or a needle pricking method. The infiltration method was conducted by pushing a needleless syringe containing the bacterial suspension against the surface of a citrus leaf supported by a finger on the opposite side of the leaf. The treated areas were immediately marked following inoculation (Chen et al., 2012). Needle-prick inoculation was performed by pricking the leaves, and droplets (10 μL) of bacterial suspensions were applied to each inoculation site. In both methods, the inoculated leaves were covered with a plastic bag for 48 h to facilitate the infection. Leaves were incubated in a growth chamber at 28°C with a photoperiod of 12 h light and 12 h dark for 4 weeks (Verniére et al., 1998; Li and Wang, 2011; Malamud et al., 2012).

PHAGE STABILITY TEST

We used *Xac* strain MAFF301080 because it was free from a XacF1 sequence in the genome. After infection with XacF1, a single colony was isolated and confirmed for its production of phage particles, the presence of XacF1 DNA in the cells by miniprep, and no integration of XacF1 DNA in the chromosome by PCR with a primer set of chromosomal sequences, 5′-ACT CGC TTT

GCA TGA AAT TCG CTA GCG AT-3′ (forward) and 5′-TTC GAT GGT CAC GGT GCC TGT AGT AGA GGC (reverse). After cultivation in NB at 28°C for several generations, random colonies spread on NA plates were picked and subjected to plaque assay, miniprep for XacF1 DNA, and PCR to detect lysogeny with the same primers as above.

Nucleotide sequence accession number

The sequence of the XacF1 genome has been deposited in the DDBJ under accession no. AB910602.

RESULTS

ISOLATION, MORPHOLOGY, AND HOST RANGE OF XacF1

A total of 20 phages were isolated from soil samples collected from citrus fields in Japan using a plaque assay on *Xac* strains (see Experimental Procedures), one of which formed small and turbid plaques (designated XacF1). A single plaque of this phage was picked for propagation, purification, and further experiments. Electron micrographs using highly purified phage particles (10^{13} pfu/mL) showed that XacF1 virions have typical filamentous phage features, with a long fibrous shape approximately 600 nm in length (**Figure 1A**). To determine the host range of the phage, *Xac* strains infecting different citrus species were tested for phage susceptibility (**Table 1**). The host range of the XacF1 phage was relatively wide, infecting 7 out of 11 *Xac* strains tested in this study (**Table 1**).

NUCLEOTIDE SEQUENCE AND GENOMIC ORGANIZATION OF XacF1

The genomic DNA of XacF1 was obtained as a replicative form (RF) from MAFF301080 as a host. XacF1 phage genomic DNA was digested using several restriction enzymes; *Eco*RI digestion produced a single band corresponding to approximately 7.3 kb on an agarose gel (**Figure 1B**, lane 4). The genomic DNA isolated from phage particles was completely digested by S1 nuclease treatment (data not shown), suggesting that the XacF1 genome is a circular single stranded DNA, like those of all other filamentous phages.

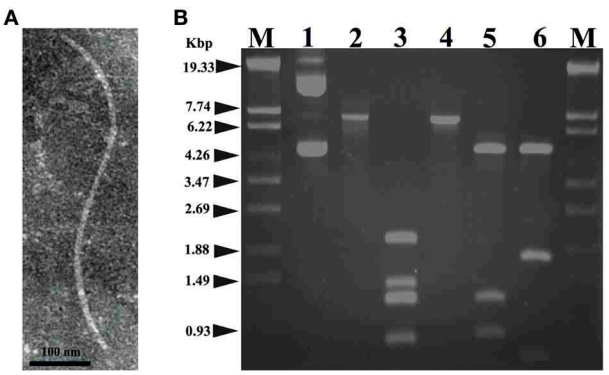

FIGURE 1 | (A) Morphology of the XacF1 phage. The purified particles of XacF1 were negatively stained with phosphotungstate and examined by transmission electron microscopy. A filamentous structure was observed (approximately 600 nm in length). **(B)** Restriction patterns of the replicative form of the XacF1 genomic DNA. Lanes: 1, undigested XacF1 DNA (RF); 2, digested with S1 nuclease; 3, *Hin*cII; 4, *Eco*RI; 5, *Eco*RV; 6, *Cla*I; M, λ *Sty*I marker.

To determine the entire nucleotide sequence of XacF1, DNA was shotgun-sequenced. The results showed that the complete genome was 7325 nucleotides long, with a G+C content of 57.8%, which was significantly lower than that of the host genome (i.e., 64.7% for strain 306, accession no. NC_003919). There were 13 putative open reading frames (ORFs), of which 11 were located on the same strand and two were on the opposite strand (**Table 2** and **Figure 2**). When databases were searched for sequences homologous to the XacF1 DNA sequence using BLAST and BLASTX programs, nine ORFs showed high similarity to ORFs previously reported for other filamentous phages, especially to ORFs of *X. campestris* pv. *citri* phage Cf1c (Kuo et al., 1991) (accession no. NC_001396), *X. campestris* pv. *vesicatoria* Cf1 phage (YP_364205.1), and *X. campestris* pv. *campestris* phi-Lf phage (X70328) (**Table 2**). XacF1 ORFs could be arranged in a similar modular structure to that of previously characterized filamentous phages of the Ff group (Model and Russel, 1988; Marvin, 1998), as shown in **Figure 2**. Within the putative replication module (**Figure 2**), we identified ORF1 and ORF2. The peptide encoded by ORF1 was homologous to filamentous phage phi-Lf replication initiation protein II (98% amino acid sequence identity) (**Table 2**). This gene encodes the pII protein, which is necessary for rolling-circle replication of phage genomes (Model and Russel, 1988). The deduced amino acid sequence encoded by ORF2 was homologous to peptides that mapped at the same position as the ssDNA binding protein (gV gene) of Ff phages, and its size was similar to that of this binding protein (**Figure 2** and **Table 2**). Within the putative structural module of XacF1, we predicted five ORFs. ORF3 showed similarity to a hypothetical *Xanthomonas* protein (**Table 2**), with 32% amino acid sequence identity to a transmembrane motif (WP_005416529), supporting the hypothesis that ORF3 belongs to the module of structural genes (**Figure 2**). Moreover, ORF4, ORF5, and ORF7 (**Figure 2** and **Table 2**) were the same size and in the same position as genes encoding the coat proteins of Ff phages. Another possible ORF included in this module was ORF6 (with similarity to coat protein Cf1c phage cp3, Kuo et al., 1991), which was similar in both size and location to *gIII* of the Ff phage. *gIII* encodes *p*III, a minor coat protein that recognizes and interacts with receptors and coreceptors on the host cells (Armstrong et al., 1981; Lubkowski et al., 1999; Heilpern and Waldor, 2003) (**Figure 2** and **Table 2**). It also showed 28% amino acid sequence identity to phage adsorption protein of *Xanthomonas citri* subsp. *citri* (YP_007649573). Therefore, ORF6 could be a homolog of g*III* in XacF1. In the third putative module of XacF1, the assembly module, we found that ORF8 showed the highest homology to the cp4 protein of Cf1c phage (**Figure 2** and **Table 2**), and to the zot protein of *Xanthomonas vesicatoria* (WP_005997731), with 59% amino acid sequence identity. Also, based on its size and position, it seems that ORF8 is a homolog of *p*I. XacF1 does not encode a *p*IV homolog, hence like many filamentous phages it must use a host encoded *p*IV homolog, outer membrane protein of the secretin family. Interestingly, we found that ORF12 might encode a regulator gene similar to those found in several filamentous phages, because amino acids encoded by this ORF exhibited similarity

Table 2 | Predicted ORFs found in the XacF1 genome.

Coding sequence	Strand	Position 5′–3′	GC content (%)	Length of protein (aa)	Molecular mass (Kda)	Amino acid sequence identity/ similarity to best homologs (no. of amino acid identical; % identity)	*E*-value	Accession no.
ORF1	+	1–1080	57.7	360	40.5	Filamentous phage phiLf replication initiation protein II (340; 98)	0.0	YP_005637352
ORF2	+	1077–1373	57.3	99	9.1	V protein *Xanthomonas* phage Cf1c (73; 99)	2e-46	NP_536673
ORF3	+	1405–1605	51.4	67	7.2	Hypothetical protein- *Xanthomonas* (65; 98)	2e-40	WP_010378728
ORF4	+	1611–1868	60.5	62	8.4	B coat protein- *Xanthomonas* phage Cf1c (62; 100)	6e-33	Q38618
ORF5	+	1928–1995	55	23	5.9	No significant similarity	–	
ORF6	+	1996–3474	55.8	493	51.7	A coat protein- *Xanthomonas* phage Cf1c (383; 96)	0.0	Q38619
ORF7	+	3474–3791	54.2	106	11.5	Hypothetical protein- *Xanthomonas campestris* (103; 98)	5e-67	WP_010378725
ORF8	+	3788–4954	59.0	389	42.8	Hypothetical protein Cf1cp4- *Xanthomonas* phage Cf1c (388; 100)	0.0	NP_040477
ORF9	+	4954–5601	59.4	216	23.5	Hypothetical protein Cf1cp5- *Xanthomonas* phage Cf1c (214; 99)	4e-148	NP_536676
ORF10	+	5617–6009	56.6	131	14.4	Hypothetical protein Cf1cp6- *Xanthomonas* phage Cf1c (130; 100)	4e-88	NP_536677
ORF11	–	6047–6430	59.7	128	14.4	Hypothetical protein Cf1cp7- *Xanthomonas* phage Cf1c (127; 100)	1e-86	NP_536678
ORF12	–	6427–6885	57.6	153	16.4	- Filamentous phage Cf1 protein- *Xanthomonas campestris* pv. *vesicatoria* str. 85-10 (146; 90)	3e-88	YP_364205
						- 18.2K protein- *Xanthomonas* phage Cf1c (164; 99)	5e-113	NP_536679
ORF13	+	7015–7203	54.8	63	6.8	Hypothetical protein- *Xanthomonas axonopodis* (59; 95)	6e-32	WP_017171337

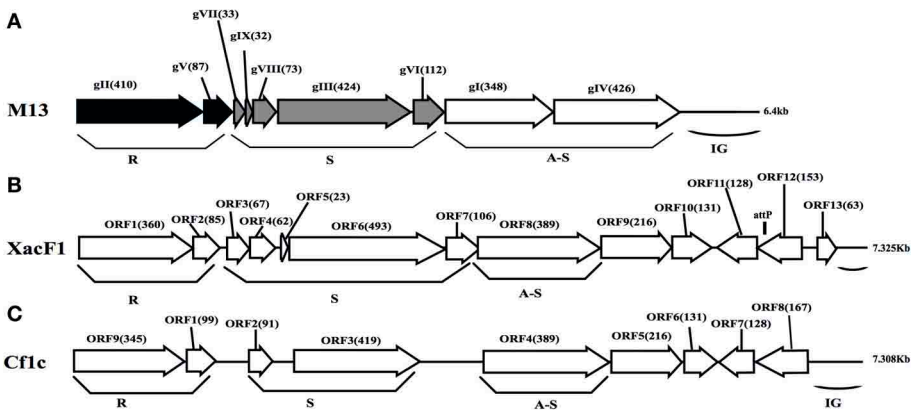

FIGURE 2 | Genomic organization of bacteriophage XacF1. Linear genomic maps of *E. coli* phage M13 **(A)**, XacF1 **(B)**, and Cf1c **(C)** are compared. Arrows oriented in the direction of transcription represent ORFs or genes. The functional modules for replication (R), structure (S), and assembly-secretion (A-S) are indicated according to the M13 model (Marvin, 1998). Map for Cf1c was drawn according to the genomic sequence (accession no. NC_001396, Kuo et al., 1991). ORF sizes (in amino acids) are in parentheses. IG (intergenic region), and *att*P are also shown.

to several putative transcriptional regulators and DNA-binding helix-turn-helix proteins of phages (e.g., Cp8 of *X. campestris* pv. *citri* phage Cf1c (99% amino acid identity) (Shieh et al., 1991); phage repressor of *Vibrio parahaemolyticus* V-223/04, exhibiting 45% amino acid identity, EVU16279, *E*-value = 0.71). ORFs 9, 10, 11, and 13 had homology to hypothetical proteins of phages and bacteria, but did not appear to belong to any of the previously described modules.

XacF1 USES HOST XerCD RECOMBINASES TO INTEGRATE INTO THE *XANTHOMONAS* GENOME

Homology searches of the DDBJ/EMBL/GenBank databases for the XacF1 sequence revealed similar sequences in the genomes of some *Xanthomonas* species. This result suggested possible integration of this kind of phage into the host genome. To test this possibility, we performed genomic Southern blot analysis of 11 strains of *Xac* using a XacF1 DNA probe. The results, shown in **Figure 3A**, indicated that eight of the 11 strains contained hybridizing bands and, among them, seven strains showed similar hybridization patterns with variations in signal intensity. Therefore, XacF1 likely has a lysogenic cycle and integrates frequently into the host genome. Regarding the integration mechanism of XacF1, we could not find any genes or ORFs that encode a phage integrase in the genome (**Table 2**). In several cases, involvement of the host recombination system by XerC/D in integration of filamentous phages into host genomes has been established, including *Vibrio cholerae* phage CTXϕ (Huber and Waldor, 2002; Das et al., 2011). In CTXϕ integration, the *dif* site of the host genome (*att*B) forms a recombination complex with *dif*-like sequences on the phage genome (*att*P) (Val et al., 2005). We therefore looked for a possible *dif*-like sequence for *att*P on the XacF1 sequence and found a 15-bp *dif* core sequence of

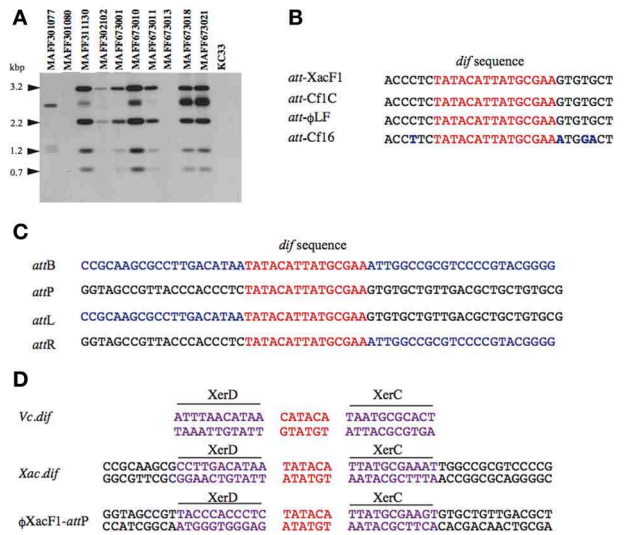

FIGURE 3 | Site specific integration of XacF1 DNA into the chromosome of *Xac*. (A) Southern blot hybridization analysis showing integration of the XacF1 phage into *Xac* host chromosomes. Genomic DNA of *X. axonopodis* pv. *citri* strains was digested with *Hin*cII and hybridized with a probe (the entire XacF1 phage genomic DNA digested with *Eco*RI). **(B)** The *att*P sequence indicated for XacF1 is compared with *att*P sequences (putative in some cases) of filamentous phages, including Cf1c (accession no. NC_001396), Cf16-v1 (M23621), and Lf (X70328) phages of *X. campestris*. The *dif* core sequences are shown in red. Changed nucleotides are shown in blue. **(C)** Alignment of *att* sequences in the XacF1 integration system. The *att*L and *att*R sequences were determined for a lysogenic strain newly established with *Xac* MAFF673010 infected with XacF1. The *att*B sequence (*dif*) of *X. axonopodis* pv. *citri* 306 was obtained from the genome database (accession no. AE008923.1, Jalan et al., 2011). Common 15 bases are shown in red and chromosomal sequences are in blue. **(D)** Putative XerC, XerD binding sites of the XacF1 system are compared with those of *Vibrio cholerae dif*1.

5′-TAT ACA TTA TGC GAA (XacF1 positions 6504–6518). This sequence showed a high degree of homology to *att*P sequences of phages Cf1c (accession no. NC_001396) (Kuo et al., 1991), Cf16-v1 (M23621), ϕLf (X70328), CTXϕ (AΦ220606), and ϕVGJ (AY242528) (**Figure 3B**). It was also reported that Cf1c, Cf1t, Cf16v1, and ϕLf phages of *X. campestris* use the XerCD recombinases of their host to integrate into the *dif* locus of the bacterial genome (Campos et al., 2003; de Mello Varani et al., 2008; Askora et al., 2012; Das et al., 2013). These results suggested that the filamentous phage XacF1 uses the host XerC/D system for integration into the host genome. To confirm this, we obtained both *att*L and *att*R fragments by PCR from newly established XacF1-lysogenic cells of *X. axonopodis* pv. *citri* strain MAFF673010. The *att*L and *att*R sequences are aligned with XacF1 *att*P and *dif* of *X. axonopodis* pv. *citri* strain 306 (accession no. AE008923.1, Jalan et al., 2011) in **Figure 3C**. From these results, we predicted XerCD binding sites according to Das et al. (2011) as shown in **Figure 3D**. However, XacF1 *att*P is located within the coding region of ORF12, so following integration into *att*B of the host chromosome, ORF12 may be split into two portions. This change in ORF12 may affect XacF1 functions because ORF12 encodes a possible phage regulator, as described above.

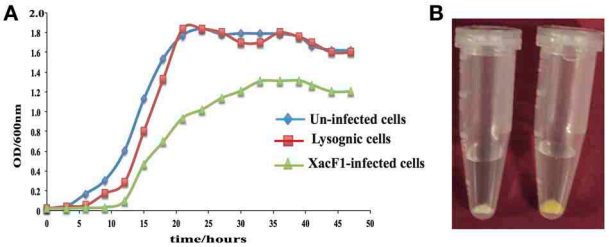

FIGURE 4 | (A) Effects of XacF1 infection on the growth of *X. axonopodis* pv. *citri* (MAFF301080). **(B)** Effects of XacF1 infection on EPS production. The pellet of uninfected *Xac* MAFF301080 cells (right) was yellow, while the pellet of XacF1-infected cells (left) was white, indicating a defect in xanthan production.

EFFECTS OF XacF1 INFECTION ON THE GROWTH RATE OF *X. AXONOPODIS* PV. *CITRI*

Unlike other bacterial viruses, the Ff phages do not kill their hosts, but establish a persistent coexistence in which new virions are continually released (Model and Russel, 1988). Because of this non-lytic mode of viral replication, it is possible to grow high-titer cultures of the virus. Similarly, infection by XacF1 did not cause lysis of host cells, but established a persistent association between the host and phage, releasing phage particles from the growing host cells. Although cells infected with XacF1 could continue to grow and divide indefinitely, the process caused the infected cells to grow at a significantly lower rate than uninfected cells (**Figure 4A**).

EFFECT OF XacF1 INFECTION ON HOST EPS PRODUCTION

EPS production was compared between uninfected and XacF1-infected cells of strain MAFF301080. The XacF1-infected cells used in this experiment were confirmed to be free from prophage by plaque assay of the culture supernatant, Southern hybridization (**Figure 3A**), and PCR. The amount of EPS produced by the infected cells was significantly lower than that of the wild-type cells. We observed that following centrifugation, the culture pellets of the infected cells turned white, reflecting a low production of xanthan, which is the major component of EPS and is responsible for the yellow color of *Xanthomona*s culture in the media (**Figure 4B**). Our prediction was confirmed by an EPS quantitation assay, which showed that the XacF1-infected cells had significantly lower EPS production (0.6 mg/ 10^{10} cfu) than uninfected cells (3.35 mg/ 10^{10} cfu).

EFFECT OF XacF1 INFECTION ON HOST MOTILITY

Swimming, swarming, and twitching motilities of uninfected and XacF1-infected cells of strain MAFF301080 were compared. A significant reduction in swimming and swarming motility was observed in XacF1-infected cells (**Figures 5A–D**). When visualized with a microscope, the colony margin of uninfected cells had a highly irregular shape, indicating proficient twitching motility, whereas the colony edge of XacF1-infected cells was smooth (**Figure 5E**), suggesting a decrease or loss of twitching motility. Because twitching motility is the surface movement associated with type IV pili (Marques et al., 2002; Meng et al., 2005),

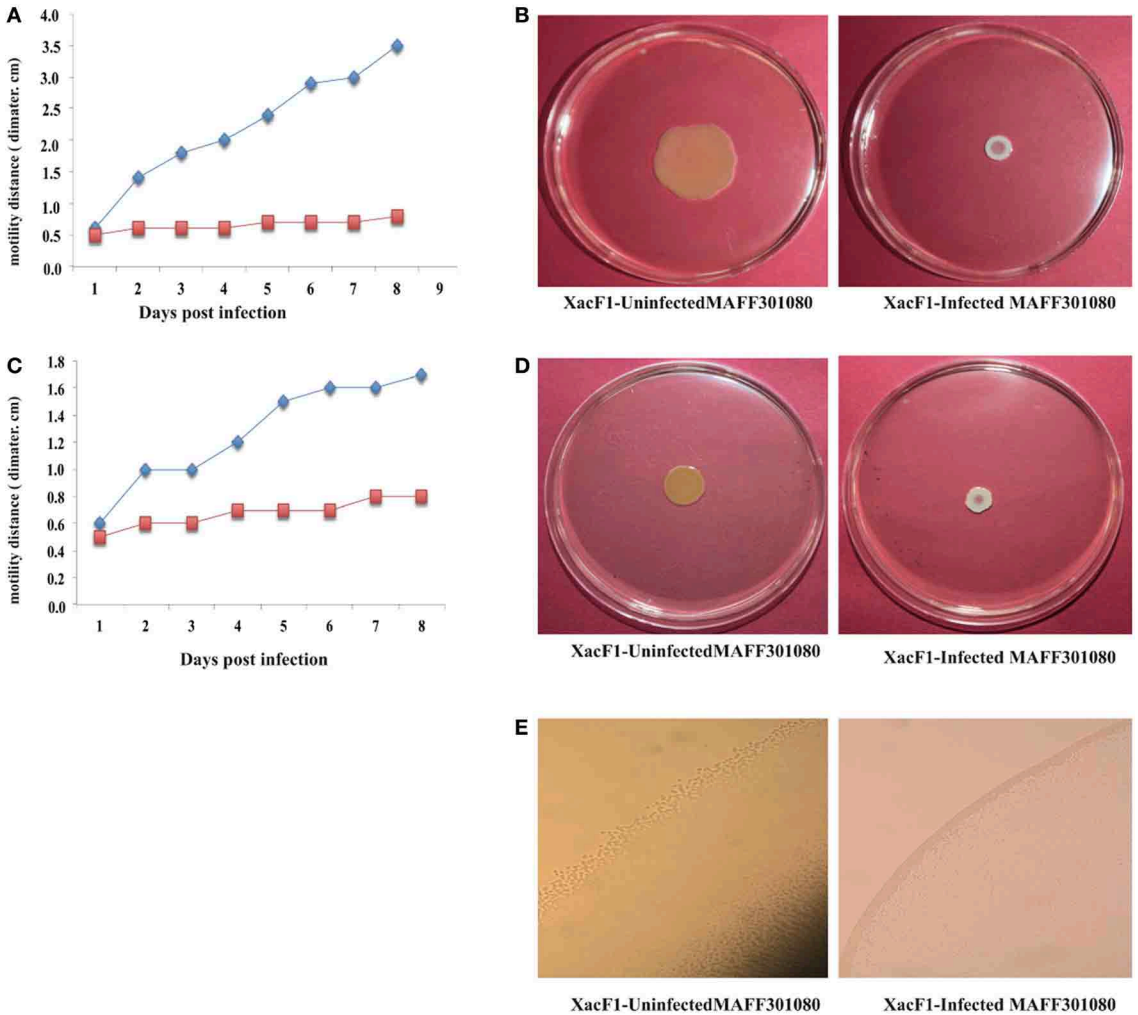

FIGURE 5 | Impact of XacF1 infection on the motility of *Xac* MAFF301080 cells. Two microliters of bacterial solution [10^8 colony forming units (CFU)/mL] were inoculated in the swimming assay [0.3% (w/v) agar] **(A,B)**, swarming assay [0.7% (w/v) agar] **(C,D)**, and twitching motility assay (minimal agar medium) **(E)**. The movement of bacterial cells was photographed 5 and 8 days post-inoculation (dpi) on the swimming and swarming plates, respectively. Twitching motility of bacteria was observed under a microscope 5 dpi on the twitching plates.

XacF1 infection may have affected the type IV pilus structures and/or functions of the host cells. We examined whether cell surface structural components were affected by XacF1 infection. Cell surface structure proteins were prepared by passing bacterial cells through a hypodermic needle, separated by SDS-PAGE, and compared between XacF1-infected and uninfected cells. XacF1-infected cells had considerably decreased levels of PilA, the major component of type IV pili, and decreased levels of FilC, flagellin (Supplemental Figure S1).

EFFECTS OF XacF1 INFECTION ON VIRULENCE OF *X. AXONOPODIS* PV. *CITRI*

Wild-type cells of strain MAFF301080 caused infection symptoms 4 days post-infection, and formed clear cankers 1 week post-inoculation (**Figure 6A**). Starting from 2 weeks post-infection, the lesion became brown in color and its center became raised and spongy or corky, typical canker symptoms (Graham et al., 2004) that reflected the aggressive virulence of this strain. In contrast, the symptoms of XacF1-infected MAFF301080 cells were relatively weak, and no mature canker symptoms were observed up to 4 weeks post-infection, except for marginal lesions formed around the pricking site (**Figure 6A**). To be more precise, we measured lesion size (**Figure 6B**), which showed that in uninfected cells, the lesions were large with a smooth center, spongy raised top, and their distribution around the infected area reached more than 6.5 mm in width 4 weeks post-infection. In contrast, the lesions formed by XacF1-infected cells remained weak and dry, and they did not expand more than 1 mm in width. Another inoculation method, in which we infiltrated the bacterial suspension into the lemon leaves, showed that XacF1-uninfected MAFF301080 cells incurred water soaking at the inoculation site 3 days post-infection, and then an erumpent tissue reaction was obvious 1 week after inoculation. The erumpent tissue expanded to an aggressive canker area on both sides of the leaf, and then

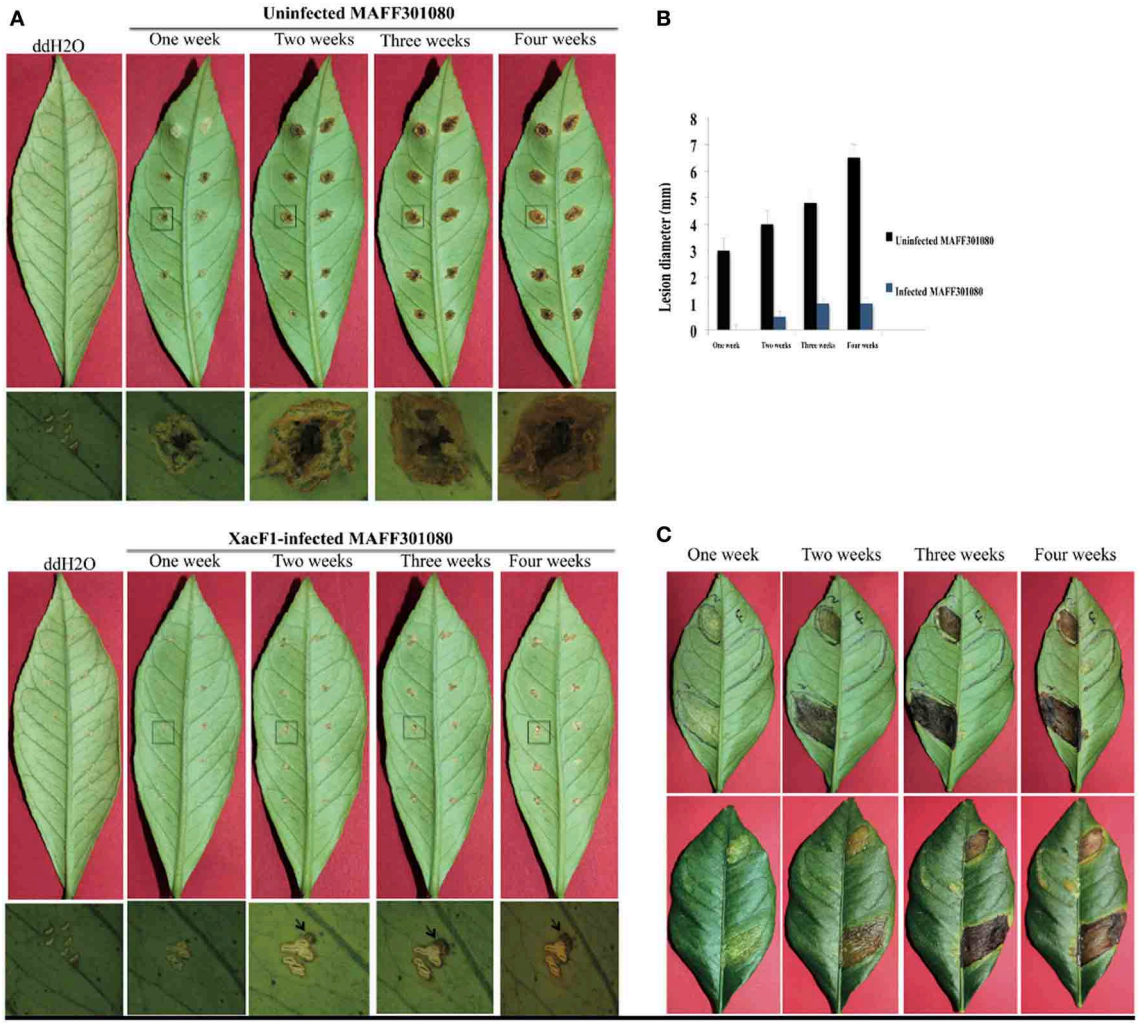

FIGURE 6 | Lesions on detached lemon leaves inoculated with cells of *Xac* MAFF301080. (A) Canker symptoms that had developed on leaves 1, 2, 3, and 4 weeks post-infection by the needle-pricking method. Leaves were inoculated with uninfected cells (upper panels) or XacF1-infected cells (lower panels). Leaf areas shown by a square were examined by photomicroscopy and the microscopic images are shown under each corresponding leaf. Characteristic canker lesions occurred with uninfected cells, while no obvious cankers developed on XacF1-infected cells. **(B)** Comparison of the size of lesions formed on lemon leaves. **(C)** Lesions formed on lemon leaves by infiltration of bacterial cells. Uninfected MAFF301080 cells were applied to two areas of the leaf (left half of the abaxial side), and XacF1-infected cells were similarly applied to the right side (upper panels). Lesions on the axial side are also shown in lower panels. Lesions on both lower and upper surfaces of leaves inoculated with the uninfected cells showed severe symptoms, expanding with time. No lesions formed on either surface of the leaves infected with XacF1-infected cells.

the lesions became dark and decayed with a yellow halo at the inoculation site 4 weeks post-infection (**Figure 6C**). However, in XacF1-infected cells, a slight water-soaking area on the leaf surface was only visible 2 weeks after inoculation, and weak canker symptoms could be seen 4 weeks post-infection. In all cases, leaves inoculated with ddH_2O showed no canker symptoms.

DISCUSSION

In this study, we isolated and characterized a filamentous phage, named XacF1, that infects *X. axonopodis* pv. *citri* strains. The isolated phage had a relatively wide range of host bacterial strains. Of particular interest, this study showed that along with the phage infection, the infected cells had decreased ability to form citrus cankers and a loss of virulence. We demonstrated that the canker symptoms of XacF1-infected lemon leaves were dramatically mitigated up to 4 weeks post-infection using both pricking and infiltration methods of inoculation (**Figures 6A–C**). The significant reduction in EPS (xanthan) production caused by XacF1 phage could be one of the reasons for such a dramatic decrease in canker formation. Virulence of numerous phytopathogenic bacteria, particularly various *Xanthomonas* species, is correlated with their ability to produce EPS (Dolph et al., 1988; Bellemann and Geider, 1992; Kao et al., 1992; Chou et al., 1997; Katzen et al., 1998; Dharmapuri and Sonti, 1999; Yu et al., 1999; Kemp et al., 2004). The multiple functions of EPS in virulence include protection of bacteria from toxic plant compounds, reduction

of bacterial contact with plant cells to minimize host defense responses, promotion of bacterial multiplication by prolonging water soaking of tissues, and supporting invasion or systemic colonization of bacterial cells (Denny, 1999). Another possible role of EPS is to confer epiphytic fitness. It was previously suggested that EPS functions during both epiphytic and pathogenic phases of infection in *X. campestris* pv. *campestris* (Poplawsky and Chun, 1998; Rigano et al., 2007). As significant differences in virulence were observed between wild-type and xanthan-deficient mutant strains of other *Xanthomonas* species, Dunger et al. (2007) proposed that in citrus canker, xanthan supports epiphytic survival in citrus canker, but is not required for colonizing nearby tissue. Without xanthan the bacteria were unable to retain water and could not withstand abiotic stress and, thus, could not survive on the leaf surface. Therefore, xanthan works in two ways: to enhance bacterial virulence and to block the host defense. The drastic reduction in host EPS production caused by XacF1 infection may explain why the XacF1-infected cells showed dramatically decreased virulence.

Another major finding is the significant reduction in the swimming, swarming, and twitching motilities of *Xac* cells following infection by XacF1. Bacteria use a variety of motility mechanisms to colonize host tissues. These mechanisms include flagella-dependent swimming and swarming for movement in liquid surfaces, and flagella-independent twitching, gliding, and sliding for movement on solid surfaces (O'Toole and Kolter, 1998; Mattick, 2002; Harshey, 2003). Recent reports propose that bacterial adhesion and motility are required in the initial stages of *Xac* biofilm formation, whereas lipopolysaccharide and EPS play important roles in the establishment of mature biofilms (Li and Wang, 2011). The reduction in motility of XacF1-infected cells may be because filamentous phages such as XacF1 assemble on the host cell membrane and protrude from the cell surface, and so the nature of the host cell surface may change drastically during phage production (Addy et al., 2012). As shown in Supplemental Figure S1, XacF1-infected cells had considerably decreased levels of PilA, the major component of type IV pili.

Frequent protrusion of XacF1 particles from the infected cell surface may somehow compete with the formation of type four pili (Tfp). As reported by Kang et al. (2002), Tfp is responsible for twitching motility and adherence to multiple surfaces and is required for virulence. Interestingly, ORF 9 of the XacF1 phage (**Table 2**) showed significant homology to a TraX family protein (H8FlE6, *E*-value = 1e-70) and a putative F pilin acetylation protein (Q3BsT0, *E*-value = 4e-70), involved in pilus modification. Therefore, the loss of virulence in the XacF1-infected cells seems to be, at least partly, caused by the reduction or modification of Tfp formation and decrease in swimming, swarming, and twitching motilities.

Several works have described the use of phages for control of bacterial citrus canker caused by *X. campestris* pv. *citri* (Balogh et al., 2010). In those cases, the bacteriophages used for foliar plant diseases interacted with the target bacteria on the leaf surface, the phylloplane. The phylloplane is a constantly changing environment: there are changes in temperature, sunlight irradiation, leaf moisture, relative humidity, osmotic pressure, pH, microbial flora, and, in the case of agricultural plants, chemical compounds (Jones et al., 2012). These factors may be harmful to bacteriophages to varying extents. Sunlight irradiation, especially in the UVA and -B range, is mainly responsible for eliminating bacteriophages within hours of application (Jones et al., 2012). To avoid quick inactivation of XacF1, we propose the application of XacF1-infected cells instead of XacF1 phage alone. The XacF1-infected cells can grow and continue to produce infectious phage, so the XacF1 phage may serve as an efficient long-lasting tool to control citrus canker by decreasing the virulence of the pathogen. Concerning the stability of XacF1-infected cells, we observed relatively high stability of "a free phage state" in the infected cells. After several bacterial generations, 100% cells contained XacF1 and more than 70% of them were at the state of producing free phages without integration into the host chromosome (confirmed by PCR) (data not shown). Even if once prophage states were established, we observed frequent spontaneous excision and production of phage particles.

Another possible way to use XacF1 for biological control may be given as a phage cocktail with other lytic phages, such as Cp1 and Cp2, originating from Japan, which can infect more than 97% of *Xac* strains and was recently characterized by Ahmad et al. (2014).

ACKNOWLEDGMENT

This study was supported in part by a Japanese Society for the Promotion of Science KAKENHI grant 25.03086 to Ahmed Askora.

SUPPLEMENTARY MATERIAL

The Supplementary Material for this article can be found online at: http://www.frontiersin.org/journal/10.3389/fmicb.2014.00321/abstract

REFERENCES

Addy, H. S., Askora, A., Kawasaki, T., Fujie, M., and Yamada, T. (2012). Loss of Virulence of the phytopathogen *Ralstonia solanacearum* through infection by ϕRSM filamentous Phages. *Phytopathology* 102, 469–477. doi: 10.1094/PHYTO-11-11-0319-R

Ahmad, A. A., Ogawa, M., Kawasaki, T., Fujie, M., and Yamada, T. (2014). Characterization of bacteriophages Cp1 and Cp2, the strain typing agents for *Xanthomonas axonopodis* pv. *citri*. *Appl. Environ. Microbiol.* 80, 77–85. doi: 10.1128/AEM.02310-13

Altschul, S. F., Madden, T. L., Schaffer, A. A., Zhang, Z., Miller, W., and Lipman, D. J. (1997). Gapped BLAST and PSI-BLAST: a new generation of protein database search programs. *Nucleic Acids Res.* 25, 3389–3402. doi: 10.1093/nar/25.17.3389

Armstrong, J., Perharm, R. N., and Walker, J. E. (1981). Domain structure of bacteriophage fd adsorption protein. *FEBS Lett.* 135, 167–172. doi: 10.1016/0014-5793(81)80969-6

Askora, A., Abdel-Haliem, M. E., and Yamada, T. (2012). Site-specific recombination systems in filamentous phages. *Mol. Genet. Genomics* 287, 525–530. doi: 10.1007/s00438-012-0700-1

Askora, A., Kawasaki, T., Usami, S., Fujie, M., and Yamada, T. (2009). Host recognition and integration of filamentous phage ϕRSM in the phytopathogen, *Ralstonia solanacearum*. *Virology* 384, 69–76. doi: 10.1016/j.virol.2008.11.007

Ausubel, F., Brent, R., Kjngston, R. E., Moore, D. D., Seidman, J. G., Smith, J. A., et al. (1995). *Short Protocols in Molecular Biology*. 3rd Edn. Hoboken, NJ: John Wiley & Sons, Inc.

Balogh, B., Canteros, B. I., Stall, R. E., and Jones, J. B. (2008). Control of citrus canker and citrus bacterial Spot with Bacteriophages. *Plant Dis.* 92, 1048–1052. doi: 10.1094/PDIS-92-7-1048

Balogh, B., Jones, J. B., Iriarte, F. B., and Momol, M. T. (2010). Phage therapy for plant disease control. *Curr. Pharm. Biotechnol*. 11, 48–57. doi: 10.2174/138920110790725302

Balogh, B., Jones, J. B., Momol, M. T., Olson, S. M., Obradovic, A., King, P., et al. (2003). Improved efficacy of newly formulated bacteriophages for management of bacterial spot on tomato. *Plant Dis*. 87, 949–954. doi: 10.1094/PDIS.2003.87.8.949

Bellemann, P., and Geider, K. (1992). Localization of transposon insertions in pathogenicity mutants of *Erwinia amylovora* and their biochemical characterization. *J. Gen. Microbiol.* 138, 931–940. doi: 10.1099/00221287-138-5-931

Brunings, A., and Gabriel, D. (2003). *Xanthomonas citri*: breaking the surface. *Mol. Plant Pathol*. 4, 141–157. doi: 10.1046/j.1364-3703.2003.00163.x

Campos, J., Martinez, E., Suzarte, E., Rodriguez, B. L., Marrero, K., Silva, Y., et al. (2003). VGJϕ, a novel wlamentous phage of *Vibrio cholerae*, integrates into the same chromosomal site as CTXϕ. *J. Bacteriol.* 185, 5685–5696. doi: 10.1128/JB.185.19.5685-5696.2003

Chen, P. S., Wang, L. Y., Chen, Y. J., Tzeng, K. C., Chang, S. C., Chung, K. R., et al. (2012). Understanding cellular defence in kumquat and calamondin to citrus canker caused by *Xanthomonas citri* subsp. *citri. Physiol. Mol. Plant Pathol*. 79, 1–12. doi: 10.1016/j.pmpp.2012.03.001

Chou, F. L., Chou, H. C., Lin, Y. S., Yang, B. Y., Lin, N. T., Weng, S. F., et al. (1997). The *Xanthomonas campestris gum*D gene required for synthesis of xanthan gum is involved in normal pigmentation and virulence in causing Black rot. *Biochem. Biophys. Res. Commun.* 233, 265–269. doi: 10.1006/bbrc.1997.6365

Civerolo, E. (1984). Bacterial canker disease of citrus. *J. Rio Grande Valley Hort. Soc*. 37, 127–146.

Das, B., Bischerour, J., and Barre, F. X. (2011). VGJϕ integration and excision mechanisms contribute to the genetic diversity of *Vibrio cholerae* epidemic strains. *Proc. Natl. Acad. Sci. U.S.A.* 108, 2516–2521. doi: 10.1073/pnas.1017061108

Das, B., Martiìnez, E., Midonet, C., and Barre, F. X. (2013). Integrative mobile elements exploiting Xer recombination. *Trends Microbiol*. 1, 23–30. doi: 10.1016/j.tim.2012.10.003

de Mello Varani, A., Souza, R. C., Nakaya, H. I., de Lima, W. C., de Almeid, P., Watabnabe-Kitajima, E., et al. (2008). Origins of the *Xylella fastidiosa* prophage-like regions and their impact in genome differentiation. *PLoS ONE* 3:e4059. doi: 10.1371/journal.pone.0004059

Denny, T. P. (1999). Autoregulator-dependent control of extracellular polysaccharide production in phytopathogenic bacteria. *Eur. J. Plant Pathol.* 105, 417–430. doi: 10.1023/A:1008767931666

Dharmapuri, S., and Sonti, R. V. (1999). A transposon insertion in the gumG homologue of *Xanthomonas oryzae* pv. *oryzae* causes loss of extracellular polysaccharide production and virulence. *FEMS Microbiol. Lett*. 179, 53–59. doi: 10.1111/j.1574-6968.1999.tb08707.x

Dolph, P. J., Majerczak, D. R., and Coplin, D. L. (1988). Characterization of a gene cluster for exopolysaccharide biosynthesis and virulence in *Erwinia stewartii*. *J. Bacteriol*. 170, 865–871.

Dunger, G., Relling, V. M., Tondo, M. L., Barreras, M., Ielpi, L., Orellano, E. G., et al. (2007). Xanthan is not essential for pathogenicity in citrus canker but contributes to Xanthomonas epiphytic survival. *Arch. Microbiol.* 188, 127–135. doi: 10.1007/s00203-007-0227-8

Dykstra, M. J. (1993). *A Manual of Applied Technique for Biological Electron Microscopy*. New York, NY: Plenum Press. doi: 10.1007/978-1-4684-0010-6

Flaherty, J. E., Jones, J. B., Harbaugh, B. K., Somodi, G. C., and Jackson, L. E. (2000). Control of bacterial spot on tomato in the greenhouse and field with H-mutant bacteriophages. *HortScience* 35, 882–884.

Graham, J. H., Gottwald, T. R., Cubero, J., and Achor, D. S. (2004). *Xanthomonas axonopodi*s pv. *citri*: factors affecting successful eradication of citrus canker. *Mol. Plant Pathol*. 5, 1–15. doi: 10.1046/j.1364-3703.2004.00197.x

Guo, Y., Sagaram, U. S., Kim, J. S., and Wang, N. (2010). Requirement of the galU gene for polysaccharide production by and pathogenicity and growth in planta of *Xanthomonas citri* subsp. *citri. Appl. Environ. Microbiol*. 76, 2234–2242. doi: 10.1128/AEM.02897-09

Harshey, R. M. (2003). Bacterial motility on a surface: many ways to a common goal. *Annu. Rev. Microbiol.* 57, 249–273. doi: 10.1146/annurev.micro.57.030502.091014

Heilpern, A. J., and Waldor, M. K. (2003). pIIICTX, a predicted CTX phi minor coat protein, can expand the host range of coliphage fd to include *Vibrio cholerae*. *J. Bacteriol.* 185, 1037–1044. doi: 10.1128/JB.185.3.1037-1044.2003

Huber, K. E., and Waldor, M. K. (2002). Filamentous phage integration requires the host recombinases XerC and XerD. *Nature* 417, 656–659. doi: 10.1038/nature00782

Jalan, N., Aritua, V., Kumar, D., Yu, F., Jones, J. B., Graham, J. H., et al. (2011). Comparative genomic analysis of *Xanthomonas axonopodis* pv. *citrumelo* F1, which causes citrus bacterial spot disease and related strains provides insights into virulence and host specificity. *J. Bacteriol*. 14, 6342–6357. doi: 10.1128/JB.05777-11

Jones, J. B., Vallad, G. E., Iriarte, F. B., Obradovic, A., Wernsing, M. H., Jackson, L. E., et al. (2012). Considerations for using bacteriophages for plant disease control. *Bacteriophage* 2, 208–214. doi: 10.4161/bact.23857

Kang, Y., Liu, H., Genin, S., Schell, M. A., and Denny, T. P. (2002). *Ralstonia solanacearum* requires type 4 pili to adhere to multiple surfaces and for natural transformation and virulence. *Mol. Microbiol.* 46, 427–437. doi: 10.1046/j.1365-2958.2002.03187.x

Kao, C. C., Barlow, E., and Sequeira. L. (1992). Extracellular polysaccharide is required for wild-type virulence of *Pseudomonas solanacearum. J. Bacteriol.* 174, 1068–1071.

Katzen, F., Ferreiro, D., Oddo, C., Ielmini, M. V., Becker, A., Puhler, A., et al. (1998). *Xanthomonas campestris* pv. *campestris* gum mutants: effects on xanthan biosynthesis and plant virulence. *J. Bacteriol.* 180, 1607–1617.

Kemp, B. P., Horne, J., Bryant, A., and Cooper, R. M. (2004). *Xanthomonas axonopodis* pv. *manihotis gum*D gene is essential for EPS production and pathogenicity and enhances epiphytic survival on cassava (Manihotesculenta). *Physiol. Mol. Plant Pathol*. 64, 209–218. doi: 10.1016/j.pmpp.2004.08.007

Kuo, T. T., Tan, M. S., Su, M. T., and Yang, M. K. (1991). Complete nucleotide sequence of filamentous phage Cf1c from *Xanthomonas campestris* pv. *citri. Nucleic Acids Res*. 19, 2498. doi: 10.1093/nar/19.9.2498

Lang, J. M., Gent, D. H., and Schwartz, H. F. (2007). Management of *Xanthomonas* leaf blight of onion with bacteriophages and a plant activator. *Plant Dis*. 91, 871–878. doi: 10.1094/PDIS-91-7-0871

Larkin, M. A., Blackshields, G., Brown, N. P., Chenna, R., McGettigan, P. A., McWilliam, H., et al. (2007). Clustal W and Clustal X version 2.0. *Bioinformatics* 23, 2947–2948. doi: 10.1093/bioinformatics/btm404

Li, J., and Wang, N. (2011). The *wxac*O gene of *Xanthomonas citri* ssp. *citri* encodes a protein with a role in lipopolysaccharide biosynthesis, biofilm formation, stress tolerance and virulence. *Mol. Plant. Pathol*. 1, 381–396. doi: 10.1111/j.1364-3703.2010.00681.x

Lubkowski, J., Hennecke, F., Puckthun, A., and Wlodawer. A. (1999). Filamentous phage infection: crystal structure of g3p in complex with its coreceptor, the C-terminal domain of TolA. *Structure* 7, 711–722. doi: 10.1016/S0969-2126(99)80092-6

Malamud, F., Conforte, V. P., Rigano, L. A., Castagnaro, A. P., Marano, M. R., Morais do Amaral, A., et al. (2012). *hrpM* is involved in glucan biosynthesis, biofilm formation and pathogenicity in *Xanthomonas citri* ssp. *citri. Mol. Plant Pathol.* 13, 1010–1018. doi: 10.1111/j.1364-3703.2012.00809.x

Marques, L. L. R., Ceri, H., Manfio, G. P., Reid, D. M., and Olsen, M. E. (2002). Characterization of biofilm formation by *Xylella fastidiosa in vitro*. *Plant Dis*. 86, 633–638. doi: 10.1094/PDIS.2002.86.6.633

Marvin, D. A. (1998). Filamentous phage structure, infection and assymply. *Curr. Opin. Struct. Biol*. 8, 150–158. doi: 10.1016/S0959-440X(98)80032-8

Mattick, J. S. (2002). Type IV pili and twitching motility. *Annu. Rev. Microbiol*. 56, 289–314. doi: 10.1146/annurev.micro.56.012302.160938

Meng, Y., Li, Y., Galvani, C. D., Hao, G., Turner, J. N., Burr, T. J., et al. (2005). Upstream migration of *Xylella fastidiosa* via pilus-driven twitching motility. *J. Bacteriol.* 187, 5560–5567. doi: 10.1128/JB.187.16.5560-5567.2005

Model, P., and Russel, M. (1988). "Filamentous bacteriophage," in *The Bacteriophages,* Vol. 2, ed R. Calendar (New York, NY: Plenum Publishing Corporation), 375–456.

Obradovic, A., Jones, J. B., Momol, M. T., Balogh, B., and Olson, S. M. (2004). Management of tomato bacterial spot in the field by foliar applications of bacteriophages and SAR inducers. *Plant Dis*. 88, 736–740. doi: 10.1094/PDIS.2004.88.7.736

Obradovic, A., Jones, J. B., Momol, M. T., Olson, S. M., Jackson, L. E., Balogh, B., et al. (2005). Integration of biological control agents and systemic acquired resistance inducers against bacterial spot on tomato. *Plant Dis*. 89, 712–716. doi: 10.1094/PD-89-0712

O'Toole, G. A., and Kolter, R. (1998). Flagellar and twitching motility are necessary for *Pseudomonas aeruginosa* biofilm development. *Mol. Microbiol.* 30, 295–304. doi: 10.1046/j.1365-2958.1998.01062.x

Poplawsky, A. R., and Chun, W. (1998). *Xanthomonas campestris* pv. *campestris* requires a functional *pigB* for epiphytic survival and host infection. *Mol. Plant Microbe. Interact.* 11, 466–475. doi: 10.1094/MPMI.1998.11.6.466

Rigano, L. A., Payette, C., Brouillard, G., Marano, M. R., Abramowicz, L., Torres, P. S., et al. (2007). Bacterial cyclic beta-(1,2)-glucan acts in systemic suppression of plant immune responses. *Plant Cell* 19, 2077–2089. doi: 10.1105/tpc.106.047944

Sambrook, J., and Russell, D. W. (2001). *Molecular Cloning: A Laboratory Manual.* 3rd Edn. Cold Spring Harbor, NY: Cold Spring Harbor Laboratory Press.

Shieh, G. J., Charng, Y. C., Yang, B. C., Jenn, T., Bau, H. J., and Kuo, T. T. (1991). Identification and nucleotide sequence analysis of an open reading frame involved in high-frequency conversion of turbid to clear plaque mutants of filamentous phage Cf1t. *Virology* 185, 316–322. doi: 10.1016/0042-6822(91)90779-B

Shiotani, H., Fujikawa, T., Ishihara, H., Tsuyumu, S., and Ozaki, K. (2007). A pthA homolog from Xanthomonas axonopodis pv. citri responsible for host-specific suppression of virulence. *J. Bacteriol.* 189, 3271–3279. doi: 10.1128/JB.01790-06

Val, M. E., Bouvier, M., Campos, J., Sherratt, D., Cornet, F., Mazel, D., et al. (2005). The single-stranded genome of phage CTX is the form used for integration into the genome of *Vibrio cholerae*. *Mol. Cell* 19, 559–565. doi: 10.1016/j.molcel.2005.07.002

Verniére, C., Hartung, J. S., Pruvost, O. P., Civerolo, E. L., Alvarez, A. M., Maestri, P. et al. (1998). Characterization of phenotypically distinct strains of *Xanthomonas axonopodis* pv. *citri* from Southwest Asia. *Eur. J. Plant Pathol.* 104, 477–487. doi: 10.1023/A:1008676508688

Vojnov, A. A., Morais do Amaral, A., Dow, J. M., Castagnaro, A. P., and Marano, M. R. (2010). Bacteria causing important diseases of citrus utilise distinct modes of pathogenesis to attack a common host. *Appl. Microbiol. Biotechnol.* 87, 467–477. doi: 10.1007/s00253-010-2631-2

Yamada, T., Kawasaki, T., Nagata, S., Fujiwara, A., Usami, S., and Fujie, M. (2007). New bacteriophages that infect the phytopathogen *Ralstonia solanacearum*. *Microbiology* 153, 2630–2639. doi: 10.1099/mic.0.2006/001453-0

Yu, J., Penaloza-Vazquez, A., Chakrabarty, A. M., and Bender, C. L. (1999). Involvement of the exopolysaccharide alginate in the virulence and epiphytic fitness of *Pseudomonas syringae* pv. *syringae. Mol. Microbiol.* 33, 712–720. doi: 10.1046/j.1365-2958.1999.01516.x

Conflict of Interest Statement: The authors declare that the research was conducted in the absence of any commercial or financial relationships that could be construed as a potential conflict of interest.

Received: 31 March 2014; accepted: 11 June 2014; published online: 01 July 2014.
Citation: Ahmad AA, Askora A, Kawasaki T, Fujie M and Yamada T (2014) The filamentous phage XacF1 causes loss of virulence in Xanthomonas axonopodis pv. citri, the causative agent of citrus canker disease. Front. Microbiol. ***5****:321. doi: 10.3389/fmicb.2014.00321*
This article was submitted to Virology, a section of the journal Frontiers in Microbiology.

参考論文
Thesis Supplements

DISEASE NOTE

OLIVE KNOT CAUSED BY *PSEUDOMONAS SAVASTANOI* pv. *SAVASTANOI* IN EGYPT

A.A. Ahmad[1], C. Moretti[2], F. Valentini[1], T. Hosni[2], N.S. Farag[3], A.A. Galal[4] and R. Buonaurio[2]

[1] Istituto Agronomico Mediterraneo, Via Ceglie 9, 70010 Valenzano (Bari), Italy
[2] Dipartimento di Scienze Agrarie e Ambientali, Sezione di Arboricoltura e Protezione delle Piante, Via Borgo XX Giugno 74, 06121 Perugia, Italy
[3] Agricultural Research Centre, Plant Pathology Research Institute, Giza, Egypt
[4] Department of Plant Pathology, Faculty of Agriculture, Minia University, Minia, Egypt

During field surveys carried out in 2008 in all olive-growing areas of Egypt, bacterial knot symptoms were observed on twigs and branches of domestic olive cultivars in El-Fayoum governorate. From colonies resembling those of *Pseudomonas savastanoi* pv. *savastanoi,* isolated from olive knots on nutrient agar, four representative isolates were selected, purified on 5% sucrose nutrient agar medium and compared with *P. savastanoi* pv. *savastanoi* reference strain LMG 2209^T. All isolates were gram negative, fluorescent on King's medium B and had only oxidative metabolism of glucose. They were negative for levan, oxidase, potato rot and arginine dihydrolase and positive for tobacco hypersensitivity. When 1-year-old olive (*Olea europea* cvs Toffahi, Agyze alshame, Picual, Manzanilla and Frantoio) and wild olive (*Olea europaca* subsp. *oleaster*) plants were inoculated with bacterial suspensions (10^8 cfu ml^{-1}) by puncturing them in wounds made in the bark, all isolates induced knots in 20-30 days in both host plants at the site of inoculation. Bacteria re-isolated from the inoculated plants were identical to the original isolates. PCR analysis revealed that all the isolates generated and amplicon with the size expected for *P. savastanoi* pv. *savastanoi iaa*L gene (Penyalver *et al.*, 2000). By rep-PCR, it was shown that the isolates have a 95-100% similarity among them and with the reference strain. Based on morphological, biochemical, physiological and pathogenicity tests as well as molecular analyses, it seems safe to conclude that the Egyptian bacterial isolates conform to the description of *P. savastanoi* pv. *savastanoi*. To our knowledge, this is the first record of olive knot disease on olive plants in Egypt.

The Authors wish to thank Prof. Dr. Sadk Ahmed El-Sadek (Minia University, Egypt) for his helpful suggestions and Mr. L. Bonciarelli for the skillful technical support.

Penyalver R., García A., Ferrer A., Bertolini E., López M.M., 2000. Detection of *P. savastanoi* pv. *savastanoi* in olive plants by enrichment and PCR. *Applied and Environmental Microbiology* **66**: 2673-2677.

Corresponding author: R. Buonaurio
Fax: +39 075 585 6482
E-mail: buonaurio@unipg.it

Received October 22, 2008
Accepted November 15, 2008

DISEASE NOTE

TRANSMISSION OF THE FIG MOSAIC AGENT BY THE ERIOPHYD MITE *ACERIA FICUS* COTTE (ACARI: ERIOPHYIDAE)

K. Çaglayan[1], V. Medina[2], A. Yigit[1], K. Kaya[1], M. Gazel[1], Ç.U. Serçe[1] and O. Çalıskan[3]

[1] Mustafa Kemal University, Plant Protection Department, 31034 Antakya-Hatay, Turkey
[2] Lleida University, Departamento de Producción Vegetal y Ciència Forestal, 25198 Lleida, Spain
[3] Mustafa Kemal University, Horticulture Department, 31034 Antakya-Hatay, Turkey

Fig mosaic disease (FMD) and its vector *Aceria ficus* Cotte are widespread in different fig growing ares of Turkey. Fig cultivars Bursa siyahı, Göklop, Sarı Zeybek and Yediveren that were heavily infested by mites, were used as source plants for attempting mite transmission of FMD (8 mites per plant) to healthy fig seedlings. Electron microscopy of donor plants prior to transmission tests showed cv. Bursa siyahı to have double membrane bodies (DMBs) in the palisade mesophyll cells, and all cvs to have long flexuous virus-like particles (LVLPs) in vascular tissues. Electron microscopy of experimentally infected seedlings showed that only those infested with mites from FMD-infected cv. Bursa siyahı contained DMBs in mesophyll cells and that no LVLPs were present. However, none of the test plants, fed on by mites coming from cvs. Göklop, Sarı Zeybek and Yediveren showed any symptoms in four months following transmission. The presence of DMBs has been linked with FMD (Bradfute *et al.*, 1970; Martelli *et al.*, 1993; Serrano *et al.*, 2004). DMBs have been observed previously in field-infected symptomatic plants in Turkey (Martelli *et al.*, 1993), however our results are the first record of FMD and associated DMBs in experimentally infected fig seedlings. These results reinforce the suggestion that an agent that elicits the production of DMBs in infected plants is involved in the aetiology of FMD.

Bradfute O.E., Whitmoyer R.E., Nault R.L., 1970. Ultrastructure of plant leaf tissue infected with mite-borne viral-like particles. *Proceedings of the Electron Microscopy Society of America* **28**: 178-179.

Martelli G.P., Castellano M.A., Lafortezza R., 1993. An ultrastructural study of fig mosaic. *Phytopathologia Mediterranea* **32**: 33-43.

Serrano L., Ramon J., Segarra J., Medina V., Achon M.A., Lopez M., 2004. New approach in the identification of the causal agent of fig mosaic disease. *Acta Horticulturae* **657**: 559-566.

Corresponding author: K. Caglayan
Fax: +90. 326 2455832
E-mail: kcaglayano@yahoo.com

Received November 6, 2008
Accepted November 22, 2008

Arabidopsis. Yeast two-hybrid screens identified protein targets in *Arabidopsis* that interact with AvrPtoB and VirPphA. Putative interactors (PIs) recovered, including cytoskeletal proteins and a receptor like-kinase may have an important role in plant defense. In this study, Northern blots were used to examine the gene expression of selected PIs after bacterial pathogen challenge using probes labeled with the isotope ^{32}P. The expression profiling of the transcripts showed different patterns including 1- *p*athogen *i*nduced *g*enes (*PIGs*), such response was observed with the protein kinase and receptor-like kinase; 2- delayed *PIGs*, this group included the 20S proteasome beta subunit, caltractin and carnitine racemase-like protein; 3- constitutive *g*ene pattern such as putative fibrillin; and 4- *p*athogen *s*uppressed *g*ene pattern (*PSG*), since it is the only gene predicted to encode 2-cys peroxiredoxin-like protein fell into this category.

B 11

BACTERIAL WILTS OF POTATO IN LEBANON. Adib Saad[1], Elias Chnais[1], Lucia Hanna[1], Mireille Kattar[2], and Karma Bouazza[1]. (1) American University of Beirut, Faculty of Agriculture and Food Sciences, Agricultural Sciences department; (2) American University of Beirut, Medical Center, Pathology department. P.O.Box 11-0236, Agricultural Sciences, FAFS, Riad El-Solh, Beirut 1107 202, Lebanon, Email: eliechnais@hotmail.com

The current study consisted of a survey that aimed to detect the quarantine pathogen *Ralstonia solanacearum* (*R.s*) and the blackleg bacterium *Erwinia carotovora* subsp. *atroseptica* (*Eca*). Three hundred and fourteen infected potato samples were collected from eleven localities in the Bekaa. One hundred and fourteen bacterial strains were isolated from these infected plants. The bacterial isolates were subjected to several biochemical and physiological tests to determine their pathogenicity, where thirty nine isolates were pathogens. A pathogenicity test was conducted on eggplants and tomato plants and rated on a scale of 1 to 4 according to the degree of virulence. Twelve isolates had a rating of 1, fourteen a rating of 2, thirteen a rating of 3, and none had a rating of 4 (highly virulent). The ability of the isolates to degrade potato tissues was assessed by rotting of potato slices and whole tubers. It was revealed that the higher the pathogenic rate the isolates had, the more likely they possessed the ability to rot potato. Resuts prooved that none of the isolates suspected as *R. s*. belonged to this species. However, *Eca* has many serotypes and it is probable that local *Eca* strains do not belong to the same serotypes previously identified which might explain why they weren't detected by the ELISA test. Sequencing of the 16S rDNA was performed on 24 out of 39 isolates selected to represent the major surveyed localities. Sequence analysis revealed that five isolates were *Eca*, eight were *Pantoea agglomerans* and four were *Agrobacterium tumefaciens*. None of the isolates were identified as *R. solanacearum*. Therefore, this study indicates that *R.s*. was not present in the surveyed areas during the period of survey. However, this study confirmed the presence of *E. carotovora* subsp. *atrospetica* in five localities in the Bekaa.

B 12

GENETIC VARIABILITY OF *PSEUDOMONAS SAVASTANOI* PV. *SAVASTANOI*. Chiaraluce Moretti[1], Franco Valentini[2], Abdelmonim A. Ahmad[2], Taha Hosni[1], Nael Alabdalla[2], Nabil S. Farag[3], Anwar A. Galal[4], M'Barek Fatmi[5], Mahmoud Abu-Ghorra[6] and Roberto Buonaurio[1]. (1) Department of Environmental and Agricultural Sciences, Faculty of Agriculture, University of Perugia, Italy, Email: chiaraluce.moretti@unipg.it; (2) Centre International de Hautes Etudes Agronomiques Méditerranéennes (CIHEAM/MAIB), Via Ceglie 9, 70010 Valenzano, Bari-Italy; (3) Agricultural Research Centre, Plant Pathology Research Institute, Giza, Egypt; (4) Department of Plant Pathology, Faculty of Agriculture, University of Minia, Egypt; (5) Institut Agronomique et Vétérinaire Hassan II, Complexe Horticole d'Agadir, Agadir, Morocco; (6) Division of (Department of) Plant Protection, Faculty of Agriculture, University of Damascus, Syria.

Olive knot disease, caused by *Pseudomonas savastanoi* pv. *savastanoi* (Pssa), poses a serious threat to many olive growing areas of the Mediterranean basin and can significantly affect olive yield and oil. The study of genetic variability of a wide Pssa population, coming from Albania, Algeria, Egypt, France, Greece, Italy, Morocco, Portugal, Serbia, Spain, Syria, Tunisia, Turkey, USA and ex-Yugoslavia, is currently in progress. This research work was undertaken following the results of the investigations carried out at MAIB-CIHEAM (Italy), in the framework of three Master theses in Integrated Pest Management, which allowed to conduct a preliminary molecular characterization of a Pssa population and to describe the disease for the first time in Egypt and Syria. Rep-PCR, and particularly, f-AFLP analyses revealed a high Pssa polymorphism which seems to be related to the country of origin and not to the olive cultivars nor to the bacterial virulence. Further Pssa characterisation was based on the establishment of the repertoire of effectors involved in the bacterium virulence. Since multi-locus sequence analysis revealed that Pssa is closely related to *P. savastanoi* pv. *phaseolicola* 1448A completely sequenced genome, primers designed on the basis of 21 bacterium effector genes were used to verify whether or not they are present in a selected number of Pssa strains.

VIRUSES DISEASES

V 1

BIOLOGICAL AND SEROLOGICAL IDENTIFICATION OF *TOMATO YELLOW LEAF CURL VIRUS* (TYLCV) AND DETERMINATION OF ITS STRAINS IN IRAQ. Rakib Akif AlAni, Mustafa Ali Adhab and Samir Abdul-Razzak Hassan Hamad, Plant Protection Department, College of Agriculture, University of Baghdad, Iraq, Email: maa_adhab@hotmail.com.

This study was conducted to identify *Tomato yellow leaf curl virus* and determine its strains in Iraq. Symptoms on indicator plants, incubation period of virus in vector, and serological properties of the virus were evaluated. Results of different isolates of the virus on